USING THE GPS TO IMPROVE TRAJECTORY POSITION AND VELOCITY DETERMINATION DURING REAL-TIME EJECTION SEAT TEST AND EVALUATION

THESIS

Christina G. Schutte, Captain, USAF

AFIT/GE/ENG/03-16

DEPARTMENT OF THE AIR FORCE
AIR UNIVERSITY

AIR FORCE INSTITUTE OF TECHNOLOGY

Wright-Patterson Air Force Base, Ohio

Disclaimer

The views expressed in this thesis are those of the author and do not reflect the official policy or position of the United States Air Force, Department of Defense, or the U. S. Government.

AFIT/GE/ENG/03-16

USING THE GPS TO IMPROVE TRAJECTORY POSITION AND VELOCITY DETERMINATION DURING REAL-TIME EJECTION SEAT TEST AND EVALUATION

THESIS

Presented to the Faculty

Department of Electrical and Computer Engineering

Graduate School of Engineering and Management

Air Force Institute of Technology

Air University

Air Education and Training Command

In Partial Fulfillment of the Requirements for the

Degree of Master of Science in Electrical Engineering

Christina G. Schutte, BSEE

Captain, USAF

February 2003

AFIT/GE/ENG/03-16

USING THE GPS TO IMPROVE TRAJECTORY POSITION AND VELOCITY DETERMINATION DURING REAL-TIME EJECTION SEAT TEST AND EVALUATION

Christina G. Schutte, BSEE
Captain, USAF

Approved:

Lt Col Mikel M. Miller (Chairman)	14 Mar 03 Date
Dr. Peter S. Maybeck (Member)	14 MAR 03 Date
Maj John F. Raquet (Member)	14 MAR 03 Date

Acknowledgments

I would first like to thank Col Steve Cameron, Col Joe Zeis Jr., and Lt Col Tom Buter for supporting my crazy idea of returning to school after an eight year sabbatical, and trusting in my abilities to complete the program. Without their encouragement and support, this journey would not have taken off.

My sponsor, Mr. John Plaga, and the folks from at the Air Force Research Lab's Human Effectiveness Division, Mr. Doug Coppess, Mr. Kris Kull, and Dr. Ted Knox, deserve my thanks and appreciation for all their help and support throughout my research and for taking me under their wing to help me understand the world of test manikins and ejection seats. Their hard work, experience, and knowledge made the testing opportunities in the multiple venues possible.

Also, I would like to thank the Barber Dodge Racing Team, the Simula Safety Systems' SEI Division team, the China Lake Naval Air Warfare Center's Supersonic Naval Ordnance Research Track team, and the Hurricane Mesa Test Track group for allowing me to use their resources. Without their help my research would not have been possible.

My advisor, Lt Col Mikel Miller, and my committee members, Dr. Peter Maybeck and Maj John Raquet deserve special thanks. Their patience and encouragement throughout the program was unwavering. They never hesitated to take time out of their busy schedules to provide guidance or explain difficult concepts to me.

I couldn't have asked for a better group of folks to take this ride with than the "NavLab" crew: Alec, Aydin, Craig, Jae, Jason, Ken, Terry, and Don. Without their help, support, and encouragement, I might have graduated, but I'm sure it wouldn't have been as much fun.

Last but not least, I want to thank my family for helping me through the hard times encouraging me to keep going when the classes and homework seemed unending.

Christina G. Schutte

Table of Contents

List of Figures

Abstract

Test and evaluation of the United States Air Force's latest aircraft escape system technology requires accurate position and velocity profiles during each test to determine the relative positions between the aircraft, ejection seat, manikin and the ground. Current rocket sled testing relies on expensive ground based multiple camera systems to determine the position and velocity profiles. While these systems are satisfactory at determining seat and manikin trajectories for sled testing, their accuracy decreases when they are used for in-flight testing, especially at high altitudes.

This research presents the design and test results from a new GPS-based system capable of monitoring all major ejection test components (including multiple ejection seat systems) during an entire escape system test run. This portable system can easily be integrated into the test manikin, within the flight equipment, or in the ejection seat. Small, low-power, lightweight Global Positioning System (GPS) GPS receivers, capable of handling high-accelerations, are mounted on the desired escape system component to maintain track during the escape system test sequence from initiation until the final landing. The GPS-based system will be used to augment the telemetry and photography systems currently being used at the Air Force (AF) and other Department of Defense's (DoD) sled track test facilities to improve tracking accuracy and reduce testing costs.

USING THE GLOBAL POSITIONING SYSTEM (GPS) TO IMPROVE TRAJECTORY POSITION AND VELOCITY DETERMINATION DURING REAL-TIME EJECTION SEAT TEST AND EVALUATION

I. Introduction

Background

Shortly after man began to fly in the early 20th century, he realized the need to escape from a crippled aircraft safely. Testing of early ejection seats began in 1912, and since then, improving the ejection seat and ways to test it adequately have been ongoing.

The testing process has come a long way in the past ninety years. Early testing used cannon-propelled parachutes to pull the aircrew member from the aircraft. Modern day testing uses instrumented Advanced Dynamic Anthropomorphic Manikins (ADAM) and the Lightest Occupant In Service (LOIS) to simulate the aircrew member. In addition, extensive sled track facilities are used to test the ejection seats, and telemetry and photography are used to monitor the entire ejection seat sequence.

The improvements in testing have resulted in scientists, physicians, and engineers understanding the dynamics encountered during an ejection sequence more fully, and have provided the manufacturers with vital information to improve the ejection seat's performance. Through this cooperative effort, the survivability rate from an aircraft escape systems increased from a mere 60 percent in the late 1940s to over 80 percent in the mid 1980s [34].

Although there has been a significant decrease in the number of injuries and fatalities encountered, the need for better ejection seats is evident. Future improvements to the ejection seat testing process provides an opportunity for scientists, physicians, and engineers to advance their knowledge further concerning the dynamics of an ejection sequence, and possibly increase the survivability rate even more.

Global Positioning System (GPS) Used for Ejection Seat Test and Evaluation

Captain Brian (Reece) Tredway [34] proposed using a GPS receiver and antenna system capable of handling the high dynamic environment of an ejection sequence. Through his research, he developed a small, low cost GPS-based system that could easily be inserted into the manikin's survival vest and provide position and velocity information for the manikin during an ejection seat test sequence.

His initial research and testing proved the system was a viable concept, and left the door open for more research in this area. This research expands on his work to incorporate a dual receiver into the survival vest using the same form fit of a single receiver, and modify the equipment to withstand the high dynamic environment of the ejection seat sequence. With these changes, not only will the system provide accurate position and velocity information to augment the telemetry and photography, but it will also provide attitude determination for the manikin through the ejection sequence.

Problem Definition

As stated above, modern day testing of ejection seats has come a long way, but the monitoring and tracking systems, which use telemetry and photography, lack the ability to track more than one target at a time. They currently provide accurate position, velocity, and altitude

measurements to within 1.5 meters. A second limitation to the current tracking and monitoring system is its inability to determine the attitude of the manikin through the ejection sequence. Knowing the manikin's attitude would help to isolate and possibly reduce the tumbling and rotational moments experienced through the ejection sequence.

The problem is to develop a tracking and monitoring system to track more than one target at a time, augment position, velocity, and altitude measurements, and incorporate attitude determination while maintaining the current accuracy standards. This thesis presents a method of adapting a differential GPS system to work in the high dynamic environment of ejection seat testing to provide a small, flexible, low cost system for the testing community.

Scope

The goal of this research is to improve the Differential GPS Independent Velocity, Position, and Altitude Collection System (DIVEPACS) [34] to augment the current video based trajectory determination system, and provide sub-meter accuracy for position, velocity, altitude, and attitude determination measurements for the manikin, ejection seat, and aircraft canopy.

Overview

This thesis is divided into five chapters and six appendices. Chapter 2 provides additional background information about ejection seat testing, the GPS, inertial navigation systems for attitude determination, and a brief outline of Kalman filtering to aid in determining the carrier-phase ambiguity. Chapter 3 details the methodology used to adapt the DIVEPACS to improve the trajectory position and provide attitude determination for ejection seat testing. Chapter 4 outlines the results of the actual tests conducted in this research. Chapter 5 summarizes the results of this research, and provides recommendations for future research and

testing. The appendices provide the schematics for the different DIVEPACS configurations, the flash report from the high-speed sled test, the antenna specifications for the antennas used, and the paper presented at the SAFE Association Symposium in October 2002.

II. Theory

This chapter presents theories used for this research and a brief discussion of previous research using the Global Positioning System (GPS) for ejection seat testing. The theories presented in this section outline GPS and the use of differential GPS to provide accurate position and velocity trajectory information for ejection seat testing. Also, to understand attitude determination, this chapter discusses inertial navigation systems (INS) theory. The last section of this chapter briefly presents previous research using GPS in conjunction with ejection seat testing.

Global Positioning System (GPS)

GPS Overview

In the late 1960's, the Department of Defense (DoD) initiated the development of the GPS satellite constellation primarily to provide the military with accurate estimates of position, velocity, and time. Although it was primarily deployed for military purposes, the DoD adapted the system to provide a degraded position, velocity, and time estimate for civilian users by introducing controlled errors into the transmitted radio navigation signal, called selective availability (SA). In May 2000, SA was deactivated [22][28].

The GPS architecture consists of three main parts—the space segment, the control segment, and the user segment. Figure 1 shows all three segments of the system's architecture. The information provided in this section is only a brief discussion of the GPS. For more information, please consult the following [15][22][28][29].

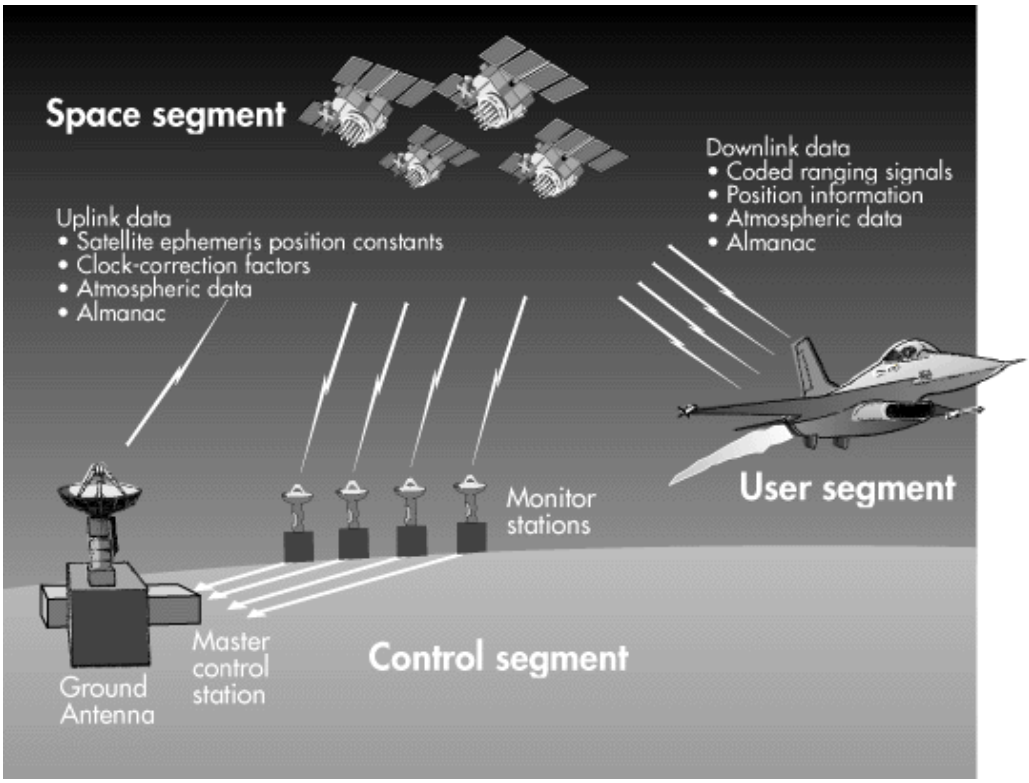

Figure 1. GPS Architecture [31]

Space Segment.

The space segment consists of the GPS satellite constellation. To provide global coverage, the constellation has a minimum of 24 satellites, and can support a maximum of 32 satellites in the constellation [22]. The satellites are distributed unevenly into six orbital planes which each have a 55 degree inclination angle. The satellites' medium earth orbit (MEO) has an orbital period of 11 hours and 56 minutes for each satellite. In turn, this orbital period allows each satellite to have an in-view time of approximately five hours, and typically users have six to eight satellites available to them to calculate a position solution. Each satellite continually broadcasts ranging signals and navigation data for the users. More information about these

signals will be presented later in this chapter. Figure 2 depicts the orbital planes located around the earth.

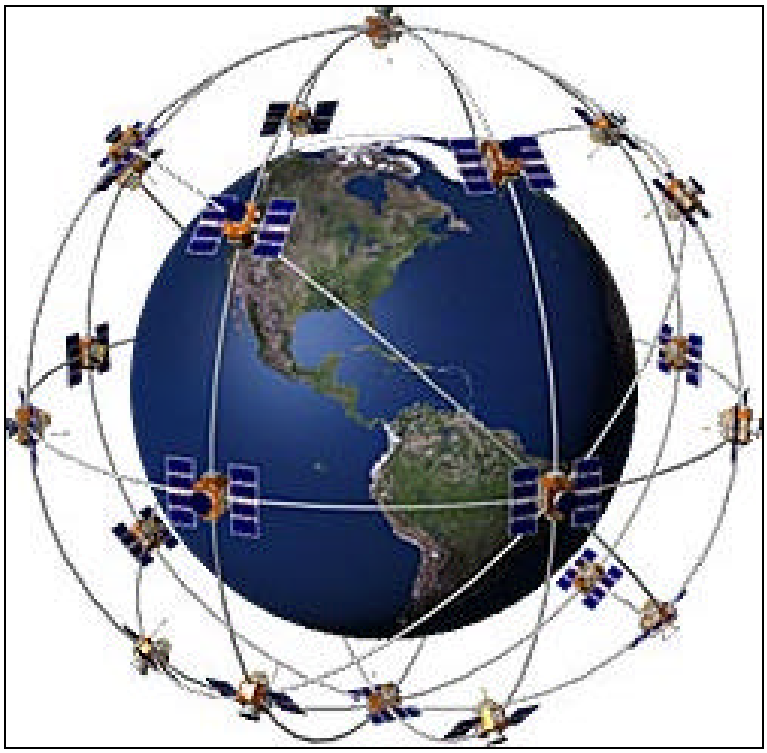

Figure 2. GPS Orbital Planes [8]

Control Segment.

The control segment consists of a master control station (MCS) located at Schriever Air Force Base in Colorado, and five unmanned monitoring stations located around the world at Hawaii, Cape Canaveral, Ascension Island, Diego Garcia, and Kwajalein. The monitoring stations have dedicated antennas and communications equipment, and the MCS controls them remotely as needed to receive telemetry from the satellite or to upload navigation messages to the satellites. These stations are responsible for monitoring the satellite orbits, maintaining the satellites' health, maintaining GPS time, predicting satellite ephemeredes and clock parameters,

updating satellite navigation messages, and commanding satellite maneuvers to maintain orbits or compensate for satellite failures [22]. Figure 3 shows the control segment locations.

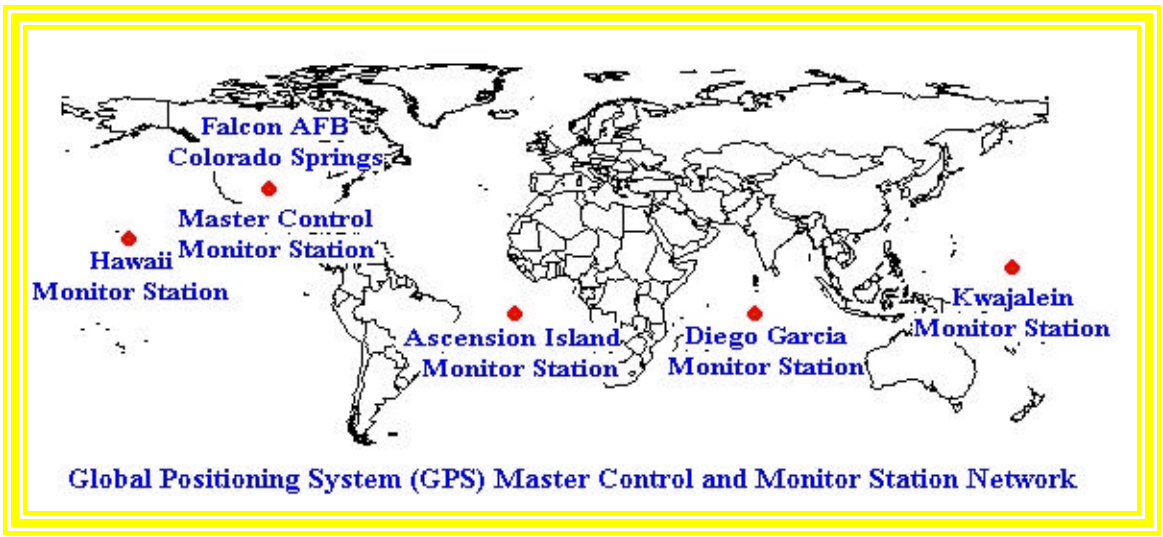

Figure 3. GPS Control Segment [29]

User Segment.

The user segment consists of anyone, military or civilian, who has a GPS receiver designed to convert the GPS signals into position, velocity and time estimates. The size, accuracy, and cost of the receiver vary greatly, from under a hundred dollars to tens of thousands of dollars, based on the user's desired GPS application [22]. For instance, a receiver mounted on a fighter aircraft would cost significantly more than a receiver used for hiking through the mountains due to the size, weight, and dynamic requirements of the airborne system. Although they both use the same basic principles to process the received signals, the sensitivity and accuracy requirements for the airborne system would be more stringent than the hand-held unit. Receiver principles will be discussed in more detail later in this chapter.

GPS Signal

As previously stated, each satellite in the GPS continually broadcasts ranging signals and navigation data. The broadcast signal of interest for this research has three components—the carrier frequency, the ranging code, and the navigation data. The two carrier frequencies of interest are the L1 at 1575.42 MHz and L2 at 1227.60 MHz. The L1 frequency is available to all users, while the L2 frequency is typically restricted to DoD-authorized users. The ranging codes or code modulating the L1 or L2 frequency are responsible for this distinction. The GPS uses two distinct ranging codes, the coarse acquisition (C/A) code and the precision (P) code. To restrict the P code for DoD-authorized users, it is encrypted into a Y code, and typically referred to as the P(Y) code. While the L1 carrier frequency is modulated with both ranging codes, the L2 frequency is only modulated with the P(Y) code.

Since all the satellites broadcast on the same frequency, the ranging code generated for each satellite must be specific to that satellite. Each satellite generates a unique sequence of ones and zeros known as a pseudo-random noise (PRN) sequence or PRN code. Figure 4 is an example of both C/A and P(Y) PRN codes.

Each element in the C/A or P(Y) is referred to as a "chip," and the number of chips per second is called it chipping rate. The C/A code consists of 1023 chips, and the sequence is repeated every millisecond. Therefore, the C/A code's chipping rate is 1.023 MHz. The P(Y) code sequence is extremely long (approximately 10^{14} chips), and has a chipping rate of 10.23 MHz. The higher chipping rate of the P(Y) code translates into a smaller chip width, which provides a more accurate range measurement. The P(Y) code repeats once a week. Table 1 is a summary of the two GPS signals [11][28].

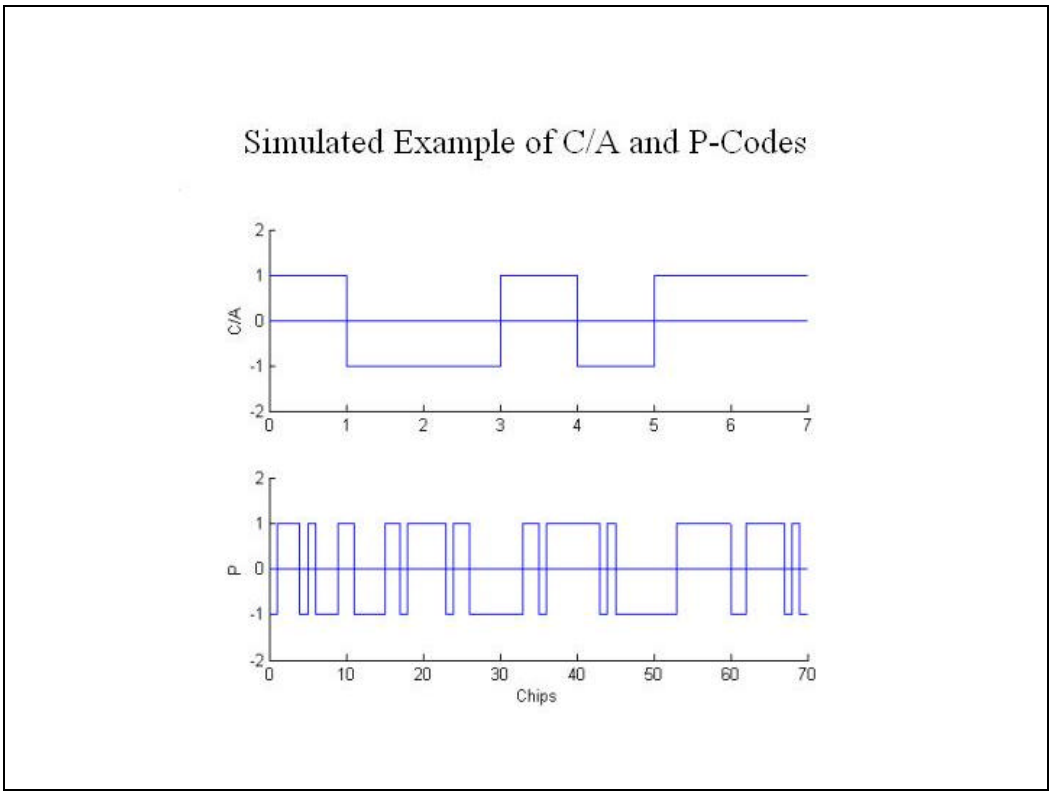

Figure 4. Example of C/A and P(Y) PRN Codes [28]

Table 1 GPS Signal Summary

Carrier	Frequency	Wavelength	Modulation	Chip Rate/ Frequency	Chip Length	Repeat Interval
L1	1575.42 MHz	19 cm	C/A Code	1.023 MHz	293 m	1 msec
			P Code	10.23 MHz	29.3 m	1 week
			Nav Message	50 Hz		12.5 min
L2	1227.60 MHz	24 cm	P Code	10.23 MHz	29.3 m	1 week
			Nav Message	50 Hz		12.5 min

The last part of the broadcast signal is the navigation data. The navigation data includes the satellite health status, satellite position and velocity (ephemeris), clock bias parameters, ionospheric models, and an almanac. The almanac provides the ephemeris for all the satellites in the constellation. The navigation message is transmitted at a 50 Hz rate with a bit duration of

20 msec. The entire message takes 12.5 minutes to receive [22]. Using modulo-2 addition, the navigation message is combined with each code. Figure 5 depicts an example of the entire broadcasted signal.

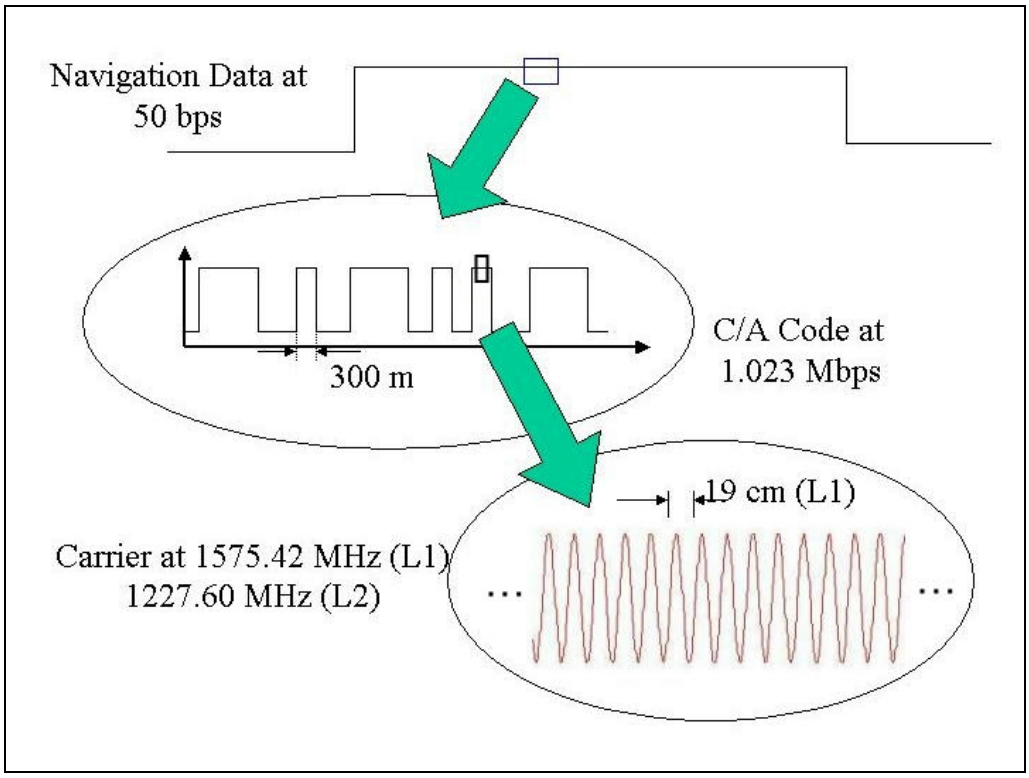

Figure 5. Broadcasted Signal [34]

GPS Measurements

To calculate a user's position, the GPS receiver measures the range between itself and the satellites it is tracking. To provide an accurate position solution, at least four satellites must be in view. Typically, receivers can output four types of measurements—code or pseudorange, carrier-phase, Doppler, and carrier-to-noise measurements. This section will discuss the code and carrier-phase measurements. More information concerning the Doppler and carrier-to-noise measurements can be found in [22] [28].

Code Measurements.

Since the code measurement is a combination of the true range measurement to the satellite and errors associated with the GPS signal, it is also known as the pseudorange measurement. When the satellite broadcasts its signal, it includes a transmit time. As the signal is received, the time of reception is noted. The time difference between the transmitted satellite signal and the received signal is the pseudorange measurement. Equation (1) defines the pseudorange measurement with all the errors listed. The errors affecting the measurement will be discussed later in this chapter.

$$r_j = r + c(dt_u - dt_{SV} + dt_{trop} + dt_{iono} + dt_{noise} + dt_{mult} + dt_{SA} + dt_{hw}) \qquad (1)$$

where

r_j = *Pseudorange measurement from satellite j*
r = *True range to receiver (m)*
c = *Speed of light (m/s)*
dt_u = *Receiver clock error (s)*
dt_{SV} = *Satellite clock error (s)*
dt_{trop} = *Errors due to tropospheric delay (s)*
dt_{iono} = *Errors due to ionospheric delay (s)*
dt_{noise} = *Errors due to receiver noise (s)*
dt_{mult} = *Errors due to multipath (s)*
dt_{SA} = *Errors due selective availability (s)*
dt_{hw} = *Errors due to hardware (s)*

Carrier-Phase Measurements.

To calculate the carrier-phase measurement, the receiver differences its internally generated signal with the carrier signal received from a satellite. The code measurement uses time

contained within the signal as a reference to determine the transmit time, but the carrier signal does not contain such a reference. The receiver can only count the number of changes in cycles it sees, so the initial number of cycles between the receiver and the satellite is unknown or ambiguous. With carrier-phase measurements, an unknown bias is added to the range measurement. This ambiguity must be resolved before a true range measurement can be achieved. Several techniques can be used to resolve or estimate the ambiguity. For additional information regarding the different techniques consult references [11][22][29]. Equation (2) defines the carrier-phase measurement.

$$f_j = \frac{1}{l}\left[\ r + c(dt_u - dt_{sv} + dt_{trop} - dt_{iono} + dt_{noise} + dt_{mult} + dt_{hw} + dt_{SA})\ \right] + N \qquad (2)$$

where

f_j = *Carrier-phase measurement from satellite j (cycles)*
l = *Carrier-phase wavelength (m)*
dt_u = *Receiver clock error (s)*
r = *True range to receiver*
c = *Speed of light (m/s)*
dt_{sv} = *Satellite clock error (s)*
dt_{trop} = *Delay due to troposphere (s)*
dt_{iono} = *Delay due to ionosphere (s)*
dt_{noise} = *Delay due to receiver noise (s)*
dt_{mult} = *Delay due to multipath (s)*
dt_{hw} = *Delay due to hardware (s)*
dt_{SA} = *Delay due to selective availability (s)*
N = *Carrier-phase integer ambiguity (cycles)*

Although the same types of errors are found in the carrier-phase measurement, the magnitude of the specific type of error will be different from those of the code measurement. One specific

error to note is the ionospheric error. Its effects on the GPS signal cause it to delay the code measurement and advance the carrier-phase measurement [22]. The effect is noted with the sign change associated with the error term found in Equations (1) and (2).

GPS Measurement Errors

As noted in the previous sections, several errors affect the user's position calculation. This section will briefly address the eight error sources: selective availability, hardware noise, satellite clock and ephemeris, receiver clock, troposphere, ionosphere, receiver noise, and multipath. Table 2 lists typical values for the errors to be discussed for standard positioning service (SPS) and precision positioning service (PPS) receivers [28]. The user equivalent range error is a combination of the errors listed in the table, and is calculated using the root-sum-square of the component errors [22] [28].

Table 2 Typical GPS Positioning Errors [28]

Error Source	Typical Range Error Magnitude (meters, 1 s)		
	SPS (w/ SA)	SPS (w/o SA)	PPS
Selective Availability	24.0	0.0	0.0
Ionosphere[a]	7.0	7.0	0.01
Troposphere[b]	0.7	0.7	0.7
Satellite Clock and Ephemeris	3.6	3.6	3.6
Receiver Noise	1.5	1.5	0.6
Multipath[c]	1.2	1.2	1.8
Total User Equivalent Range Error (UERE)	25.3	8.1	4.1

a – For SPS: 7.0 is typical value of ionosphere after applying ionospheric model. Actual values can range between approximately 1-30m.
b – Residual error after using tropospheric model
c – For PPS: Includes increase in multipath that results from using L1 and L2 code measurements to remove ionospheric error.

Selective Availability (SA) and Hardware Noise Errors.

When the DoD developed the GPS, one of its primary objectives was to provide the U. S. military with an accurate positioning system worldwide, and at the same time prevent its enemies from using the system to their advantage. The DoD originally used SA to achieve this objective. SA intentionally dithered the satellite clock and induced errors into the broadcasted ephemeris values, which affected the ranging. As can be seen from Table 2, SA was the dominant error. In May of 2000, SA was deactivated [22][28]. Hardware noise errors are typically small in comparison to the other errors present in the signal, and they are often neglected (as they are here).

Satellite Clock and Ephemeris Errors.

Accurate timing is at the core of the GPS. One microsecond of error in time can result in approximately a 300 meter positioning error. Although the satellites use very accurate rubidium or cesium atomic clocks, they can still drift or develop a bias due to aging or other environmental factors. The MCS continually monitors the satellites' clocks, and uploads corrections. Along with the clock corrections, the MCS uploads ephemeredes to the satellites daily, and the satellites broadcast the predicted position within the navigation message. The difference between the actual satellite position and the predicted position is the ephemeris error. Even with the corrections, a residual error remains which adds approximately 2 meters root mean square (RMS) error to the position solution [22].

Receiver Clock Errors.

To calculate the x, y, and z position of a receiver requires four satellites. Through trilateration, the receiver can estimate a three-dimensional position, but the fourth satellite is

needed to estimate the receiver's clock error. Figure 6 depicts how positioning is determined using trilateration [24].

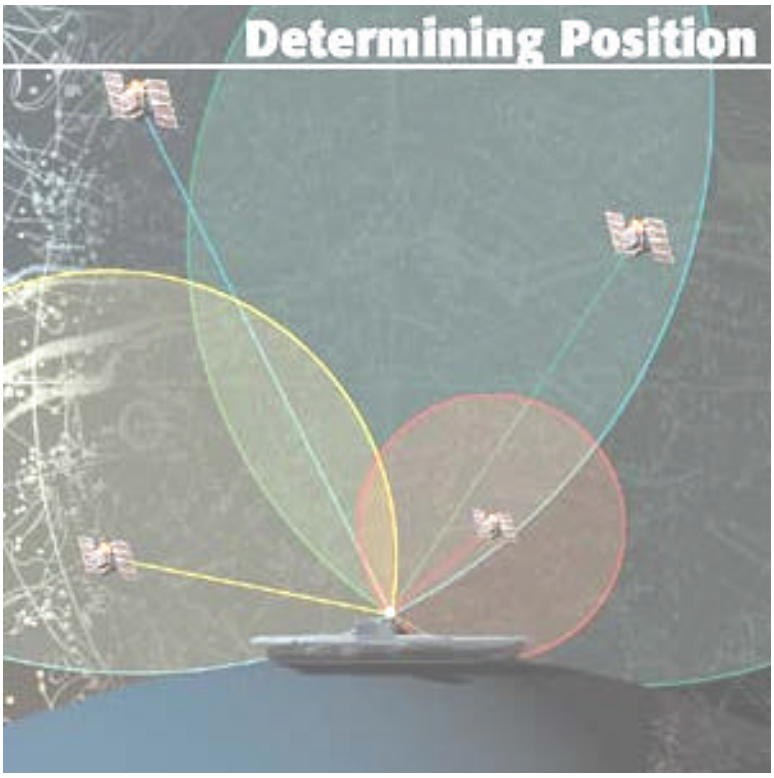

Figure 6. Position Determined by Trilateration [24]

Tropospheric Errors.

As radio frequencies propagate through the atmosphere, different layers of the atmosphere affect how they propagate. The troposphere is the lowest layer of the atmosphere, extending up from sea level to approximately 50 km above sea level [28]. The dry gases and water vapor in the lower atmosphere delay both the code and the carrier-phase signals. The first 10 km of the atmosphere is responsible for 75 percent of the tropospheric error [28]. Since the signals must travel through more of the atmosphere at lower elevation angles, a larger error is associated with

the position solution for such elevation angles [22]. Accurate modeling of meteorological conditions can reduce the error to 0.1 to 1 meters [22].

Ionospheric Errors.

The ionosphere is the upper portion of the atmosphere that contains charged particles. The concentration and variability of charged particles depends on solar activity, satellite's elevation angle, the user's latitude, and the time of day [22]. The maximum ionospheric errors typically occur in the afternoon around 2:00 p.m. locally. Figure 7 is an example of the ionospheric errors recorded at East Port Maine on January 15, 2002 from a single GPS receiver.

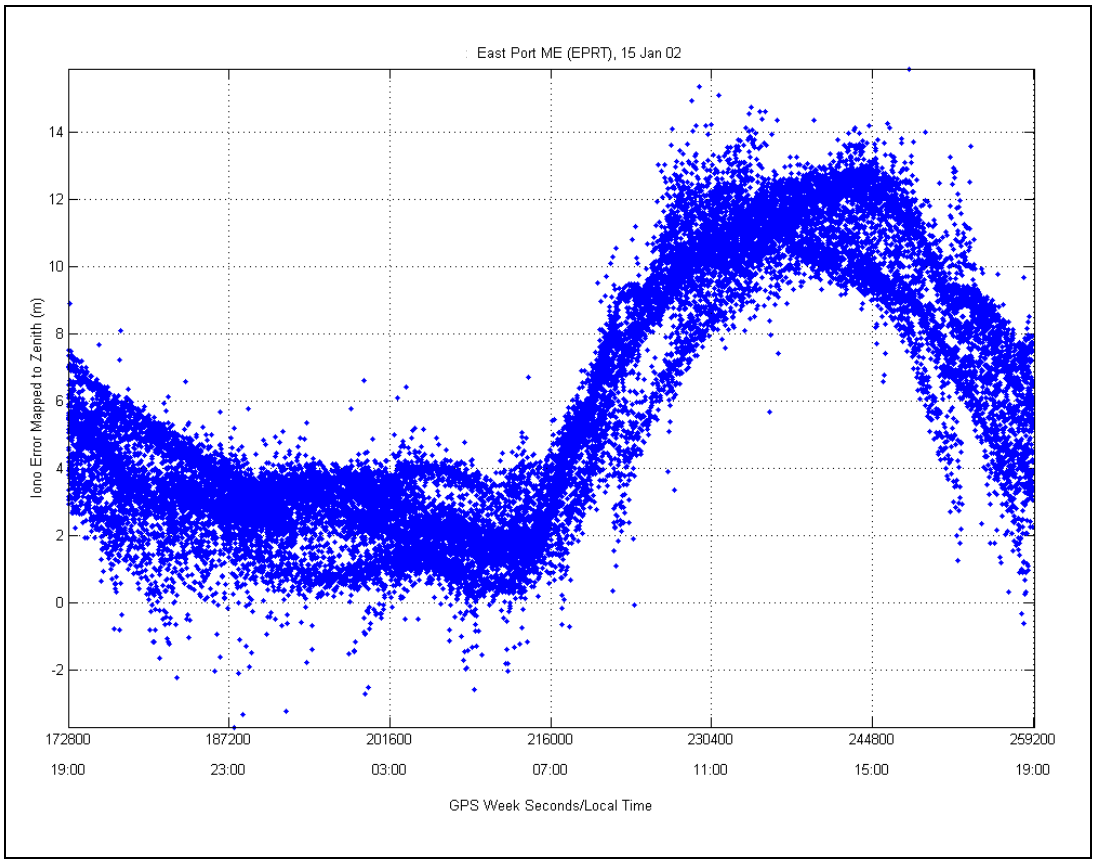

Figure 7. Ionospheric Errors

The amount of error induced on a signal is frequency dependent. The ionosphere affects lower frequencies more than higher frequencies, which accounts for the ionospheric error sign difference in Equations (1) and (2) previously noted, delaying the code signal and advancing the carrier-phase signal. Through the use of ionospheric models or differencing the L1 and L2 frequencies, the error can be mitigated with a residual error of 1 to 5 m [22].

Receiver Noise Errors.

Receiver noise is inherent to the receiver's design. It is uncorrelated in time and with other receivers, but is correlated with the signal-to-noise ratio [22][28]. A lower signal-to-noise ratio results in a larger receiver noise error [28]. Careful receiver design can help to mitigate the error, but it cannot be completely removed.

Multipath Errors.

Multipath errors occur when the same signal is received through two or more paths due to reflections from structures or obstacles surrounding the antenna. Multipath affects both code and carrier-phase measurements, but the magnitude of the code multipath errors are significantly larger than the phase multipath errors [22]. The code multipath error can vary from 1 to 5 meters, while the carrier-phase multipath error is much smaller, 1 to 5 cm [22]. Placing the antenna in an obstacle-free environment mitigates the error.

Dilution of Precision (DOP)

Along with the measurements errors listed above, the geometrical distribution of the satellites in view surrounding the user plays a role in the accuracy of the position solution. To help quantify the contribution of the satellite distribution on the position estimate, a dilution of

precision (DOP) parameter is used. Figure 8 shows an example of good and poor user-satellite geometry [22][28].

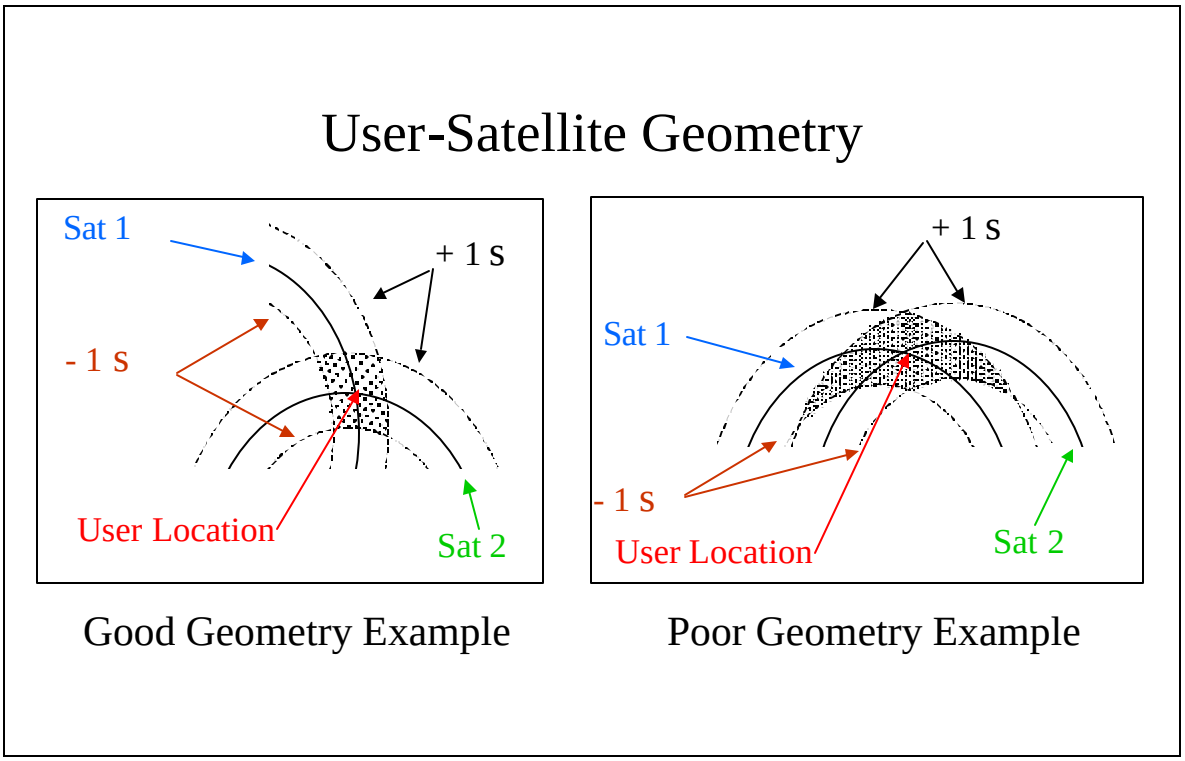

Figure 8. User-Satellite Geometry [22]

Typically, the lower the DOP value, the better the estimated position solution. Combining the position DOP value with the user equivalent range error (UERE) from the previous section, a three-dimensional root mean square error value can be established. For ease of use, the UERE is converted into a local level coordinate frame such as longitude, latitude, altitude reference frame or an east, north, up frame. Equation (3) expresses the three-dimensional RMS value in terms of the PDOP and UERE. For more information concerning PDOP or other DOP values consult the references [22][28].

$$RMS\ 3\text{–}D\ Error = \sqrt{s_E^2 + s_N^2 + s_U^2} = s_{UERE} \cdot PDOP \qquad (3)$$

where

s_{UERE} = *Standard deviation of the user estimated range error*
s_E^2 = *Variance of the east component*
s_N^2 = *Variance of the north component*
s_U^2 = *Variance of the vertical (up) component*

GPS Receivers

As GPS has grown and garnered greater acceptance in many fields, the size and cost of receivers has decreased, but the receiver's basic operating principles have not changed. One difference to note between older receivers and newer ones is that many older receivers limited their satellite tracking to the best four satellites visible based on their DOP. The newer receivers typically track all satellites in view. Regardless of which type of receiver is used, the receiver still acquires GPS signals and processes them in its tracking loops to provide precise position, velocity, and time data for the user. Along with position, velocity, and time data, the receiver can output raw measurements, signal-to-noise ratios, satellite PRNs and formatted messages derived from its tracking loops [34]. The receiver uses two tracking loops, the phase lock loop (PLL) and the code tracking loop, which are discussed below. Figure 9 depicts both tracking loops within the receiver [29][34].

GPS Receiver Tracking Loops

Each channel within the receiver uses a code tracking loop and a PLL. The inner loop is used to detect and track the PRN code of the satellite, while the outer loop acquires and tracks

the carrier frequency. Both tracking loops consist of three main parts, the predetection integrators, discriminators, and loop filters. Both must be working properly for the receiver to work.

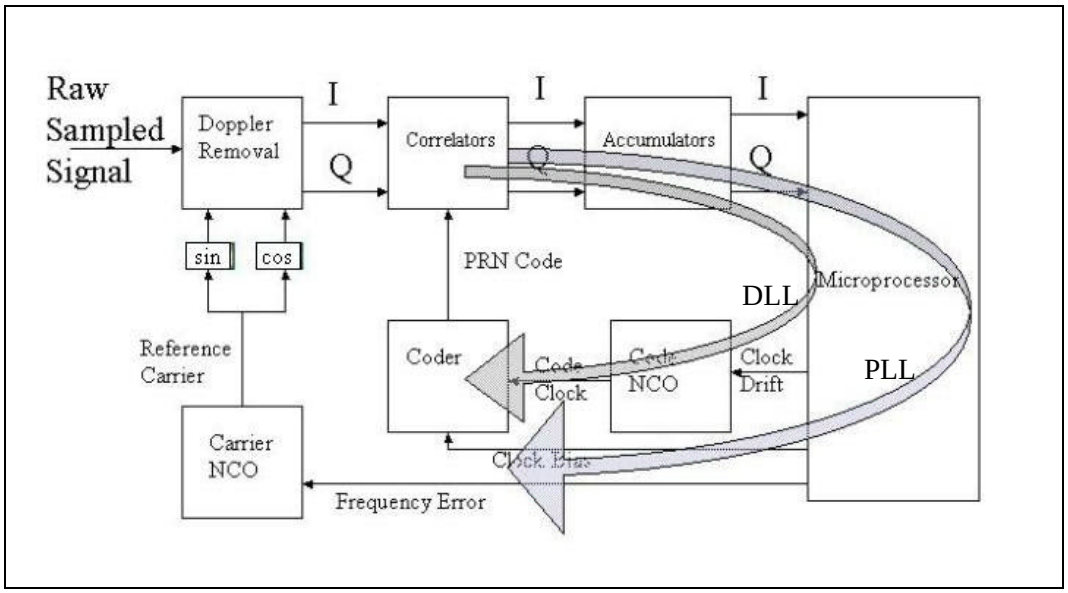

Figure 9. Tracking Loops [29]

Code Tracking Loop.

As the raw signal is brought into the receiver, the Doppler is removed, and the signal is broken into in-phase (I) and quadrature-phase (Q) signals. Through the use of the almanac, the receiver determines which satellites are in view. Using this information, the correlators use the receiver's internally generated C/A codes for the satellites in view, and compares it with the received code. As the correlators shift the internally generated code against the received signal, a sharp peak in the correlation signal is created when the internal code matches an incoming satellite C/A code. The accumlators integrate the I and Q data to ensure the correlators have actually acquired a satellite, and have not locked onto noise. Inside the microprocessor, the signal is tracked using early, late, and prompt detectors to determine how the signal has shifted in

time. The numerically controlled oscillator uses the information from the early, late, and prompt detectors to adjust the internal signal so it can maintain lock. Through this feedback loop, also known as the delay lock loop, the code is tracked [22][29].

Phase Lock Loop.

The outer loop is similar to the inner loop, but tracks the carrier signal instead of the code. The receiver also generates a sinusoidal frequency to match the incoming signal's frequency and phase. After the code is removed, the phase lock loop tracks the changes in the frequency and measures the Doppler shift of the incoming frequency. More information concerning the tracking loops can be found in references [22][29].

Differential GPS (DPGS)

In the early years of GPS when SA was activated, the requirement for a more accurate position solution drove the development of DGPS. DGPS uses two GPS receivers in close proximity to each other. One receiver is used as a reference receiver with a well-known or surveyed location, while the second receiver is mounted at an unknown location or is used as a mobile receiver. The reference receiver determines the difference between the measured distances to the satellites and the calculated distances. For real-time DGPS, this difference is sent to the second receiver as a correction term to its calculated distance or logged in a file for post-processing DGPS. Depending on the accuracy requirements and computational resources available, one of three types of DGPS measurements—code-only DGPS, carrier-smoothed DGPS or carrier-phase DGPS—can be used. A brief discussion of each one is provided below. For more detailed information refer to [15][22][28].

Code-Only DGPS

Code-only DGPS uses a reference receiver in conjunction with a mobile receiver to reduce common errors affecting the accuracy of the GPS position solution. The reference receiver calculates pseudorange corrections, and those corrections are then applied to the mobile receiver's pseudorange calculations to reduce the common errors between them. The code-only DGPS improves the accuracy of the position solution from approximately 10 meters RMS to 3 meters or less RMS [22][34].

Carrier-Smoothed

Carrier-smoothed DGPS uses the code measurement and the carrier-phase measurement contained within the GPS signal. The code measurements provide an estimate of the carrier-phase wavelength cycle ambiguity. The carrier-phase measurement is a more precise measurement. The combination of the two measurements improves the position accuracy to half a meter RMS. More information concerning carrier-phase measurements is provided below and in [15][22][28].

Carrier-Phase DGPS

Carrier-phase DGPS uses the carrier-phase measurement contained within the GPS signal. The carrier frequency for L1 is 1575.42 MHz (approximately 635 x 10^{-12} seconds per cycle), and its wavelength is 19 cm [22][28][34]. The carrier-phase signal does not contain time tagged information to denote the start or stop of a cycle. The receiver can count the number of cycles, but the receiver can not determine which cycle it is seeing. This uncertainty is defined as integer ambiguity. By tracking the carrier-phase and counting the cycles over time, the integer ambiguity can be resolved, and millimeter accuracy can be achieved. The main disadvantage of

carrier-phase DGPS and its difficult implementation is due to cycle slips. A cycle slip occurs when tracking is lost for any length of time. The receiver must start the counting process again, since there is no way to determine how many cycles passed over the outage [3][22].

DGPS Differencing Techniques

Since some of the errors previously discussed are highly correlated between two receivers in close proximity of each other, differencing their code or carrier-phase measurements can improve the accuracy of the position solution. Single differencing and double differencing are the two most common techniques. For simplicity only the code measurements will be presented. For more information on carrier-phase measurement differencing, consult [22][28][29].

Single Differencing.

Differencing simultaneous pseudorange measurements between two receivers and one satellite is single differencing. The primary advantage of single differencing is that it removes the satellite clock error. If the baseline between the receivers is relatively small, it also reduces the ionospheric and tropospheric errors. The disadvantage with single differencing is that it increases the multipath and receiver noise errors by a factor of $\sqrt{2}$. Figure 10 is an example of single differencing [34].

Using the notation developed in Equation (1), the single differencing of the pseudorange measurement is accomplished using Equation (4):

$$\begin{aligned} \Delta r_{12}^{j} &= r_{1}^{j} - r_{2}^{j} \\ &= \Delta r_{12}^{j} + c(\Delta dt_{u12}^{j} + \Delta dt_{trop12}^{j} + \Delta dt_{iono12}^{j} + \Delta dt_{noise12}^{j} + \Delta dt_{mp12}^{j}) \end{aligned} \qquad (4)$$

where

Δ = *Single difference DGPS*

Δr_{12}^{j} = *Single difference between receivers 1 and 2 from the* j^{th} *satellite*

Δr = *Single difference of true range to the satellite (m)*

c = *Single difference of speed of light (m/s)*

Δdt_{u12}^{j} = *Single difference of receiver clock error(s)*

Δdt_{trop12}^{j} = *Single difference of tropospheric error (s)*

Δdt_{iono12}^{j} = *Single difference of ionospheric error (s)*

$\Delta dt_{noise12}^{j}$ = *Single difference of receiver noise error (s)*

Δdt_{mp12}^{j} = *Single difference of multipath error (s)*

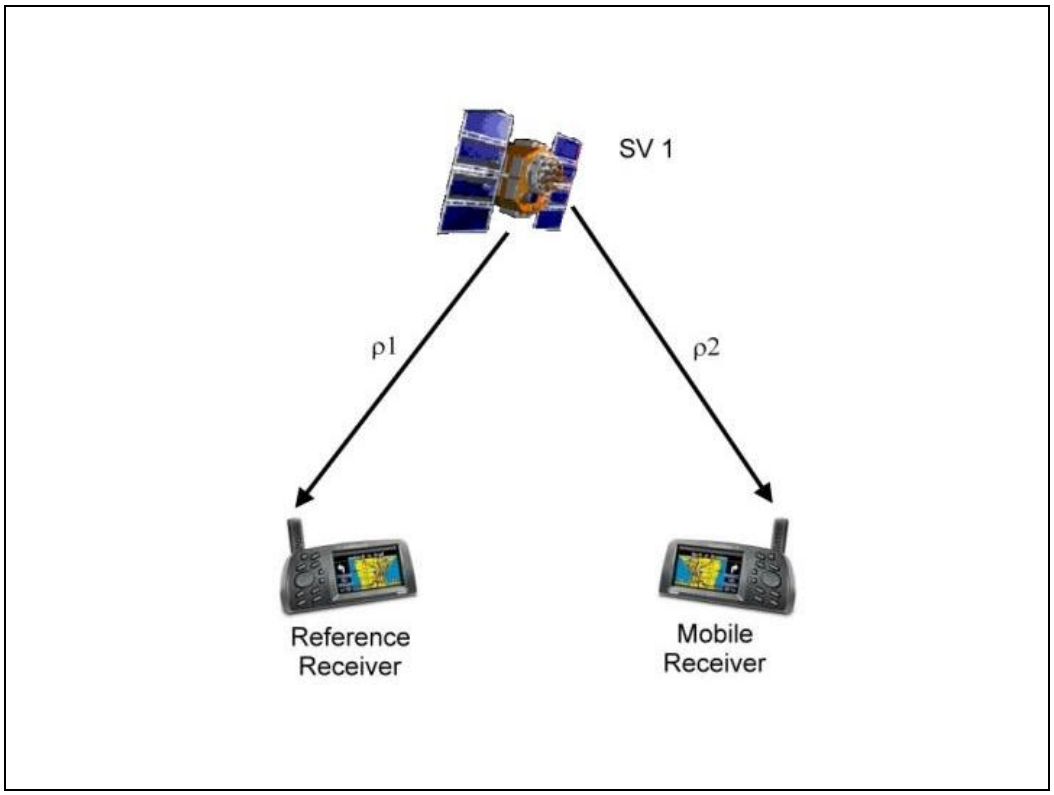

Figure 10. Pseudorange Single Differencing [34][28]

Double Differencing.

Similar to single differencing, double differencing simultaneously differences the pseudorange measurement between two receivers and the same two satellites. As with single differencing, there are advantages and disadvantages. The primary advantage of double differencing is that it not only removes the satellite's clock error, but also the receiver's clock error. Tropospheric and ionospheric errors are reduced, but multipath and noise errors are now amplified by a factor of 2. Figure 11 shows how double differencing is accomplished, and Equation (5) is the mathematical representation of pseudorange measurement double differencing [34].

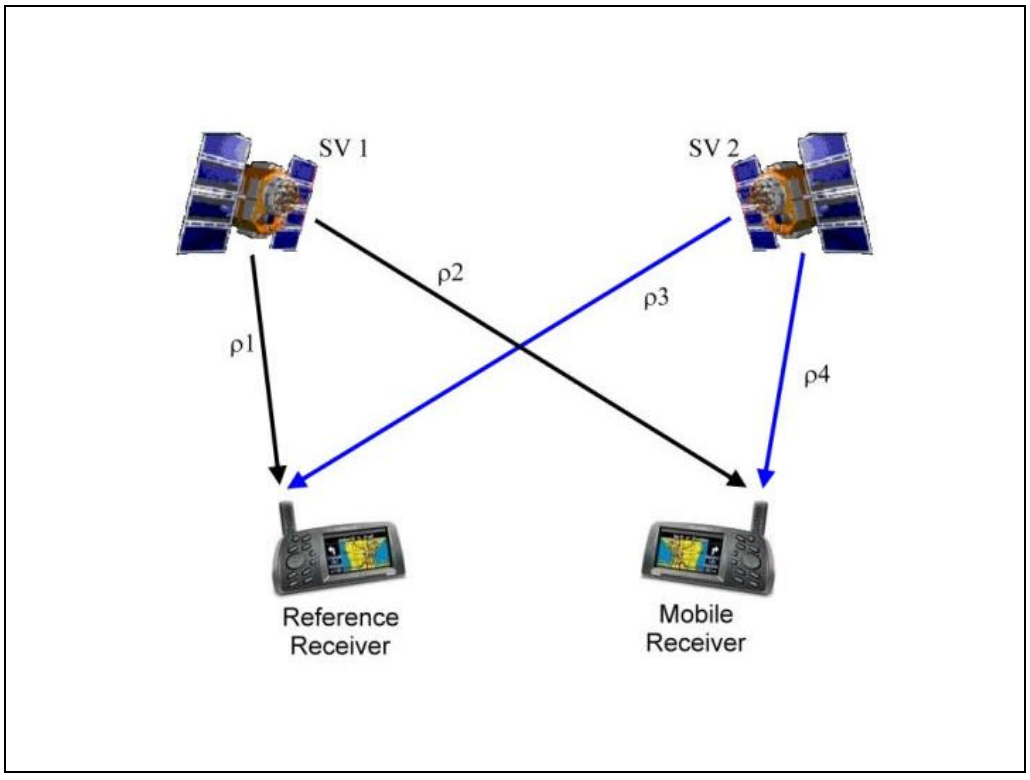

Figure 11. Pseudorange Double Differencing [34]

$$\nabla\Delta r_{12}^{SV1SV2} = \Delta r_{12}^{SV1} - \Delta r_{12}^{SV2}$$

$$= \nabla\Delta r_{12}^{SV1SV2} + c(\nabla\Delta dt_{trop12}^{SV1SV2} + \nabla\Delta dt_{iono12}^{SV1SV2} + \nabla\Delta dt_{noise12}^{SV1SV2} + \nabla\Delta dt_{mp12}^{SV1SV2}) \qquad (5)$$

where

$\Delta\nabla$ = *Double difference DGPS*

$\nabla\Delta r_{12}^{SV1SV2}$ = *Double difference between receivers 1 and 2 and satellite vehicles (SV) 1 and 2*

$\nabla\Delta r_{12}^{SV1SV2}$ = *Double difference of true range to satellites (m)*

c = *Double difference of speed of light (m/s)*

$\nabla\Delta dt_{trop12}^{SV1SV2}$ = *Double difference of tropospheric error (s)*

$\nabla\Delta dt_{iono12}^{SV1SV2}$ = *Double difference of ionospheric error (s)*

$\nabla\Delta dt_{noise12}^{SV1SV2}$ = *Double difference of receiver noise error (s)*

$\nabla\Delta dt_{mp12}^{SV1SV2}$ = *Double difference of multipath error (s)*

DGPS Errors

Although DGPS provides a more accurate solution than a single GPS receiver, it does not completely eliminate all the errors. As stated above in the differencing techniques, the satellite clock and receiver clock errors can be removed, but there are still residual tropospheric and ionospheric errors. As long as the baseline between the two receivers is kept relatively small (within a few hundred kilometers), the signal passes through relatively the same atmosphere, and the correlated errors can be minimized. The uncorrelated errors of multipath and receiver noise are not reduced through DGPS, but are actually amplified.

Attitude Determination

Attitude determination is the ability to determine the angular orientation of a body within a plane [33]. Two gyroscopes mounted with their sensitive axes orthogonal to each other within the plane to determine the angular orientation of the body. As the plane is tilted, the gyroscopes sense the change and produce an output to counter the tilt motion. Measuring the amount of force needed to correct the tilt provides attitude information such as pitch and roll for that plane. To determine a body's attitude in three dimensions requires the use of three gyroscopes mounted orthogonally to each other [25]. The three-dimensional configuration provides pitch, roll, and yaw attitude measurements.

Using a carrier-phase DGPS receiver and antenna system to replace each gyroscope described above allows the carrier-phase DGPS to measure the relative position, which can be used to determine attitude, but the implementation is not as easy as it sounds. Placement of the receiver and antenna systems becomes an issue. Since the space available on a manikin is limited, the size and weight of the receiver and antenna systems changes the ejection properties of the manikin. Limiting the attitude determination to two dimensions versus three reduces the number of receiver and antenna systems required, and still provides valuable measurement information to the engineers. With two receiver and antenna systems to consider, the placement of the antennas becomes critical. Due to the accuracy of the position and velocity measurements previously discussed for carrier-phase DGPS, the antennas must be placed far enough apart to provide good resolution of the attitude [22]. Implementing carrier-phase DGPS to provide attitude information is possible, but antenna placement and planar locations must be carefully examined.

Global Positioning System (GPS) Used for Ejection Seat Test and Evaluation

Captain Brian (Reece) Tredway [34] proposed using a GPS receiver and antenna system capable of handling the high dynamic environment of an ejection sequence. The following sections summarize his research in this area, and provide insight into areas warranting further investigation.

Initial Design Criteria

The first step to solving the augmentation of the position, velocity, and altitude measurements was to select a GPS receiver capable of handling the high dynamics of the ejection environment [3][10][11][34]. After carefully considering the initial design, Captain Tredway selected a receiver, antenna system, and a data logger to meet the operating parameters of the ejection environment. Before moving to his development test program, Captain Tredway had to integrate the three systems into a single package. The package, called the Differential GPS Independent Velocity, Position, and Altitude Collection System (DIVEPACS), was packaged to ensure a proper form fit to the manikin.

DIVEPACS Phase I Testing

Following the integration of the three systems, the next step was to model and simulate the system's performance. The modeling phase required several assumptions concerning the receiver's ability to acquire and track the GPS constellation under heavy gravity loading and high vibrations [10][11][34]. After establishing the model, he simulated flight profiles and various GPS constellation configurations for the receiver. The flight profiles and constellation changes tested the receiver's ability to maintain lock and provide an accurate position solution.

In the simulations, the G12 receiver was able to handle straight line accelerations up to 400 meter per second, and the DGPS RMS for latitude and longitude proved to be under 2 meters. Additional hardware tests profiled the receiver, antenna and data logger's operating characteristics. The system passed all the preliminary criteria, and was ready for Phase II testing.

Phase II Testing

Phase II testing was a natural progression to freefall flight [34]. The freefall flight was an inexpensive but effective way to simulate a portion of the ejection sequence. It tested the DIVEPACS' ability to reliably track and calculate a three-dimensional position and velocity measurement solution, and it provided insight into the system's ability to withstand g-forces during canopy deployment. The results of the freefall proved the DIVEPACS could maintain lock and track the skydiver's position and velocity through several rotations, and withstand the g-force of the initial canopy opening. After analyzing the data collected during the freefalls, the results indicated the system was ready for Phase III testing.

Phase III Testing

Phase III testing incorporated the DIVEPACS into the manikin's survival vest and helmet for an actual ejection sequence [34]. Two attempts were made to collect data at the Hurricane Mesa Test Track (HMTT) in southern Utah. The standard telemetry and photography systems monitored and tracked both ejection sequences, and were used to evaluate the DIVEPACS' performance. Both tests simulated a very high-speed ejection, with over 600 knots equivalent airspeed (KEAS) from an F-15 aircraft [34]. The KEAS value provides an airspeed value

adjusted for the effects of altitude, air pressure, temperature, and wind speed so tests conducted at different locations can be measured against a common standard.

Due to the high speed of the ejection, the first test was not completely successful [34]. As the manikin started its ejection and entered the wind stream, the DIVEPACS and one of the manikin's legs separated from the manikin's torso, and established their own flight paths. Although the DIVEPACS was damaged, it did have some useable data recorded. The DIVEPACS was able to track through the four motor firings of the sled to provide position and velocity measurements, but did not track the position of the manikin during the ejection sequence. After repairing the DIVEPACS and modifying the antenna location on the helmet, Captain Tredway installed it onto the second manikin's survival vest for the next test.

The second test did not fair well for the manikin or the DIVEPACS [34]. Again, as the manikin entered the wind stream, the DIVEPACS separated from the manikin. The second test results were consistent with the first test. The initial sled movement caused the DIVEPACS to lose lock on several satellites, and corrupted the position and velocity measurements.

Although the ejection tests in Phase III were not successful, they did provide insight into areas requiring further study. With some modifications to the DIVEPACS, it may be able to handle the high dynamic environment of the ejection sequence based on the results from the Phase II testing. Also, testing the DIVEPACS at a lower ejection speed, under 450 KEAS, would more accurately simulate a real ejection sequence. In addition to addressing these issues, this research explores the possibility of adding a second receiver, antenna system, and data logger to provide for attitude determination as well as position, velocity, and altitude measurements.

Summary

This chapter presented the basic theory behind the GPS. The first section provided a brief history of why GPS was developed and how the signals are generated. The next section outlined some of the errors associated with estimating a position solution, and it also described various DGPS techniques. The third section discussed attitude determination and why it is important to this research. The final section contained information on previous research conducted to use GPS for ejection seat testing. The next chapter outlines the methodology for expanding the previous research.

III. Methodology

Overview

Chapter 3 presents the Differential GPS Independent Velocity, Position and Attitude Collection System's (DIVEPACS') development and testing methodology. To distinguish the original research from the follow-on research, the term "first generation" will be associated with the original research while the term "second generation" will denote this follow-on research. This chapter describes the different DIVEPACS configurations for each phase of testing, and outlines the type of data collected and analyzed for each testing phase.

DIVEPACS Configuration

The original research established design criteria and assumptions concerning the operating parameters of the DIVEPACS. The follow-on research adapted the design to conform to the type of testing being conducted and to incorporate recommended changes from the original research. Information presented in this chapter concerning first generation DIVEPACS was taken directly from the research completed by Capt Brian (Reece) Tredway [34].

First Generation

The DIVEPACS was designed to fit into the pockets of a standard aircrew survival vest. Figure 12 shows the first generation DIVEPACS configuration.

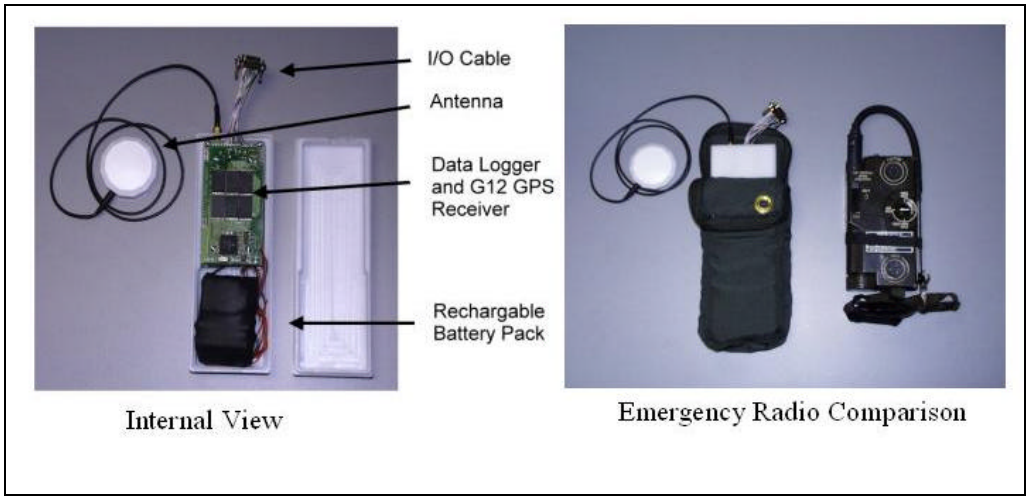

Figure 12. First Generation DIVEPACS Configuration [34]

The components shown are placed on the aircrew survival vest that is worn by the manikin. This configuration keeps the components located close to the center of mass of the manikin. It is important that any bulky items placed on the manikin are positioned symmetrically around the manikin center so that the equipment doesn't cause the manikin to become unstable in flight and tumble when it enters the airstreams [34]. Figure 13 shows the DIVEPACS placed into the manikin's survival vest.

GPS Receiver and Antenna.

In a typical ejection sequence, the ejection components experience accelerations as high as 20g's [34]. In order to handle the high dynamics, the DIVEPACS incorporated the Ashtech® G12 GPS Receiver [9][34]. The G12 is an original equipment manufactured (OEM), 12-channel, single frequency (L1), coarse acquisition (C/A) code and carrier receiver. The receiver offers consistent and reliable tracking with peak acceleration rates greater than 23g's, over 450 g/s of jerk, and vibration levels of 0.1 G^2/Hz.

Figure 13. First Generation DIVEPACS in the Survival Vest [34]

The re-acquisition time is 2 seconds, and the hot start time to first fix is 11 seconds. The G12 can output National Marine Electronics Association (NMEA) messages, Ashtech® proprietary messages, and raw measurements [9][34]. The DIVEPACS G12 is limited to a 20 Hz sampling rate, but based on the test data from previous ejections, a 20 Hz sample rate should be adequate to determine the manikin's position and velocity [34]. In addition, when the G12 sample rate is set to either 10 or 20 Hz, only 8 satellites are used to calculate a position solution [34]. Appendix A shows the schematic for the first generation DIVEPACS.

One of the design constraints on the system was that it was small enough to fit into the pockets of the survival vest shown in Figure 12. The size of the G12 is 108 mm x 58.4 mm. It weights 2.8 ounces and has a power consumption of 2.1 Watts including the power applied to the antenna. The antenna is external from the receiver and is located on top of the helmet shown in Figure 13. The manikin will wear a standard Air Force issue aircrew helmet, with the antenna located inside the plastic shell toward the front of the helmet. With the antenna placed inside the

helmet shell, the antenna may not be able to acquire all the satellites in view due to shielding effect of the helmet. A typical aircrew helmet and ejection harness is shown in Figure 14 [34].

Figure 14. Aircrew Member in an Ejection Seat [34]

Data Logger.

All the data collected from the DIVEPACS GPS receiver was stored in an H.O. Data Compu-Log RS-12DD data logger for post processing [13][34]. The data logger was designed to collect and store the output from any RS-232 source at a rate of up to 115,000 bits per second (bps). A separate 9-volt battery powers the data logger. The data was placed into non-volatile memory, so it was protected in the event of power loss. Due to the high dynamics, the original container and input/output (I/O) connections were replaced with a ruggedized container and connectors prior to the start of actual ejection tests [34].

Post-Processing Software.

After test completion, the data was downloaded from the data logger and reference receiver, and the files processed using MATLAB® and Ashtech® software loaded on a desktop PC or laptop [32][34][39]. At this point, the files could be processed separately to provide a stand-alone GPS position, velocity, and attitude solution from the data logger, or the files could be synchronized and processed together for a more accurate differential position, velocity, and attitude solution. The method of differential correction dictates the accuracy level of the solution. The three types of differential correction methods are code-corrected, carrier-smoothed code, and carrier-phase differential, see Chapter 2 for more details. Carrier-phase differential is the most accurate [34].

Second Generation

The second generation of DIVEPACS incorporated two Ashtech® G12 GPS receivers and two H. O. Data Compu-Log RS12-DD data loggers into one package [9][13][34]. The new single package was still required to meet the size constraints listed above. Figure 15 shows the dual DIVEPACS configuration, and its schematic is contained in Appendix B.

Since two antennas must be mounted on the manikin, the Sarantel GeoHelix-H antenna replaced the Antenna Technologies Inc antenna for a better form fit, see Appendix E for antenna specifications [30][34]. Although the Sarantel GeoHelix-H has a lower overall gain specification, the difference in mounting placement should compensate for it. The original antenna was mounted inside the helmet during an ejection to prevent it from separating from the manikin as it entered the windstream. This antenna placement caused shielding and impacted the antenna's reception capability. To provide a large enough distance separation between the two Sarantel GeoHelix antennas for attitude determination, the new antennas would be attached on

each shoulder without any obstructions, and the antenna cables were to be secured under the harness and survival vest. Figure 16 depicts the size difference between the two antennas.

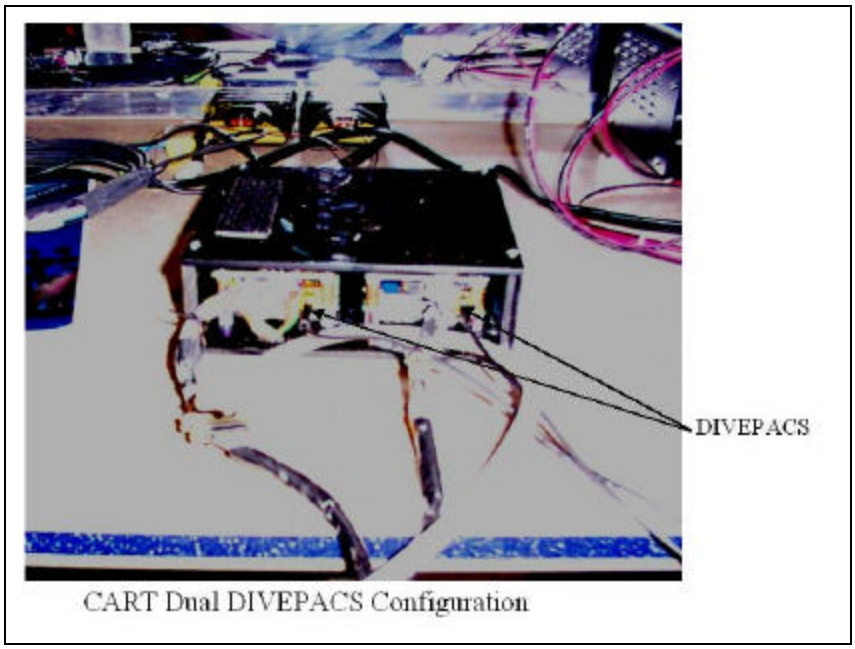

Figure 15. Dual DIVEPACS Configuration [34]

Figure 16. Antenna Comparison [34]

In addition to the hardware changes, modifications to the differential functions in MATLAB® were needed to improve the carrier-phase integer ambiguity resolution [32]. Through the use of several algorithms, the functions would be more robust, and would be able to handle cycle slips in the data easier.

Phase I Testing

The testing process for both generations of DIVEPACS used a phased approach. Each phase had exit criteria established, and gradually expanded the operating envelope of the DIVEPACS. When possible, only one part of the DIVEPACS' configuration was changed in each phase to isolate and validate its performance for the second generation testing.

First Generation

Phase I testing integrated the receiver and data logger into a single package and bench tested them using different satellite configurations. One of the most challenging aspects of this phase was developing a hardened case able to withstand 15g's and ensure the data logger was able to retain the data even if the I/O cables were damaged and the battery disconnected.

Second Generation

This phase consists of repackaging the two DIVEPACS into a single unit. By mounting the two antennas within the same plane, a two-dimensional attitude determination could be made, provided the resolution for differential GPS solution was high enough. In addition to modifying the differential MATLAB® code, a minimum separation baseline for the antennas had to be established and tested. As part of this testing phase, the single unit dual DIVEPACS was mounted into a Barber Dodge Championship Auto Racing Team (CART) car with one antenna

mounted on the front of the car and the second antenna mounted on the rear of the car. Data was collected as the car qualified for an upcoming race to observe the car's yawing as it traversed the course. Figures 17 and 18 show the placement of the DIVEPACS and antennas on the CART car.

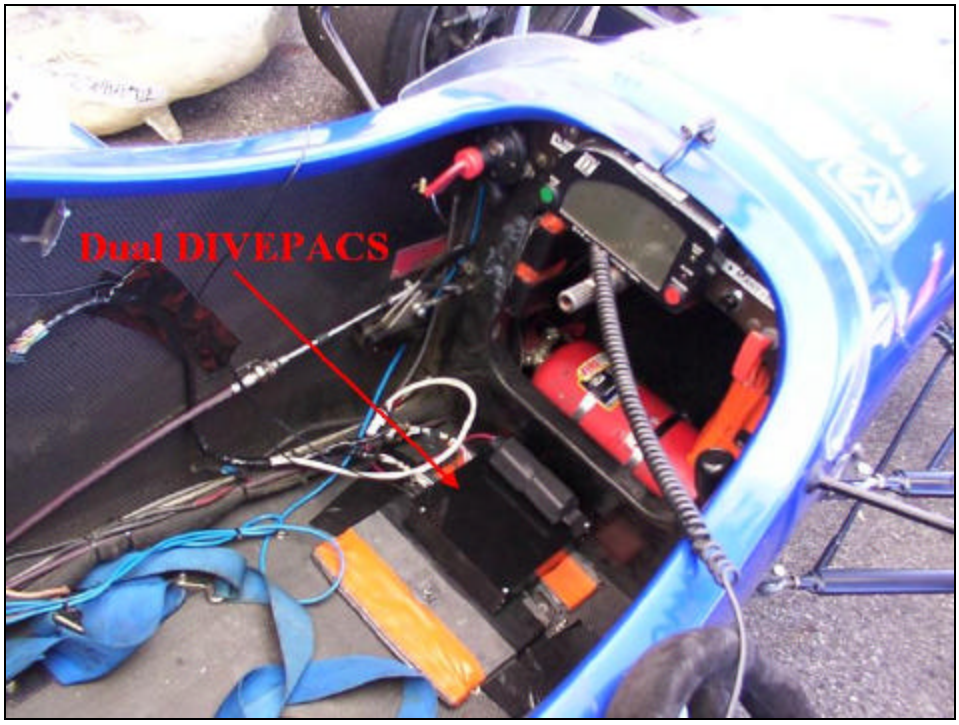

Figure 17. CART DIVEPACS Placement

Figure 18. CART Antenna Placement

Phase II Testing

First Generation

Phase II testing was the first step in validating the DIVEPACS ability to track enough satellites to calculate a three-dimensional position and velocity solution in a medium dynamic environment. The DIVEPACS was configured for freefall flight. Figure 19 shows the DIVEPACS freefall configuration [34].

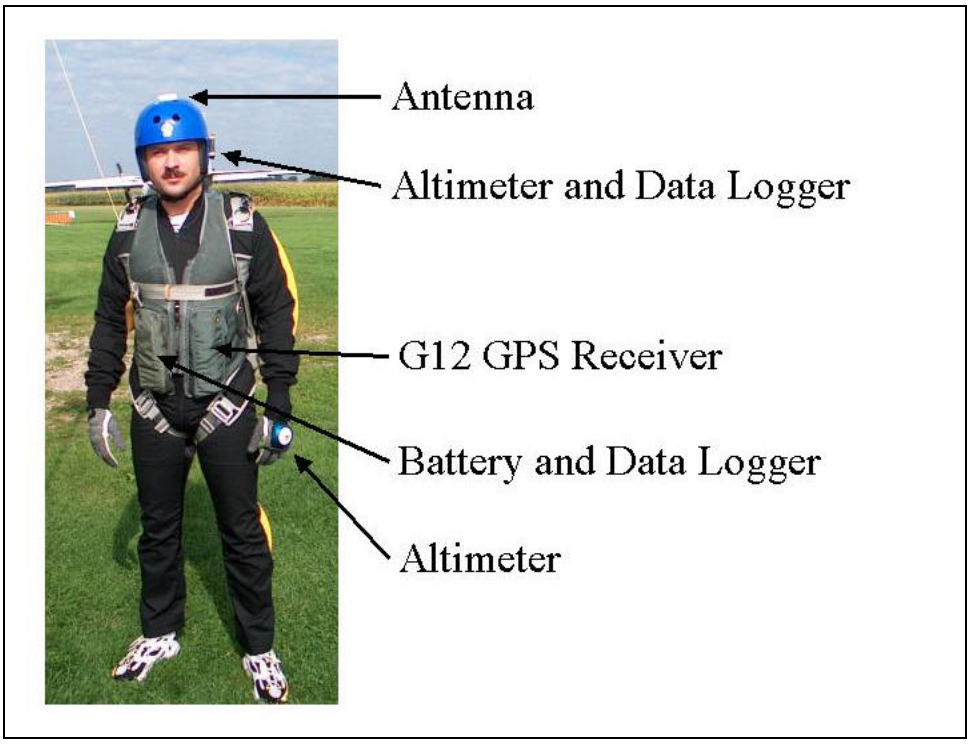

Figure 19. DIVEPACS Freefall Configuration [34]

Freefall flight simulates a portion of the manikin's natural flight profile during an ejection sequence. Although the maximum velocity and acceleration experienced during a freefall don't match those of an actual ejection seat test prior to the parachute opening, they are very similar after the parachute has been deployed. The freefall tests provided a low cost test alternative to evaluate the DIVEPACS performance in a medium dynamic environment [34].

Second Generation

Second generation phase II testing was a follow-on to the freefall testing, and had two parts. The first part expands on the initial freefall tests. In the previous tests, a human subject completed the freefall, and he was able to keep the GPS antenna oriented toward the sky, minimizing the loss of lock. For the second generation phase II testing, one DIVEPACS was mounted internally to a manikin, and the manikin was pushed from an aircraft on a static line.

The natural tumbling and rotations of the manikin before its parachute deployed helped characterize the rotating motion of the manikin in a freefall state and the system's ability to maintain lock through the rotations. Figure 20 shows the deployment configuration for the manikin.

The second part of this phase uses the dual DIVEPACS configuration for attitude determination. Once the minimum separation of the antennas can be validated, the dual DIVEPACS will be mounted into a survival vest similar to that used in the previous freefall testing with the use of two antennas. One antenna will be mounted on each shoulder of the parachutist.

Figure 20. DIVEPACS Manikin Deployment

Phase III Testing

First Generation

The last phase of testing consisted of configuring the DIVEPACS for placement onto a manikin for an actual ejection seat test. The manikin's survival vest radio pocket held the DIVEPACS, and the antenna was mounted inside the manikin's aircrew helmet. To provide a differential GPS solution, a reference station was established within 5 km of the sled track [34].

Second Generation

Second generation phase III testing consists of placing the dual DIVEPACS on a manikin for an actual ejection seat test. Due to the cost and limited availability of these tests, the data collected from the second generation phases I and II will be used as the primary data source for analysis.

DGPS Reference Station

For each phase of testing, a DGPS reference station was established for the first generation testing, and the requirement for a DGPS reference station for second generation testing was unchanged. The first generation testing used an Ashtech® Z-Surveyor system for its DGPS reference station, and the same system was used for all the second generation testing [34][39].

Summary

This chapter presented the different phases of testing and described the differences between the first generation DIVEPACS and second generation DIVEPACS. The next chapter presents the results and analysis of the three testing phases described in Chapter 3.

IV. Results and Analysis

Overview

This chapter presents the results and analysis from each phase of testing outlined in Chapter 3. The first part of this chapter discusses the dual DIVEPACS used for the Championship Auto Racing Team (CART) cars during Phase I. Next, the Phase II results from the canopy testing are discussed and analyzed. Finally, the chapter presents the Phase III results from the actual ejection seat test and sled track testing.

Phase I Testing

Dual DIVEPACS Stand-alone Results

As outlined in Chapter 3, the purpose of this phase was to place both DIVEPACS into a single package, and then mount the antennas on a single plane on the CART car as shown in Figures 17 and 18. The actual testing was conducted at the Mid-Ohio Race Track located approximately 13 miles southwest of Mansfield, Ohio on the 8th and 9th of August 2002. Figure 21 is an aerial photograph of the track [23][38]. As noted in the photograph, the track has three covered bridges that obstruct the sky view for the GPS antennas. In addition to the bridge obstructions, the east side of the track had large trees shadowing the course. Also, the location for the Ashtech® Z-Surveyor base station used for post-processing differential GPS is noted on the photograph.

For the qualification runs conducted on August 8, 2002, both of the DIVEPACS' receivers were set at 1 Hz sampling rate, and the POS and GGA National Marine Electronics Association (NMEA) messages were logged. Figure 22 is the stand-alone position solution for both

Figure 21. Mid-Ohio Race Track Aerial Photo [38][23]

DIVEPACS. The three breaks in the track coincide with the three bridges shown in Figure 21. The dual trace at the lower right corner of the track denotes the track's entrance into pit row. The small broken loop under the straight-away and pit row area is the entry point, on the right, and the exit point, on the left, for the cars to access the track from the maintenance area.

Despite the dropouts from the bridge coverage, the DIVEPACS provided an accurate representation of the car's course around the track. Due to the DIVEPACS' reacquisition time and the car's velocity when it passes under the bridge, the width of the outages appears much

larger than the actual width of the bridges shown in the aerial photograph. The reacquisition time for the first bridge located to the left of pit row varied between 4 to 6 seconds, and the average speed was 85 miles per hour (mph). The second bridge located at the top of the plot had a reacquisition time of 5 seconds, and the average speed for this portion of the track was 73 mph per hour. The third bridge located to the right of pit row had the largest variation for reacquisition time. The reacquisition time varied from 4 to 7 seconds. The average speed at this point around the track was 90 mph. The large reacquisition time from the third bridge is not as noticeable in the 1 Hz data as it is in the 20 Hz data that was collected on August 9, 2002. More information concerning the reacquisition time is discussed further in the following section.

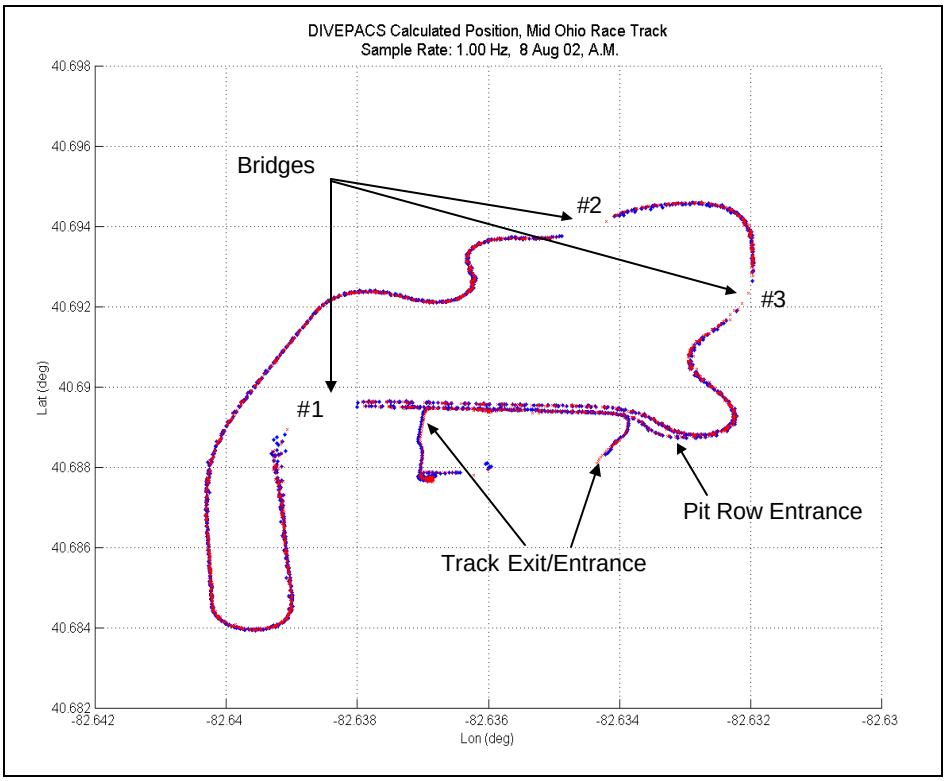

Figure 22. Mid-Ohio DIVEPACS 1 Hz Sampling Rate

On August 9, 2002, the DIVEPACS sampling rate was changed to 20 Hz, but the NMEA messages remained the same. Figure 23 represents a single DIVEPACS stand-alone position

solution for multiple laps around the track at the 20 Hz sampling rate. Although dual DIVEPACS were used for this test, one of the DIVEPACS experienced problems with its data logger, and did not capture the event.

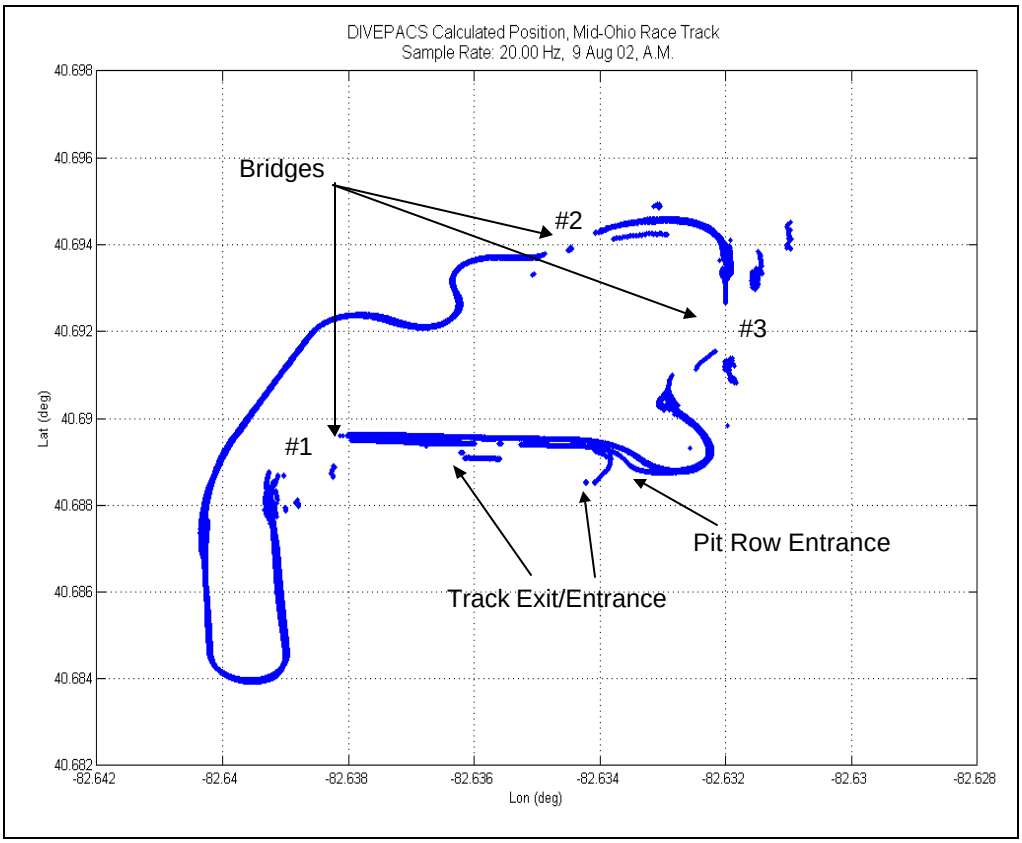

Figure 23. Mid-Ohio DIVEPACS 20 Hz Sampling Rate

At the higher sampling rate the bridge outages are more pronounced. Due to the higher sampling rate, variations in the number of satellites being tracked were much higher than with the 1 Hz rate. This could be attributed to the way the DIVEPACS' receivers calculate a position solution at the 20 Hz sampling rate. At this rate, the receivers internally select and use the best eight satellites in view to calculate the position solution [9]. As the number of satellites being tracked decreased, the DOP for the position solution increased, causing larger errors in the position solution. This effect can be seen in Figure 23 at each of the outages caused by the

bridges. The large cluster of data points to the right of the third bridge is not a set of stray data points, but an example of the position solution based on a large DOP value. Figure 24 represents the ground speed, the number of satellites being tracked, and the position DOP for the first lap of the qualification run, and helps to illustrate the effects of DOP on the position solution.

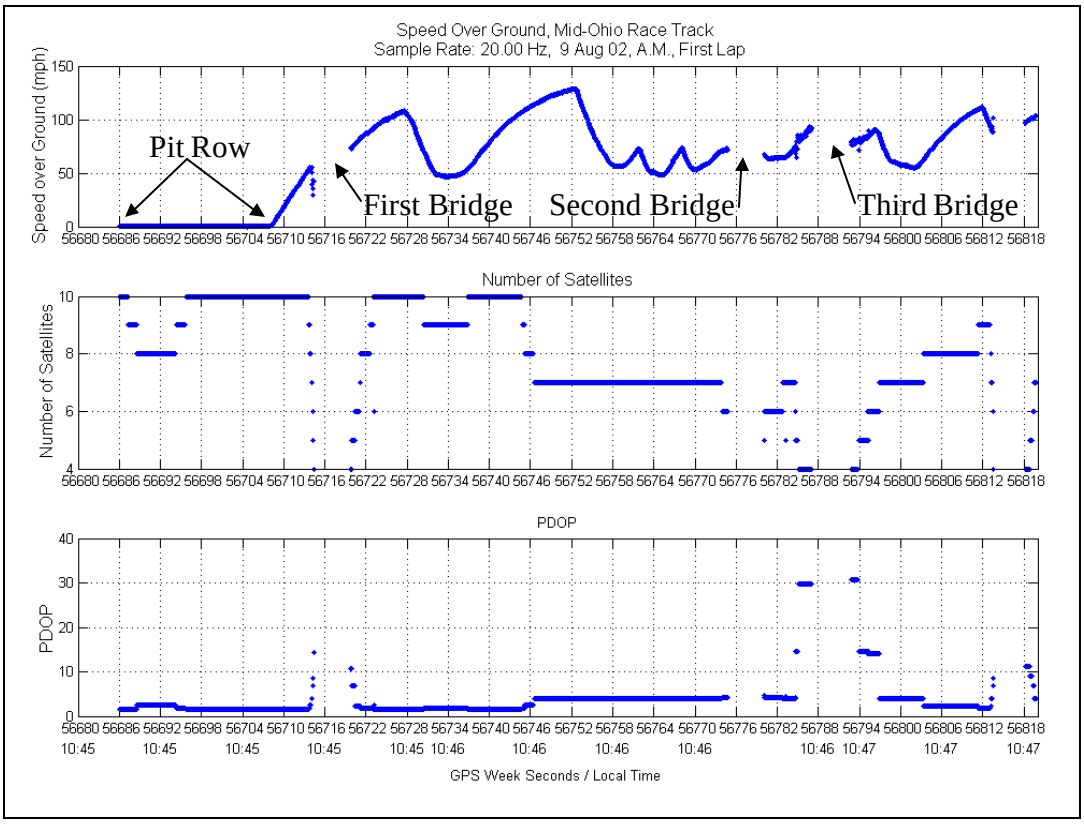

Figure 24. Effects of Ground Speed, Number of Satellites Tracked, and PDOP

While the car was sitting in pit row, the number of satellites being tracked dropped from 10 to 8 due to maintenance personnel masking the antennas. As the car accelerated out of pit row and entered the track, it encountered the first bridge where the number of satellites being tracked decreased dramatically and the position DOP increased. After 5 seconds, the DIVEPACS reacquired enough satellites to provide a position solution. As the car accelerated through the straightaway, the DIVEPACS were able to regain tracking on 10 satellites again. While

cornering through the 180-degree turn, a satellite was dropped due to its low elevation angle and its relative position to the car's antenna. As the car accelerated through the back straightaway, the number of satellites being tracked dropped from 10 to 7 due to masking from the grand stands and tree growth on the northwest side of the track. After completing the s-turns, the car encountered the second bridge, and the DIVEPACS could not maintain lock on the satellites. The DIVEPACS reacquired satellite tracking after 4 seconds, and it was able to track 7 satellites again before encountering the third bridge. In addition to the bridge on this side of the track, the large overgrowth of the trees caused the reacquisition time to be longer than the two previous outages. Although the DIVEPACS was able to reacquire 7 satellites, the geometry of the satellites being tracked caused the position DOP to be extremely large for this portion of the track, and the effects of the large position DOP were noted in Figure 23.

Dual DIVEPACS DGPS Results

Although a reference station was established to calculate the DGPS solution for each DIVEPACS, the raw data messages required for the calculation were missed in the DIVEPACS setup and thus not recorded at testing time. Technical difficulties with the equipment caused the error with the DIVEPACS setup. Unfortunately no DGPS data could be extracted from this round of testing. Differencing the dual DIVEPACS receiver positions could be used to determine a rough attitude, particularly if the two receivers are tracking the same set of satellites.

Phase II Testing

Single DIVEPACS Stand-alone Results

Phase II testing for the second generation DIVEPACS was designed to expand on the freefall testing completed for the first generation DIVEPACS as outlined in Chapter 3. The testing was conducted at the Skydive Carolina Parachute Center in Chester, South Carolina on August 20 and 21, 2002. A manikin similar in size and weight to ones used for ejection seat testing was placed into the aircraft. Once the aircraft climbed to the predetermined altitude, it would circle the airfield until the DIVEPACS indicated a minimum of five satellites were being tracked. At that time, the manikin would be pushed from the aircraft using a static line to deploy its parachute, and allow it to glide into the drop zone. A maximum of four drops were allocated for this phase of testing.

Before testing could begin, the manikins had to be configured to place the DIVEPACS inside the chest cavity, and the GPS antennas had to be secured to them. Initially two different antenna configurations were used to test the Sarantel GeoHelix's antenna placement, and evaluate its performance against the Antenna Technology's placement in the first generation testing [30][34]. Figure 25 shows the different antennas and their placement on each manikin.

After configuring the manikins, they were loaded into the aircraft and positioned to simulate a military static line drop configuration. The manikin's body position as it exits the aircraft factors into the amount of tumbling it encounters as it enters the windstream. Figure 26 shows the initial seated position of the manikin. Due to the interference from the aircraft's wing and fuselage, the GPS antenna did not have a clear sky view, therefore the DIVEPACS could not meet the satellite tracking criteria for this phase of testing. The arm-mounted antenna encountered the same interference and also could not be used in the seated position.

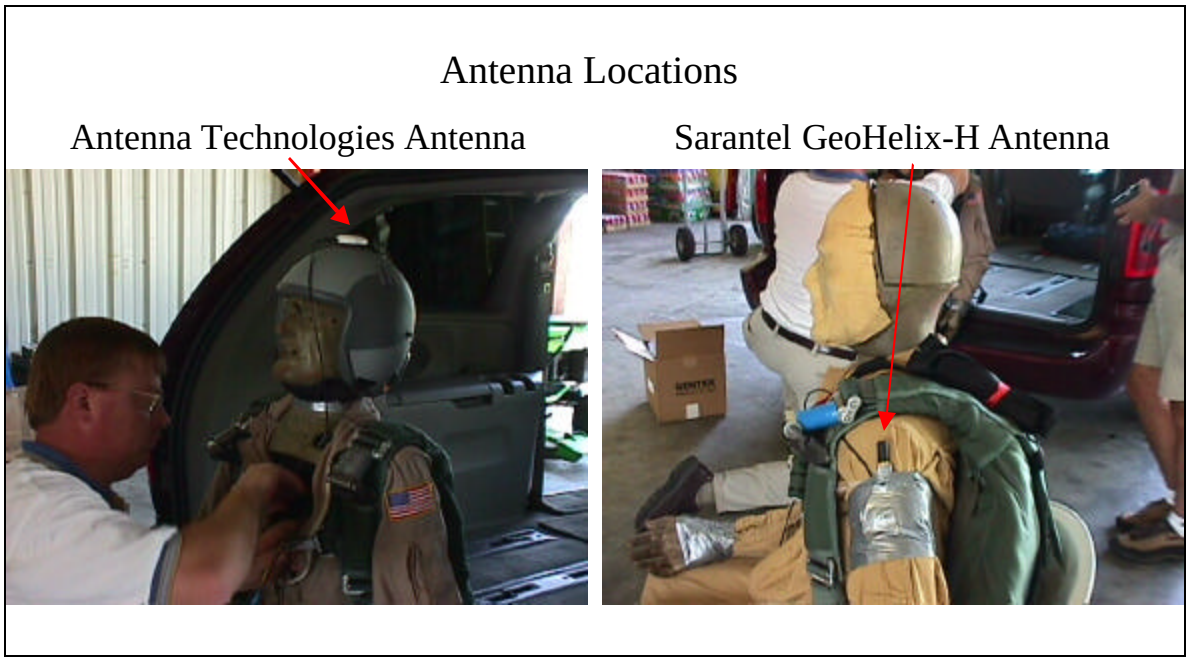

Figure 25. Antenna Placement

Figure 26. Manikin in Seated Position

Figure 27 depicts how the manikin was repositioned to allow the DIVEPACS to acquire and track the minimum number of satellites for the test. After repositioning the manikin, the first drop was attempted. The aircraft climbed to the designated altitude, and once the minimum number of satellites was being tracked, the tether holding the manikin in place was cut. Figure 28 is a three-dimensional view of the aircraft's climb, circling maneuvers to acquire the appropriate number of satellites, the manikin's exit from the aircraft, and its descent once it was under a full canopy. Figure 29 plots the latitude, longitude, and altitude components for the first drop. The first loss of data in the plots denotes the manikin's exit from the aircraft, and second data loss denotes the manikin's landing.

Figure 27. Manikin Repositioned

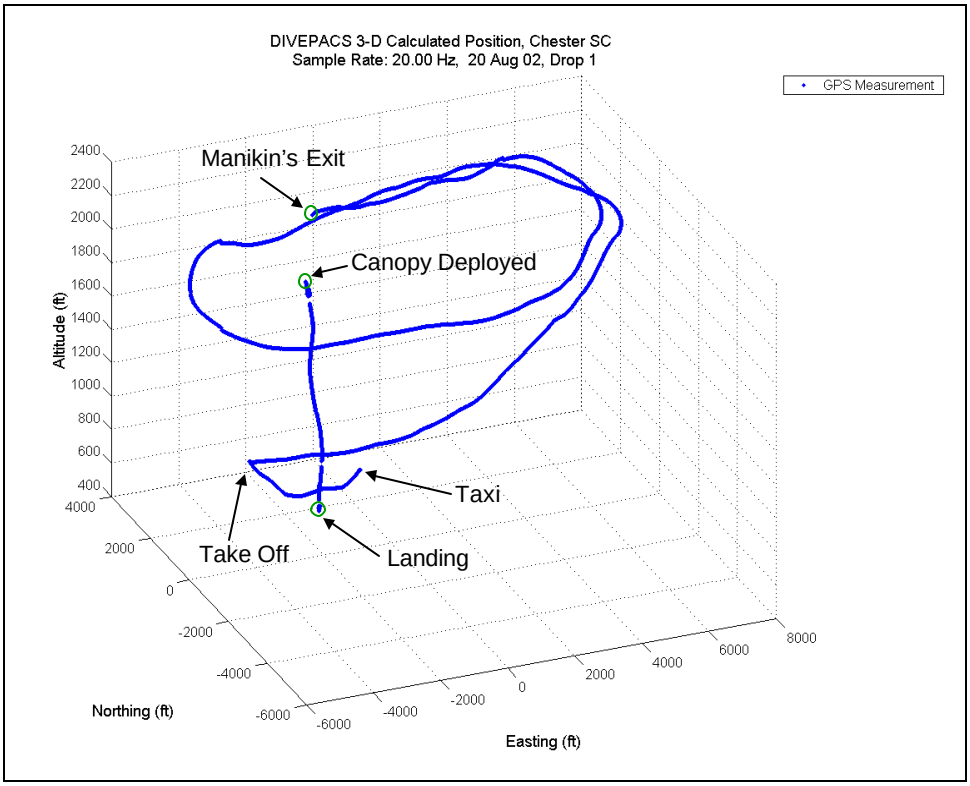

Figure 28. Manikin Drop 1 Three-dimensional View

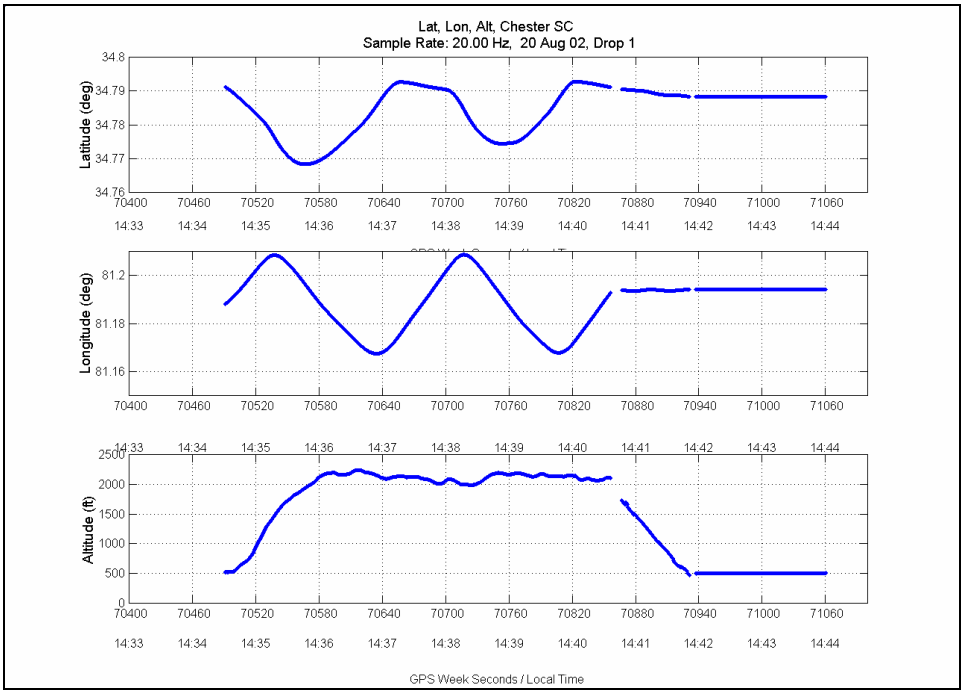

Figure 29. Manikin Drop 1 Latitude, Longitude and Altitude View

When the tether was cut, the manikin fell backwards into the windstream and tumbled several times. The DIVEPACS lost lock for approximately 10 seconds until the pilot chute deployed enough to stabilize the manikin's rotation. During this time the manikin fell approximately 350 ft before the DIVEPACS could reacquire enough satellites to provide a position and velocity solution. Figure 30 shows the loss of lock and altitude loss encounter for the first drop. One of the critical parameters of the canopy testing is the descent rate of the manikin as it exits the aircraft and its descent rate just prior to the canopy opening. The DIVEPACS loss of lock time needed to be minimized. After reviewing the videos from the first three drops and discussing the issue with the jumpmaster, a different drop method was planned for the last drop. Following trial runs with the manikin's departure from the aircraft on the ground, the manikin was reloaded into the aircraft for the fourth drop. The loss of lock time was reduced in the last drop, but was not eliminated.

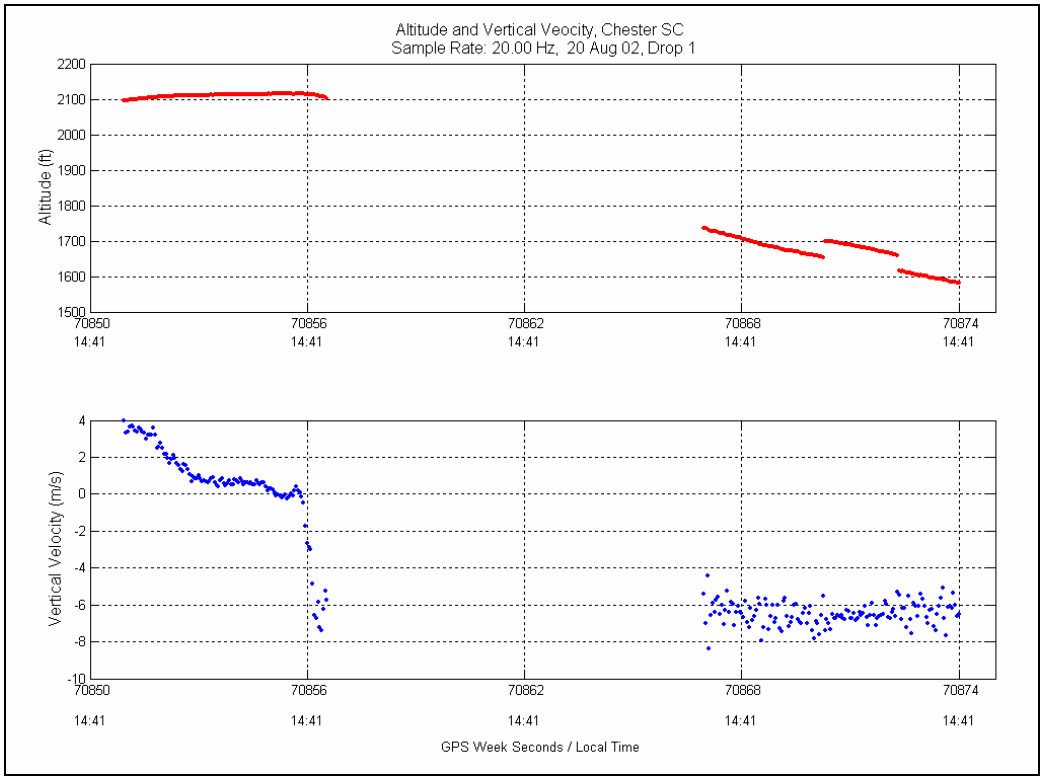

Figure 30. Altitude Loss Drop 1

For the fourth drop, the manikin's feet were placed outside the aircraft before the tether was cut. This allowed the manikin to maintain a more heads-up attitude initially in the windstream. Although it still tumbled significantly, the loss of lock time was reduced to approximately 6 seconds with an altitude loss of approximately 250 ft. Figure 31 is a three-dimensional view of the aircraft's climb, circling maneuvers to acquire the appropriate number of satellites, the manikin's exit from the aircraft, and its descent once it was under a full canopy. Figure 32 plots the latitude, longitude, and altitude components for the fourth drop, and Figure 33 shows the loss of lock and altitude loss encounter for the fourth drop.

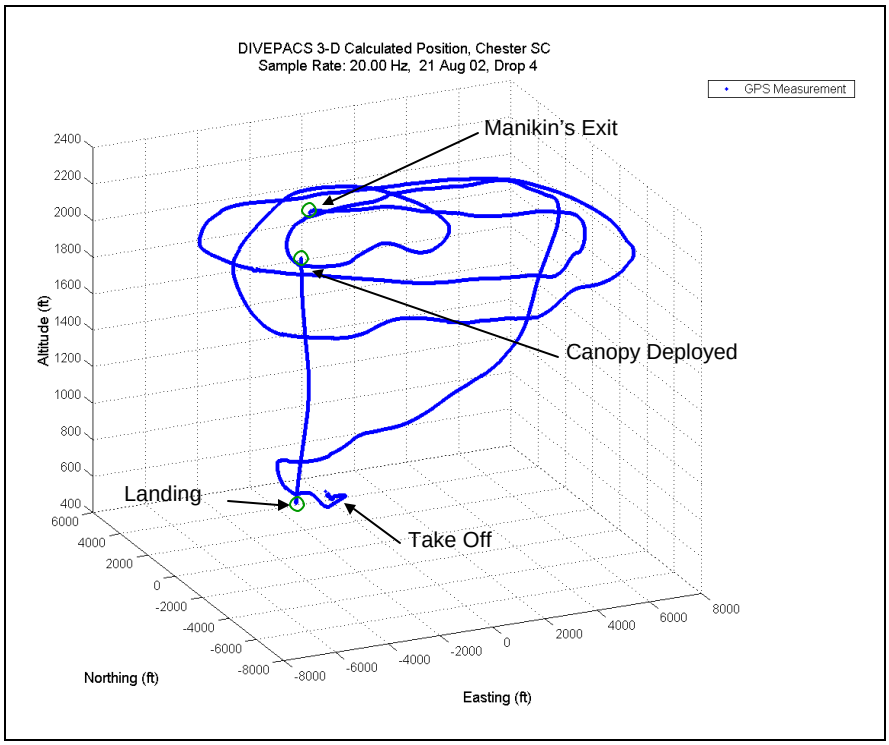

Figure 31. Manikin Drop 4 Three-dimensional View

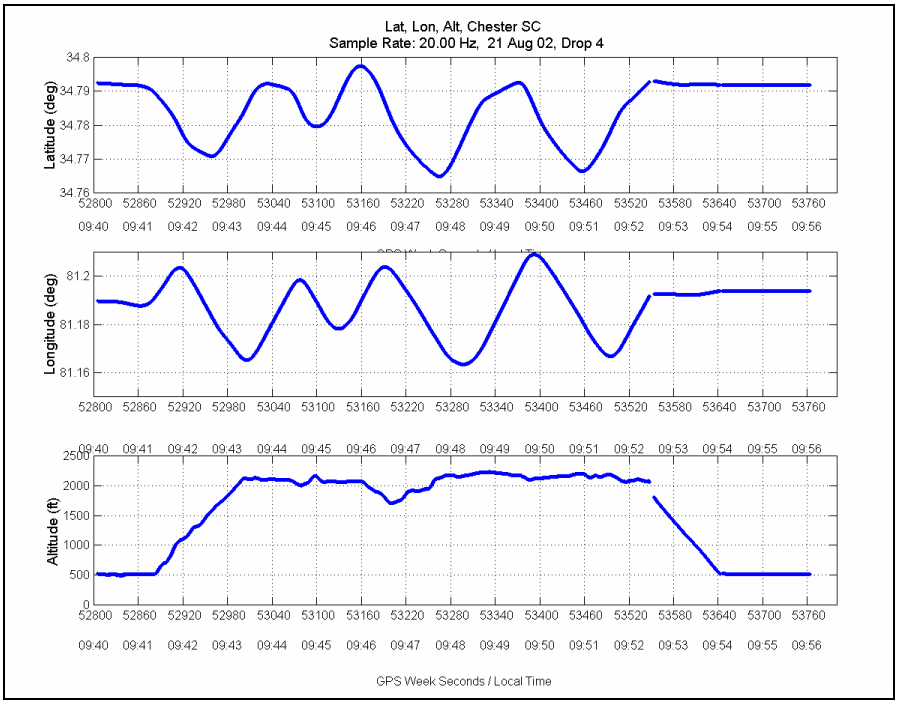

Figure 32. Manikin Drop 4 Latitude, Longitude and Altitude View

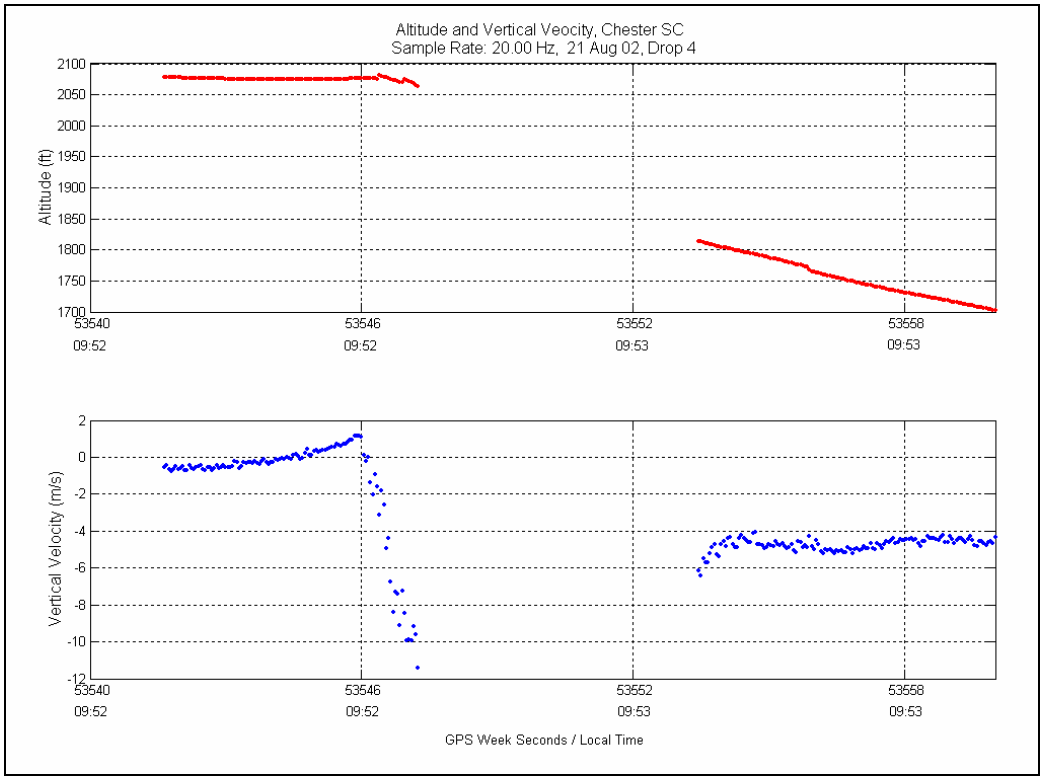

Figure 33. Altitude Loss Drop 4

Phase III Testing

Based on the results and recommendations from the first generation testing, the Phase III testing for this research was broken into two parts. The first part involved validating the single DIVEPACS ability to withstand a lower velocity ejection sequence and maintain satellite tracking to provide a position and velocity solution for the manikin through the entire ejection seat sequence. This testing was conducted at China Lake Naval Air Warfare Center (NAWC) in Ridgecrest, CA. The second part incorporated the dual DIVEPACS configuration to establish attitude determination for the ejection sequence. This testing was conducted at the Hurricane Mesa Test Track (HMTT) near LaVerkin, Utah.

China Lake Ejection Seat Test

The ejection seat test at China Lake was designed primarily to test the neck loads produced by the Joint Helmet Mounted Cueing System and new survival gear for the U. S. Navy. The test was conducted on September 11, 2002 using a Hybrid III manikin placed in an F-18C ejection seat system. The target velocity for the test was 450 KEAS.

Since the DIVEPACS testing was added on a non-interference basis, minor changes in the DIVEPACS configuration were made in regard to the DIVEPACS power control circuitry, the type of antenna used, and its placement on the manikin. The power control circuitry modification enabled the DIVEPACS to be activated remotely through a 500 ft ethernet cable if needed (see Appendix A for the schematic). Due to the sequence of events at test time, the ethernet cable was not used. The system was activated on the manikin approximately 10 minutes prior to the rocket motor firing. Due to the neck-loading test, the antenna could not be mounted inside the helmet, and had to be mounted on the manikin's body. To avoid interference with the harness or other equipment, the best placement for the antenna was on the manikin's left arm. Since the Sarantel GeoHelix-H antenna was more suited for this orientation, it was used instead of the Advanced Technology antenna used with the first generation DIVEPACS. In Figure 34 the picture on the left shows the antenna's placement on the manikin's arm, and the picture on the right shows the DIVEPACS in the survival vest pocket.

As with all previous testing, a reference station was established at the site using the Ashtech® Z-Surveyor [39]. The base station was placed approximately 150 ft west and 200 ft north of the sled's starting point.

Figure 34. China Lake DIVEPACS Configuration

The results from the first generation testing indicated that the DIVEPACS needed 5 to 10 minutes to acquire and track the greatest number of satellites visible for its location. Based on that recommendation, the test review board scheduled the DIVEPACS to be turned on approximately 10 minutes prior to the rocket motor firing. Unfortunately, the data logger within the DIVEPACS malfunctioned after collecting data for approximately 10.5 minutes, and did not capture the entire ejection sequence. From the telemetry data collected, it appears the data logger malfunctioned just prior to the rocket motor firing. Figure 35 shows the maximum number of satellites the DIVEPACS collected and ground speed prior to the malfunction.

Although the DIVEPACS did not record the ejection sequence, it remained attached to the manikin through the lower speed ejection, which was a significant improvement from the first generation testing. Figure 36 depicts the China Lake track layout and the position of the manikin, its body parts, and the seat following the ejection [16].

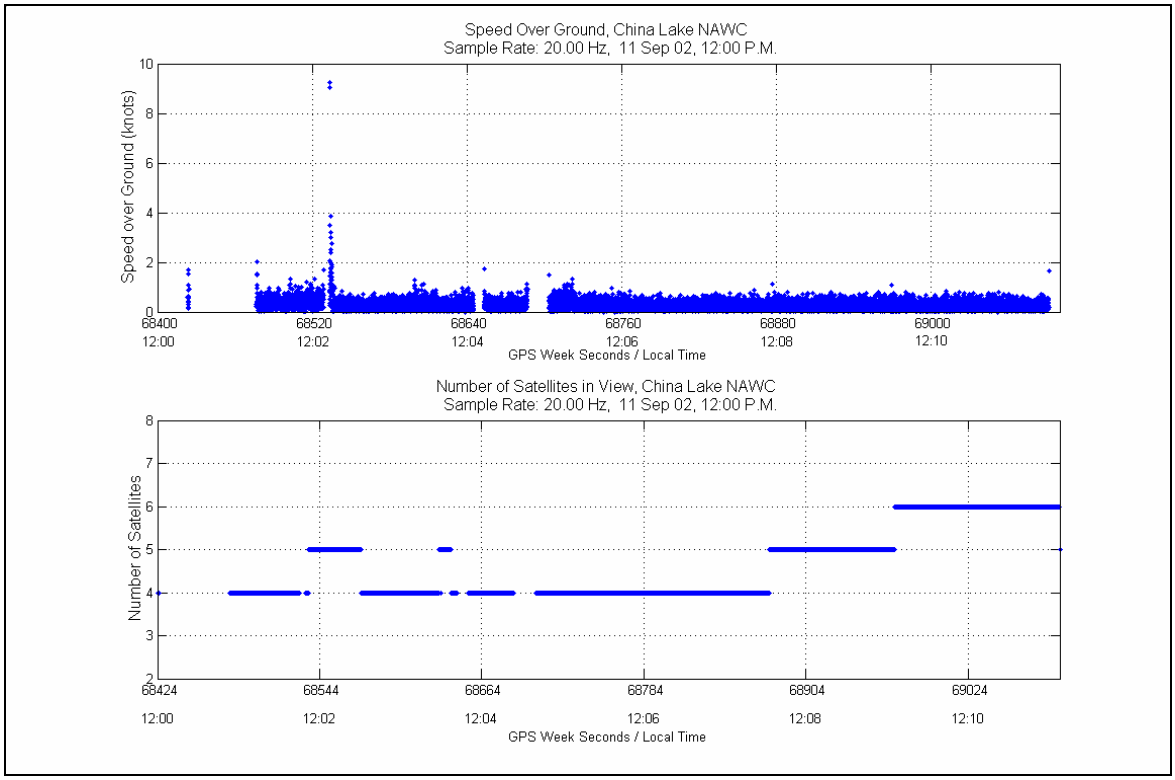

Figure 35. China Lake Data

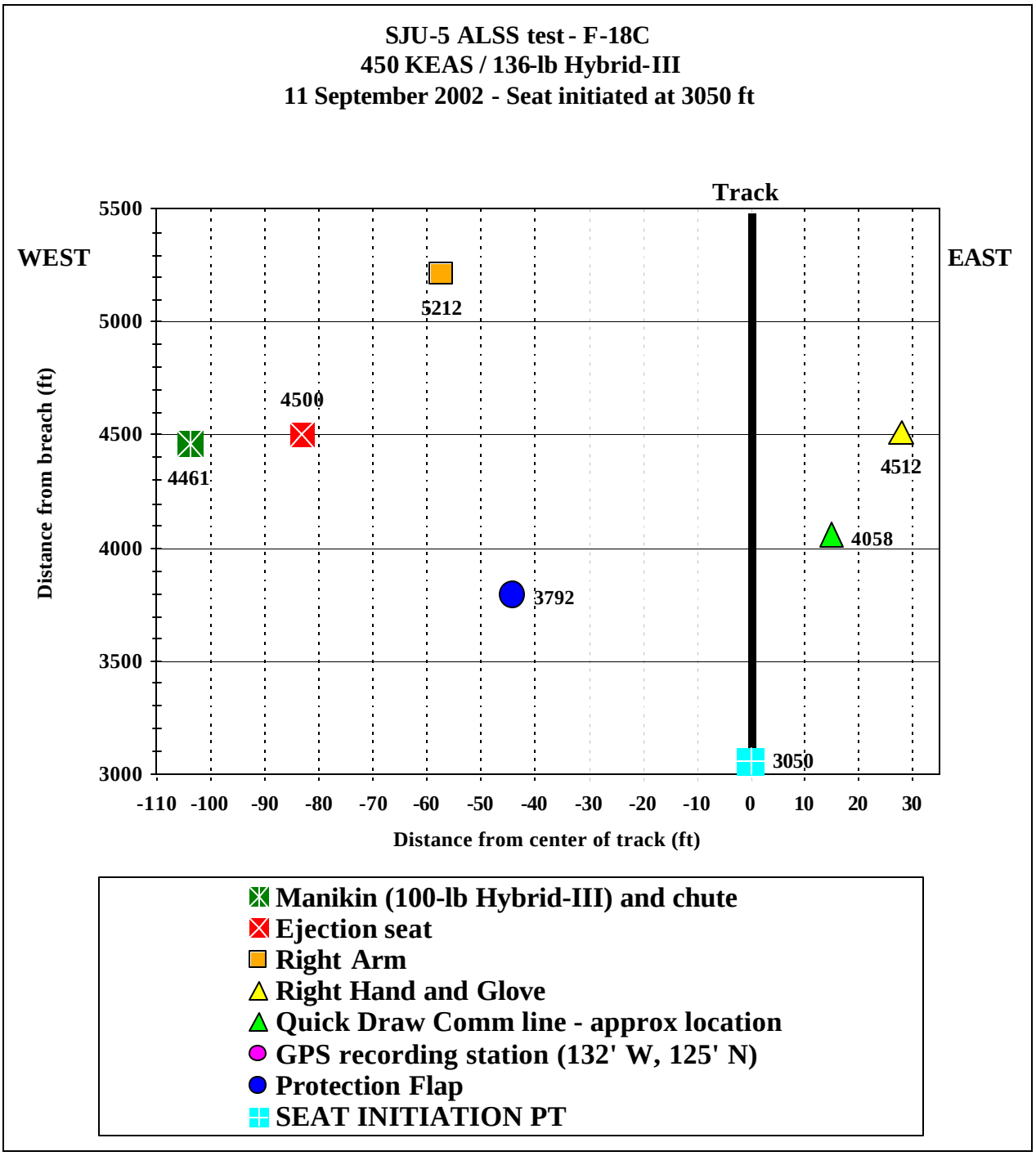

Figure 36. China Lake Track Layout

Hurricane Mesa Sled Track Test

For this part of the Phase III testing, two single DIVEPACS were mounted on an aircraft fore-body to investigate the system's ability to provide attitude determination for a sled track test. The test was conducted on November 21, 2002 using the F-15 sled body with a projected velocity of 600 KEAS; see Appendix D for the test flash report containing all the meteorological conditions.

The two single DIVEPACS were configured to log the same NMEA messages, but not at the same sampling rate. Due to previous problems with the data logger at China Lake, that DIVEPACS' sampling rate was reduced to 10 Hz to extend the logging time and hopefully capture the entire event. In addition to the different sampling rates, the DIVEPACS with the 10 Hz sampling rate used a Mighty Mouse II 28 dB antenna, and the other DIVEPACS used a SM 66 30 dB antenna (see Appendix E for antennas specifications) [4][36]. Although identical test equipment was preferred, the intermittent problem with the data logger forced the change in the sampling rate, and the different antennas were used to investigate the increased gain requirement from the previous research. The known good DIVEPACS was given the higher gain antenna to provide the best opportunity of ensuring some data was collected from the test.

The DIVEPACS were placed inside the aft portion of the sled body with foam packing surrounding them to help reduce the vibrations from the motor firings. The antennas were mounted on the aft portion of the sled for maximum separation, 19.5 inches on centers. The antenna separation distance was to be used for the heading and distance baseline for post-processing differential GPS. Figure 37 shows the DIVEPACS mountings for the sled test. The lower sampling rate DIVEPACS is located on the left side of the sled.

Figure 37. HMTT DIVEPACS Mounting

As in the China lake test, the DIVEPACS contained power control relays to allow for remote activation. The DIVEPACS were turned on 8 minutes prior to the rocket motors being fired to allow sufficient time for them to acquire the maximum number of satellites visible. Within 30 seconds after the rocket motors are fired, the entire event was complete. Figure 38 shows the ground speed and the number of satellites being tracked for the 10 Hz sampling rate, and Figure 39 depicts the 20 Hz sampling rate. Although the slower sampling rate did allow the data logger to remain active throughout the test, it could not track the dynamics of the test.

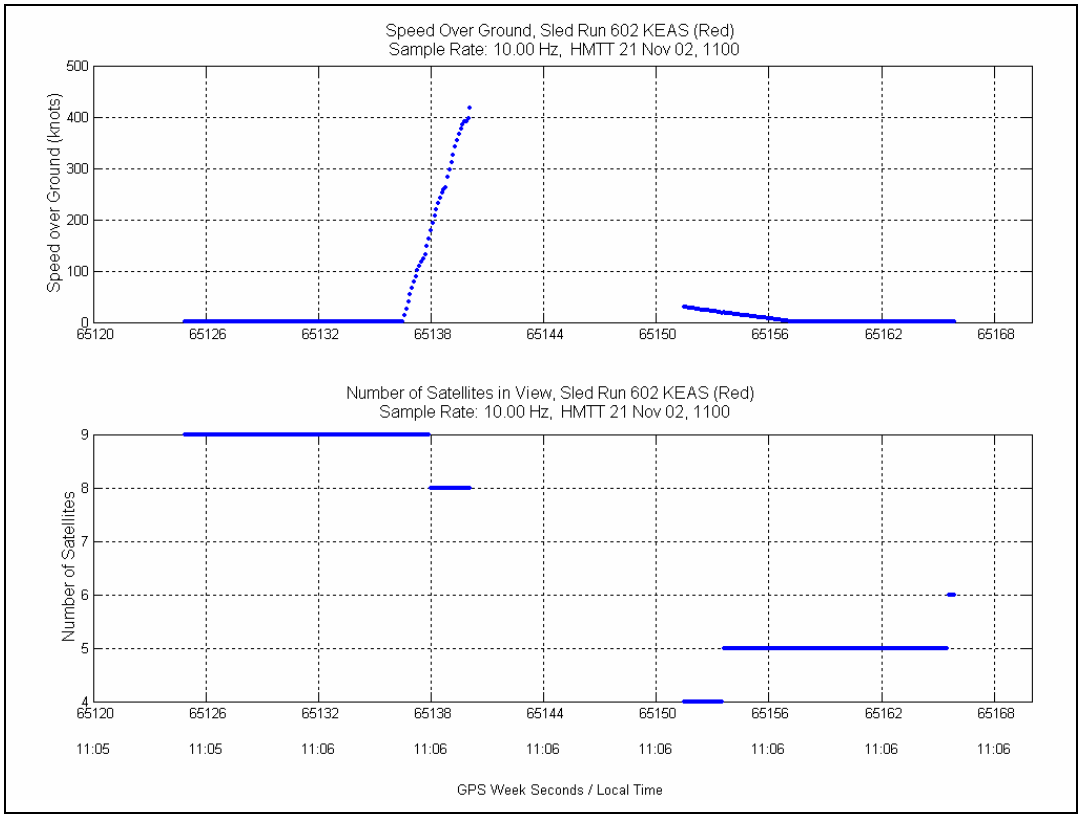

Figure 38. HMTT 10 Hz Sampling Rate

Figure 39 presents the 20 Hz sampling rate data. The small humps on the ascending side of the ground speed plot coincide with a set of rocket motors firing. A total of six motor firings occurred, and the accelerations associated with the firings were 7.536 g, 8.567 g, 8.545 g, 8.759 g, 7.903 g, and 5.641 g, respectively [12]. The peak in the ground speed plot denotes the burnout of the last motor firing, and the loss of data corresponds to the sled impacting the water brake. Comparing the ground speed plot to the number of satellites tracked, it can be noted that at each motor firing the DIVEPACS lost lock on one or more satellites. Although the G12 receiver performed well during the simulations for straight-line accelerations in the previous research, the real-world performance for high accelerations or jerk moments was not as good. By the time the sled hit the water brake, only 4 satellites were being tracked. In addition to the rapid deceleration and jerk, the large water spray could have contributed to the total loss of lock

noted in the plot. The DIVEPACS did reacquire the satellites within the 2-second time frame outlined in the G12's specifications, and continued to track the sled until it came to a full stop. Additional high-g testing needs to be accomplished to characterize the receiver's actual g tolerance envelope more fully, which is discussed in Chapter 5.

Using the data from the plot, the DIVEPACS calculated the peak velocity to be 651 knots, which corresponds to 602 KEAS [26]. As noted in Chapter 3, the KEAS is a way to standardize testing by adjusting the airspeed to account for differences in altitude, air pressure, temperature, and wind at different testing locations. The actual time from the initial motor firing until the sled came to a complete stop was 20 seconds.

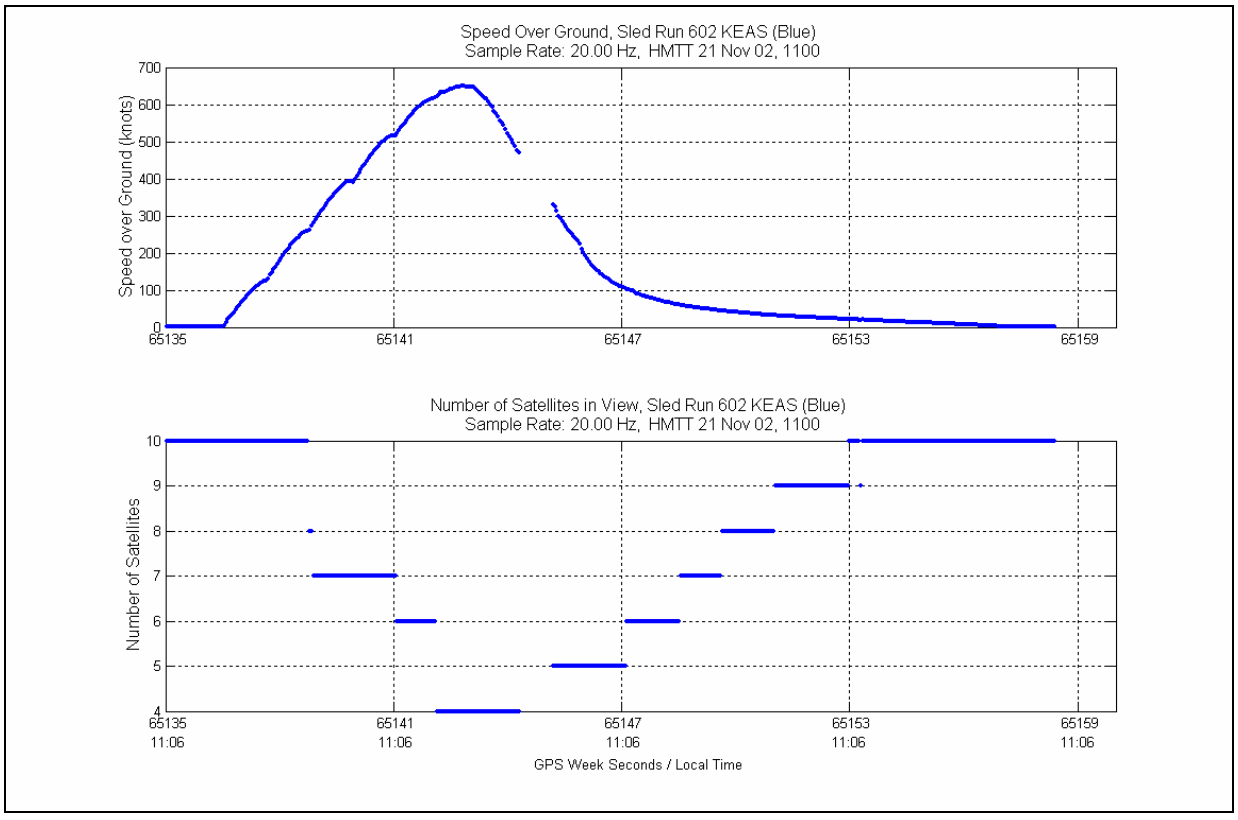

Figure 39. HMTT 20Hz Sampling Rate

Figure 40 is an East, North, Up plot that shows the track's orientation. The HMTT runs from the northeast to the southwest, and has a slight increase in elevation. According to the flash report, the sled traveled 7,094 ft or approximately 2,162 meters. Averaging the first 100 and last 100 samples of the north, east, and up components of the DIVEPACS data, the distance was calculated to be 2,160.83 meters. The large jump in the altitude plot is due to the number of satellites being tracked dropped to 4, and the position DOP increased from 3 to 24. Following the 2-second reacquisition time, the position DOP returned to a value of 3.

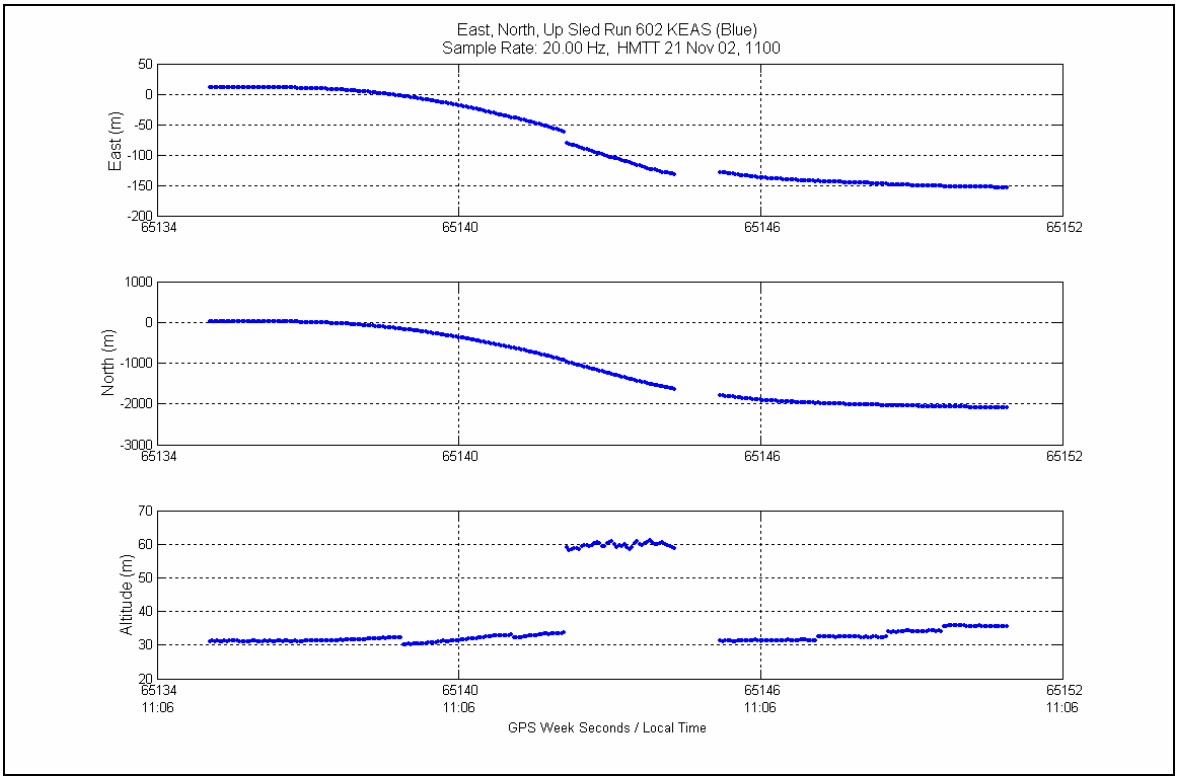

Figure 40. HMTT East, North, Up Plot

As with the other tests conducted, a reference station was placed at the 5,200 ft marker alongside the track. One configuration change was made to the HMTT configuration. Since the Z-Surveyor had to be set up over two hours prior to the actual sled initiation time, a laptop computer was added to record the base station data as a back-up to the Z-Surveyor's memory

card. Figure 41 shows the reference station, which was placed near the 5,200 ft marker on the track.

Due to problems not discovered in the reference station set up, the laptop and the memory card did not record data during the test. Attempts to access the GPS Continuously Operated Reference Stations (CORS) data were unsuccessful. The two closest stations, Echo Canyon in Nevada and Fredonia in Arizona, only had 30-second sample data available. The difference between the CORS data sampling rate and that of the DIVEPACS caused problems with trying to synchronize the two data files to determine a differential position solution. Since the entire test run was completed in 20 seconds with the main point of interest only lasting 10 seconds, no useful differential GPS could be derived for the actual sled run.

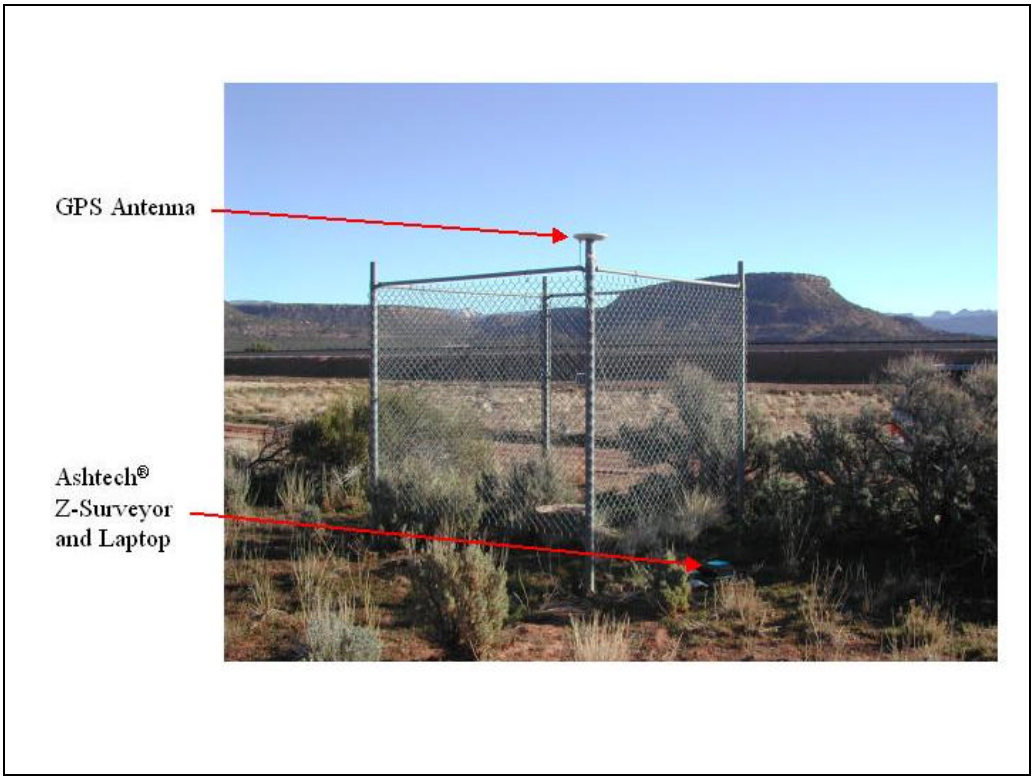

Figure 41. HMTT Base Station

Summary

This chapter presented the results and analysis of all three testing phases. Although the attempts at gathering differential data were not good, the DIVEPACS versatility was evident, and the stand-alone results provided insights into changes that could be made to make the DIVEPACS more robust for future testing. To help overcome the data loss due to overhead obstructions or tumbling motions encountered by the manikin, a tightly coupled GPS-INS should be investigated. The loss of satellite lock under high-g environment is another area of concern warranting further investigation. Chapter 5 will discuss these changes and recommend future testing challenges.

V. Conclusions and Recommendations

Overview

The previous chapters described the theory and background information, the research methodology, and the tests and analysis conducted for this research. The first part of this chapter presents the results of the research, and summarizes the DIVEPACS' ability to determine a test article's position and velocity accurately in various highly dynamic environments. The remaining portion of this chapter provides recommendations for additional testing and future research opportunities in this area. In the appendices following this chapter, the reader can reference Appendix F, which contains the paper presented at the SAFE Association Symposium in October 2002, for a brief summary of the research.

Conclusions

Throughout this research, the DIVEPACS proved to be a viable solution to provide a small low-cost versatile tool for determining position and velocity information in several highly dynamic environments. In spite of the problems encountered during the different phases of testing, the information gained in each phase helped define the operating envelop of the DIVEPACS. Also, the multiple reconfigurations of the DIVEPACS led to compact design for the dual DIVEPACS to be used in future testing.

The results from the Phase I testing showed the DIVEPACS could provide accurate position and velocity information in the harsh environment of the CART cars. Since the DIVEPACS were mounted directly to the frame of the CART car, they experienced the vibration effects from the high engine revolutions and rough ride from the car's stiff suspension system. Despite the

shock and vibrations encountered, the DIVEPACS maintained lock through the open areas of the course. Although the bridges caused a problem with the DIVEPACS' ability to maintain lock, the outages helped characterize the DIVEPACS performance, and led to possible improvements, which will be discussed later in this section.

The canopy testing in Phase II helped to characterize the DIVEPACS ability to determine the position and velocity accurately of an object in a free fall situation. Although the DIVEPACS captured the manikin's descent under a full canopy, its reacquisition time due to the manikin's tumbling was significantly longer than experienced during the free fall testing completed in the previous research [34]. For future testing, additional equipment may be needed to help the DIVEPACS reacquire satellites more quickly.

For the Phase III testing, two concerns with the DIVEPACS performance were addressed. The first issue dealt with the DIVEPACS' ability to remain attached to the manikin during a lower velocity ejection test, 450 KEAS versus 600 KEAS in the original research, and track the manikin's position and velocity. The second issued addressed the dual DIVEPACS' ability to provide an attitude determination baseline during a high-speed sled test. The first Phase III test at China Lake did prove that the single DIVEPACS configuration was a valid form fit for an ejection seat test at a slower ejection velocity. Unfortunately, due to equipment problems, the DIVEPACS was unable to provide position and velocity information for the manikin's ejection. For the second Phase III testing at Hurricane Mesa, additional equipment problems prohibited establishing an attitude determination baseline, but the data collected helped to characterize the DIVEPACS' ability to maintain lock during high accelerations or jerk.

With minor modifications to the original DIVEPACS configuration, the DIVEPACS was easily adapted for the different phases of testing conducted in the research. Phase I testing

involved combining two single DIVEPACS units into a compact dual system that could be mounted under the seat of a CART racing car, while the Phases II and III testing required the original single DIVEPACS configuration. The lessons learned through the multiple reconfigurations of the DIVEPACS led to the most recent configuration, which can be seen in Figure 42, see Appendix C for the schematics. While the new compact dual DIVEPACS configuration is slightly longer than the original configuration, it is still approximately the same size and weight as the emergency radio, which was used as the design template for the single DIVEPACS configuration.

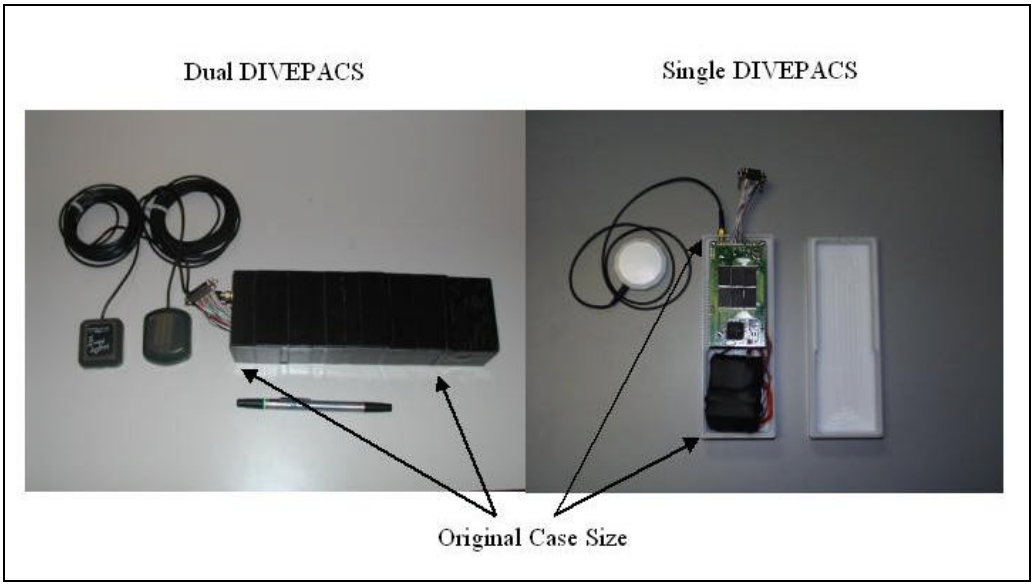

Figure 42. Dual DIVEPACS New Configuration

Recommendations

Although the research helped characterize the DIVEPACS performance in various highly dynamic environments, additional research, development, and testing is required to validate the DIVEPACS real world performance versus its performance seen in the original bench testing. Additional free fall testing or riding a roller coaster with the dual DIVEPACS could provide

more information on the DIVEPACS reacquisition time after loss of sky view. To provide the best opportunity for a successful test, sky plots for the test day could be initiated. The sky plots, which show the azimuth and elevation of all visible satellites in the sky, could allow the tester to choose the best time of day to conduct the test based on the maximum satellites in view and their geometry in relation to the testing location.

Although the DIVEPACS was placed in a ruggedized case for the original research, the data logger developed an intermittent problem that affected three tests. Once the problem was isolated, the data logger was replaced. As a result of this problem, new data loggers were researched to find a system with a faster download time and one that could handle more than one data stream at a time. Two systems looked promising and warrant further investigation [6][35]. The new data logger could reduce the size of the DIVEPACS, and with a faster download time, additional testing could be conducted within a single testing window.

From the Hurricane Mesa test, the data shows that a difference in the DIVEPACS sampling rate had an impact on the data's quality. A new GPS receiver has been developed that provides a 100 Hz sampling rate [14]. The new GPS receiver board has the same pin configuration as the G12 receiver board used for the current DIVEPACS configuration, and the new GPS receiver board is slightly smaller than the G12. The new card could easily be incorporated into the current DIVEPACS configuration.

To help overcome the problem with outages due to overhead obstructions or the manikins tumbling, a tightly coupled micro electrical mechanical (MEMS) INS/GPS system should be investigated. The tightly coupled system could provide the DIVEPACS with information that would allow it to reacquire satellite tracking faster. The outages pose a significant problem with resolving the carrier-phase ambiguity. In addition to the MEMS INS/GPS, the ambiguity

resolution, enhanced filtering, and smoothing techniques described in the research conducted by Capt Paul Henderson [11] and Capt Terry Bouska [2] could be used to in post processing of the data. The techniques used for ambiguity resolution would help to reduce the number of candidate ambiguity sets and select the best one for post-processing, while the smoothing techniques would provide a better solution more quickly by reducing the convergence time of the filter.

Appendix A. DIVEPACS Configuration for Ejection Tests

Appendix A is the schematic for the DIVEPACS configuration developed for the original research. Also, this configuration was used for both the China Lake NAWC ejection seat test and the Hurricane Mesa Test Track sled test.

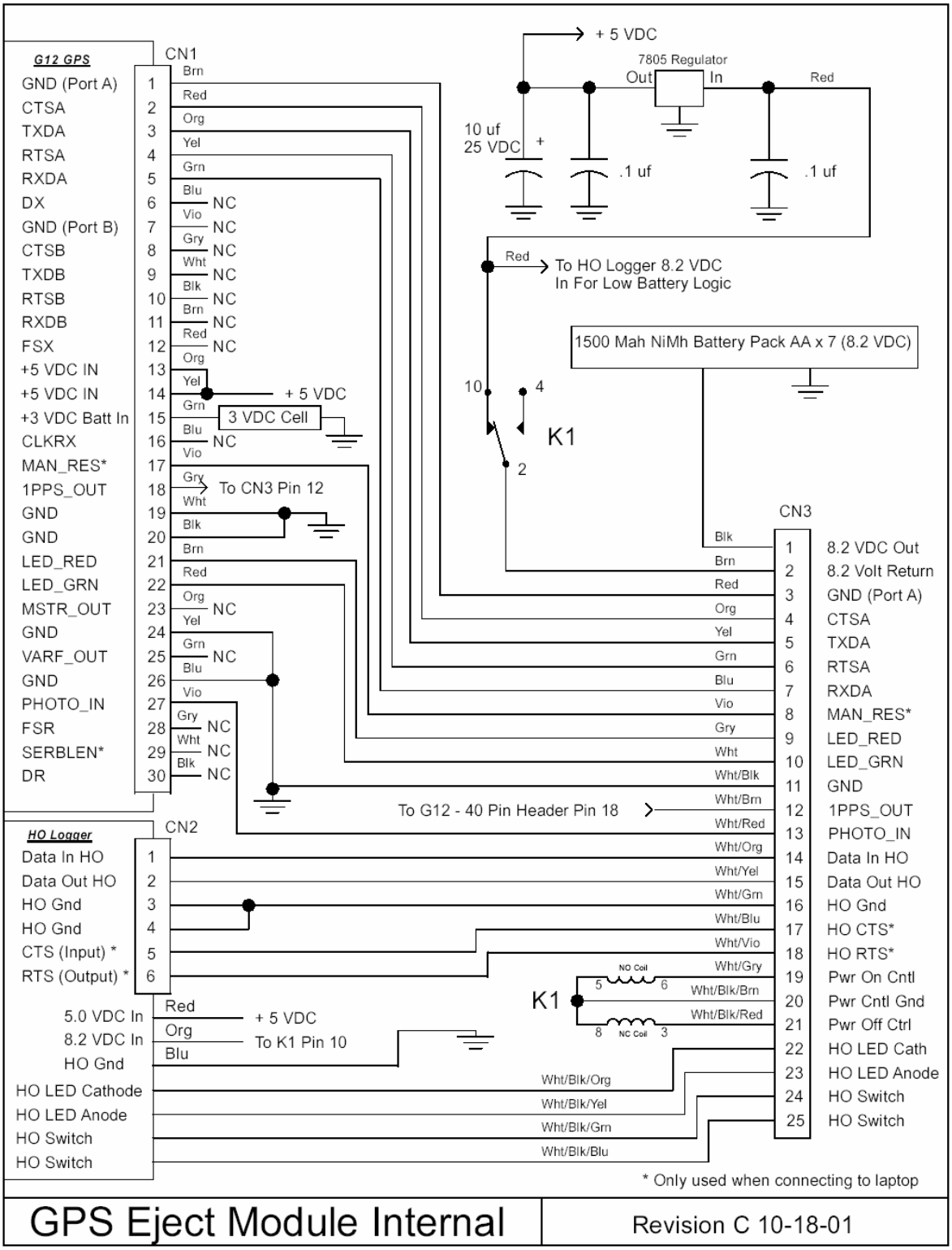

Figure 43. GPS Eject Module Internal

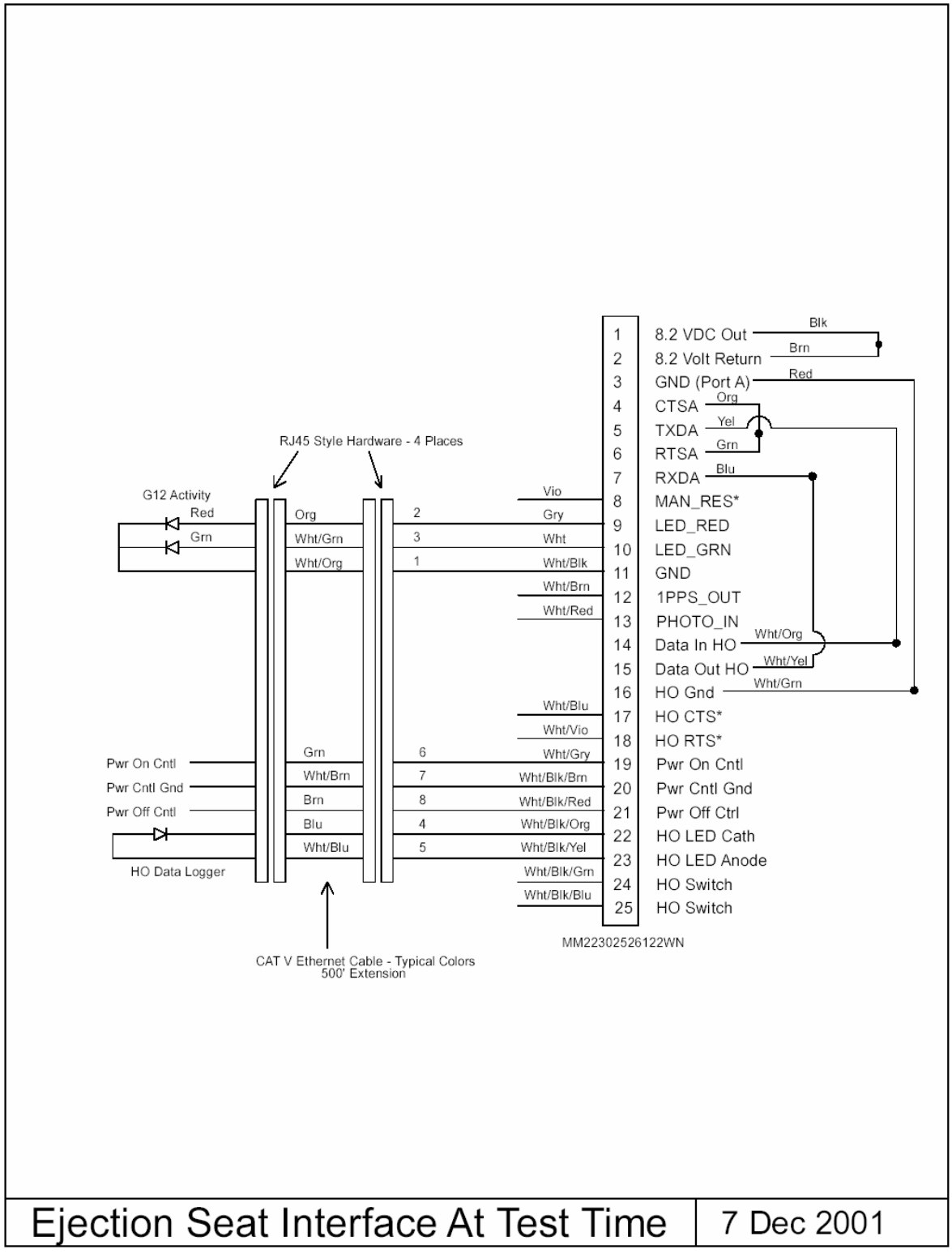

Figure 44. Ejection Seat Interface at Test Time

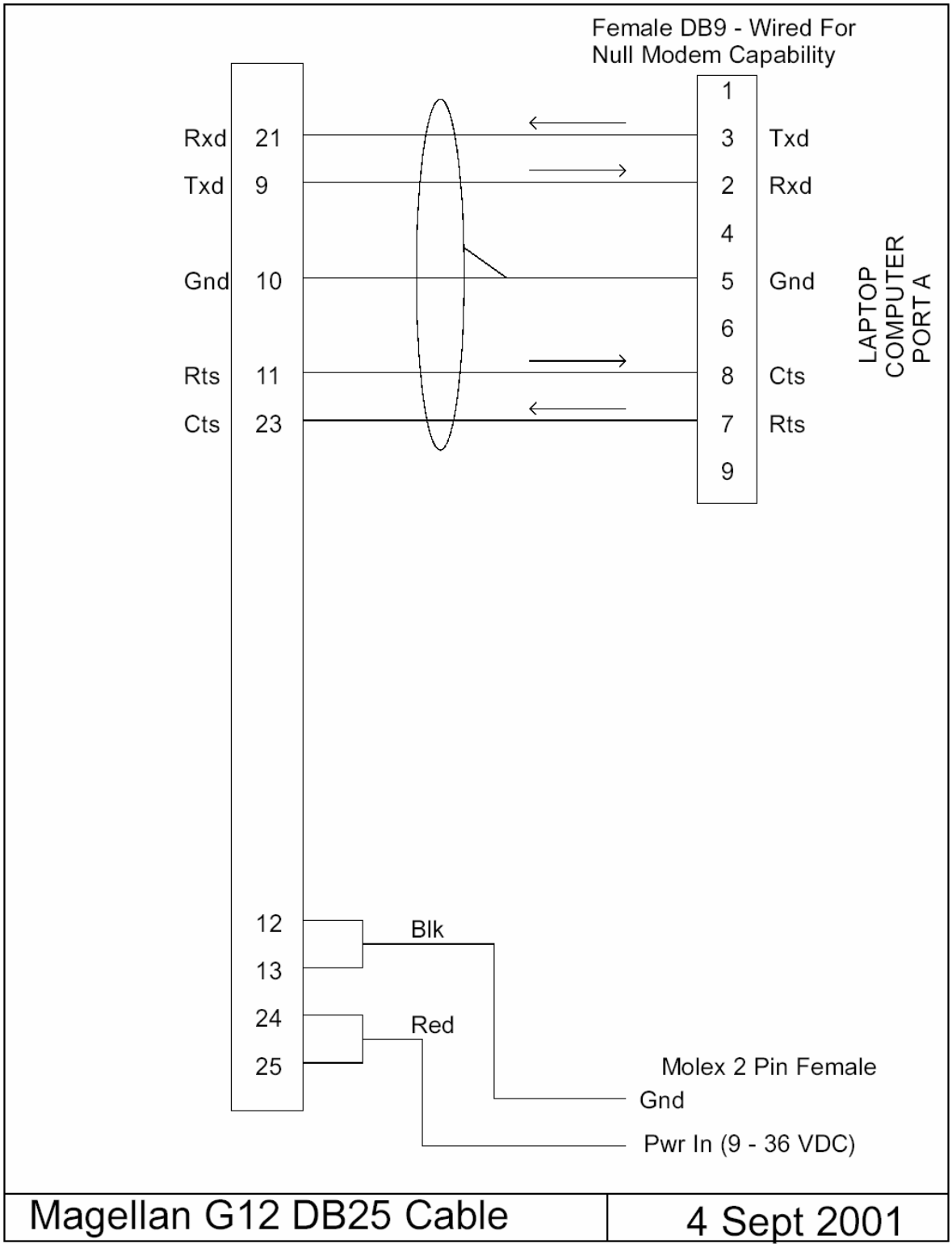

Figure 45. Magellan G12 DB25 Cable

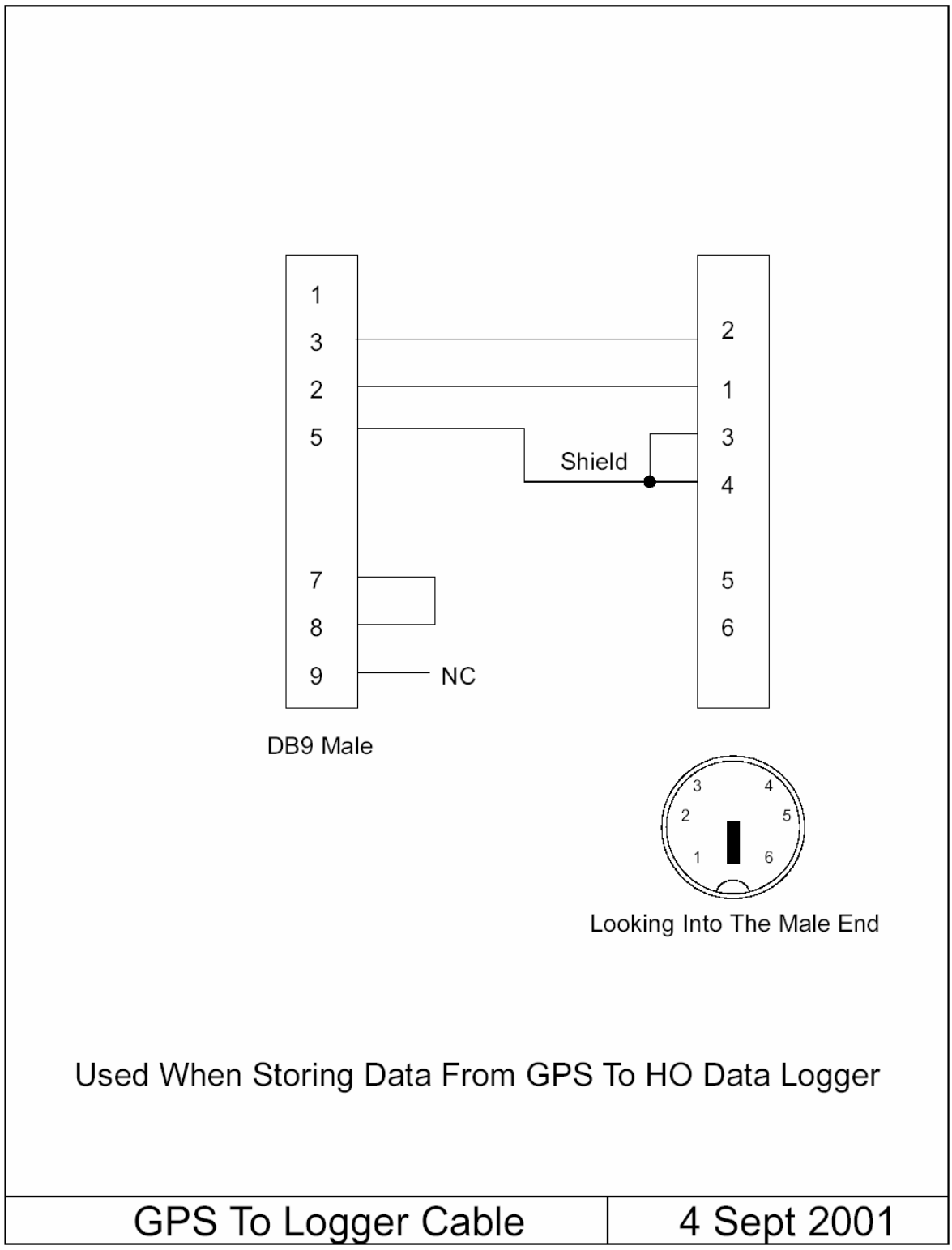

Figure 46. GPS to Logger Cable

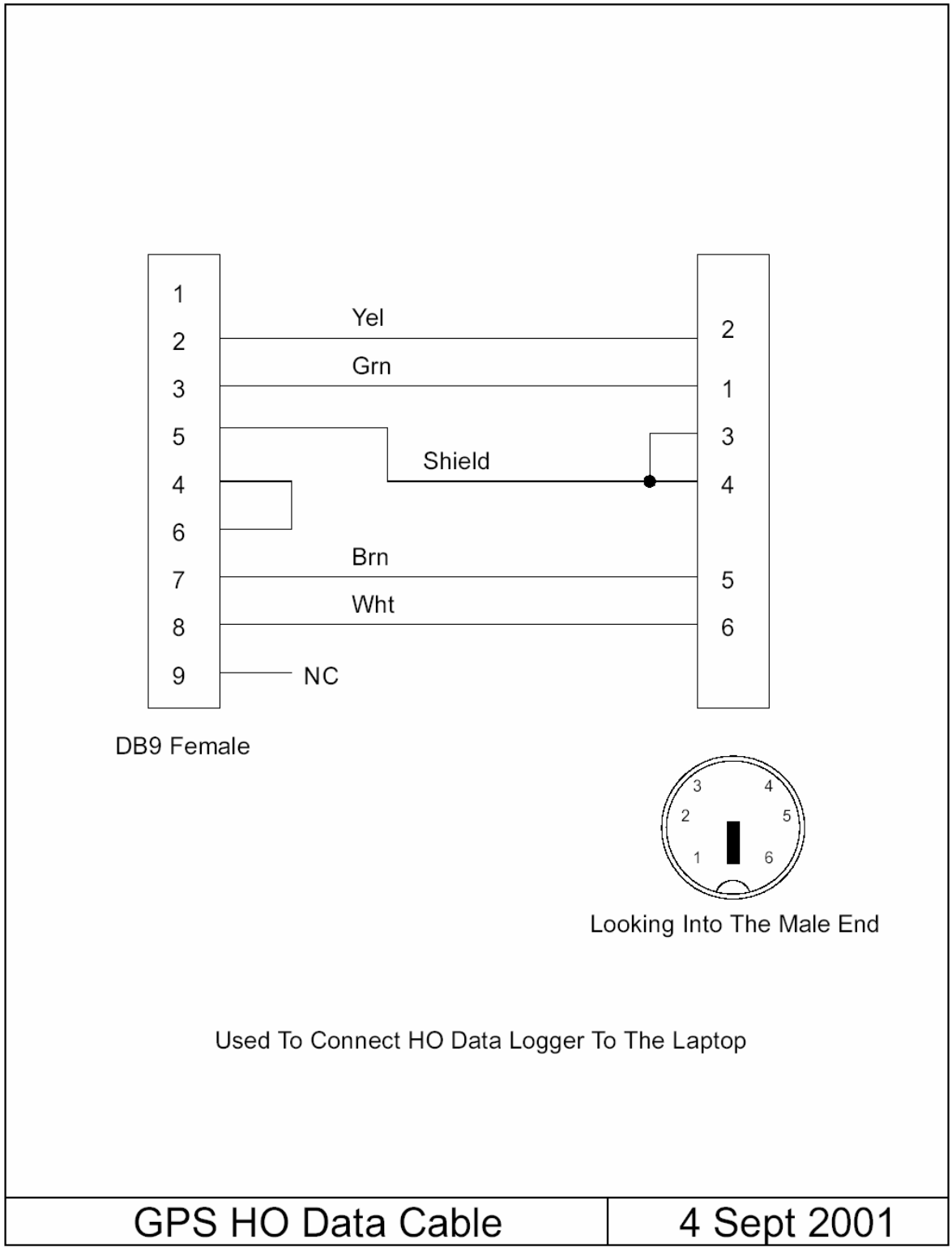

Figure 47. GPS H.O. Data Cable

Appendix B. CART Car Dual DIVEPACS Configuration

Appendix B is the schematic for the DIVEPACS configuration used in the Barber Dodge Championship Auto Racing Team car.

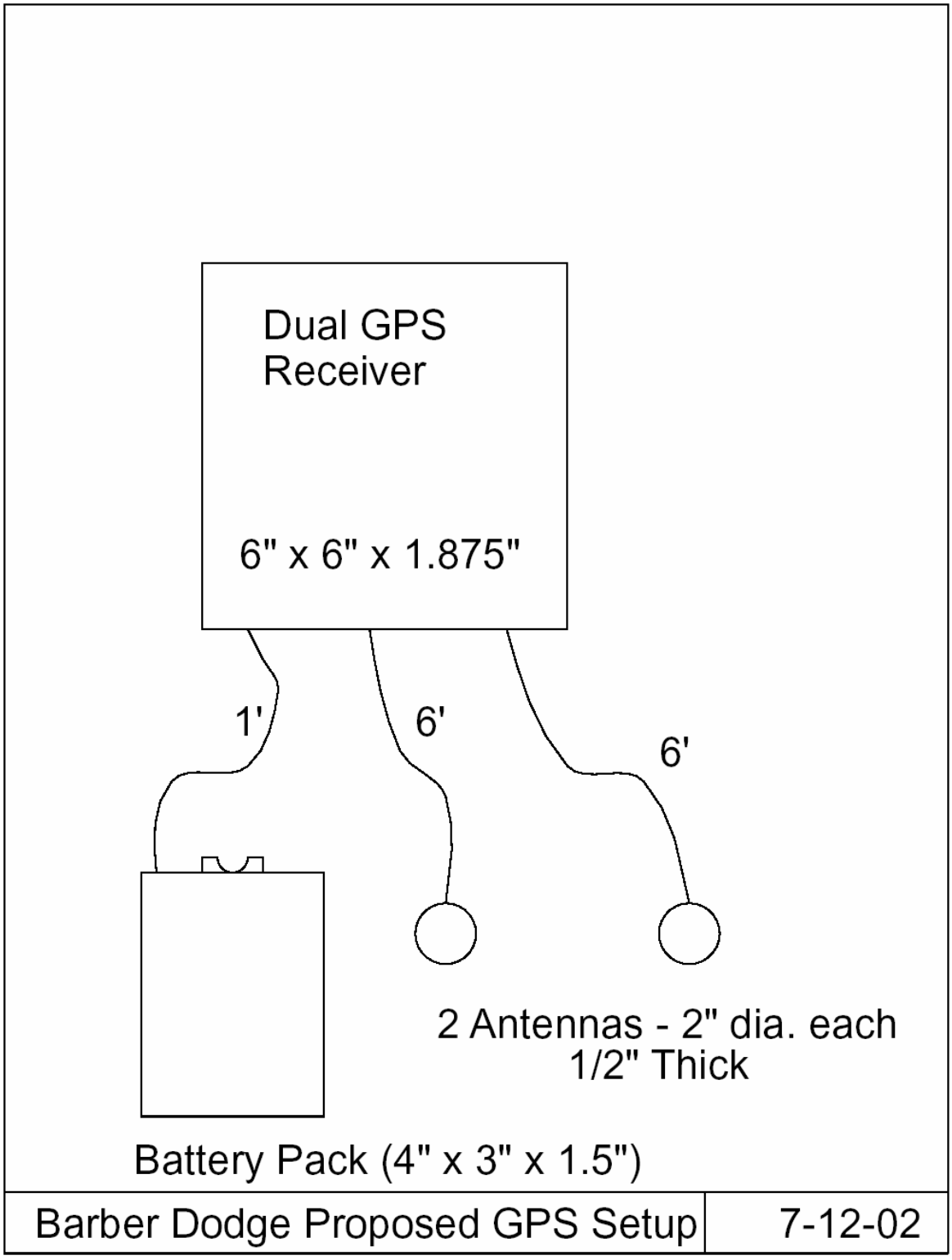

Figure 48. Barber Dodge GPS Conceptual Setup

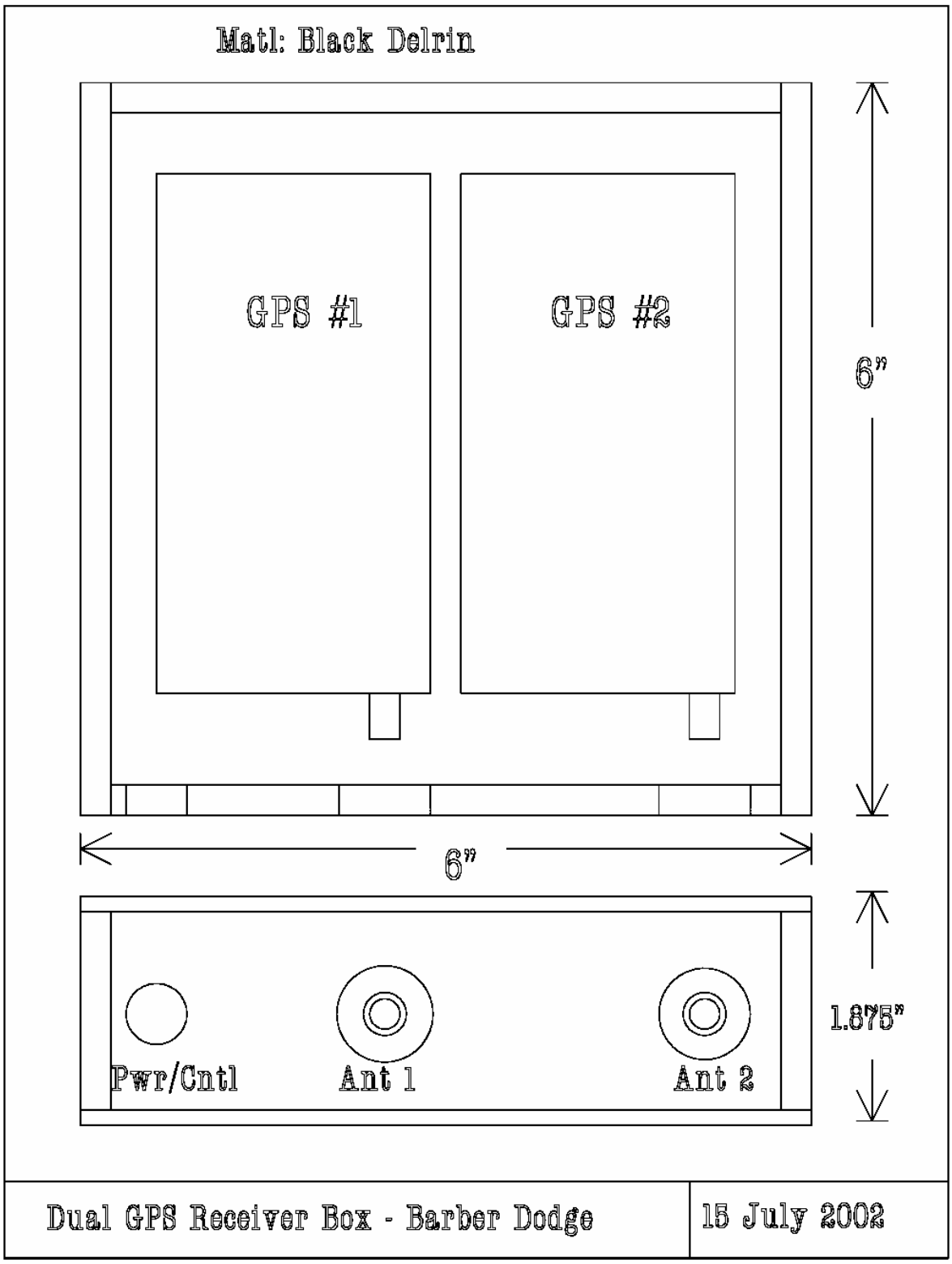

Figure 49. Dual GPS Receiver Case

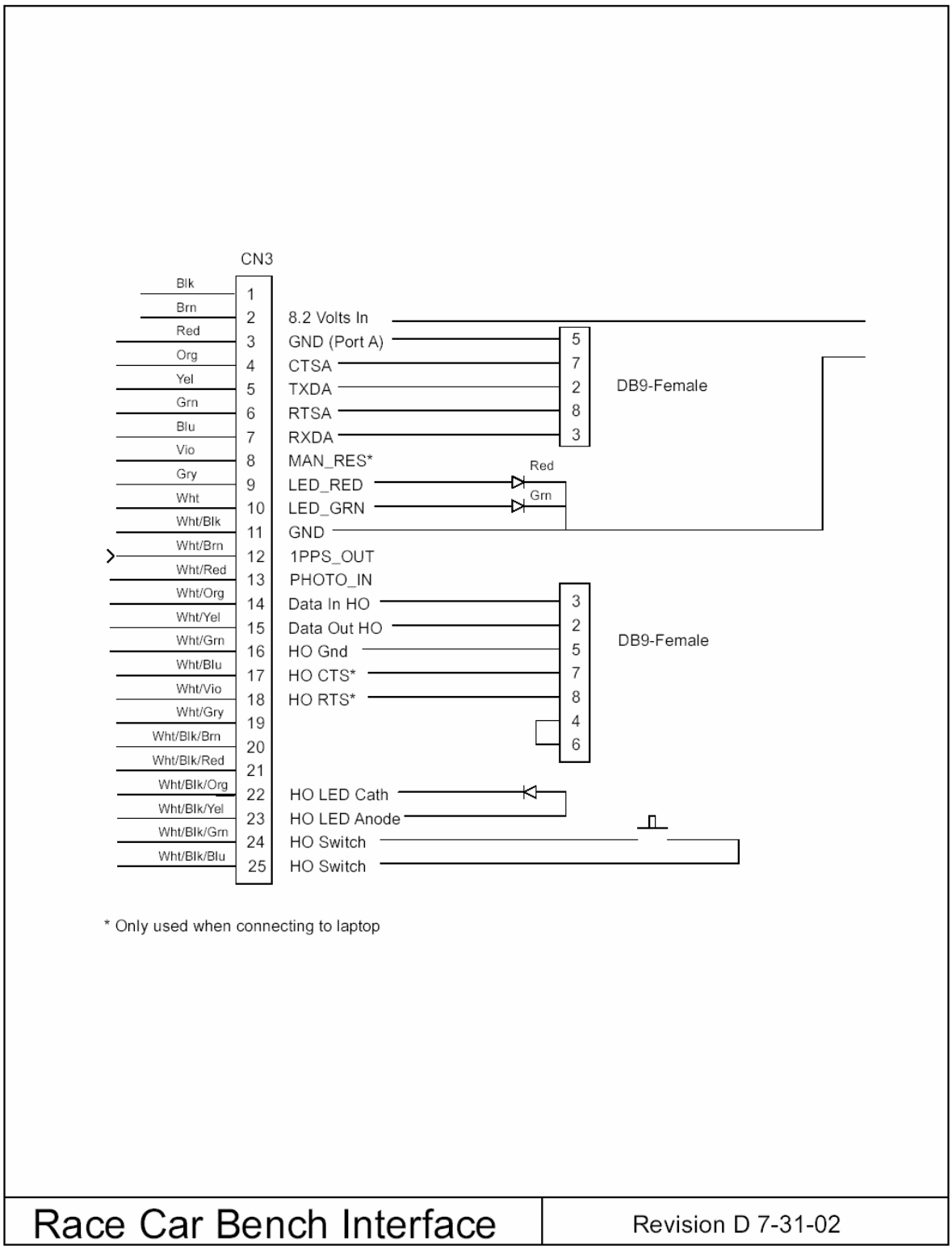

Figure 50. Dual GPS Receiver Bench Interface

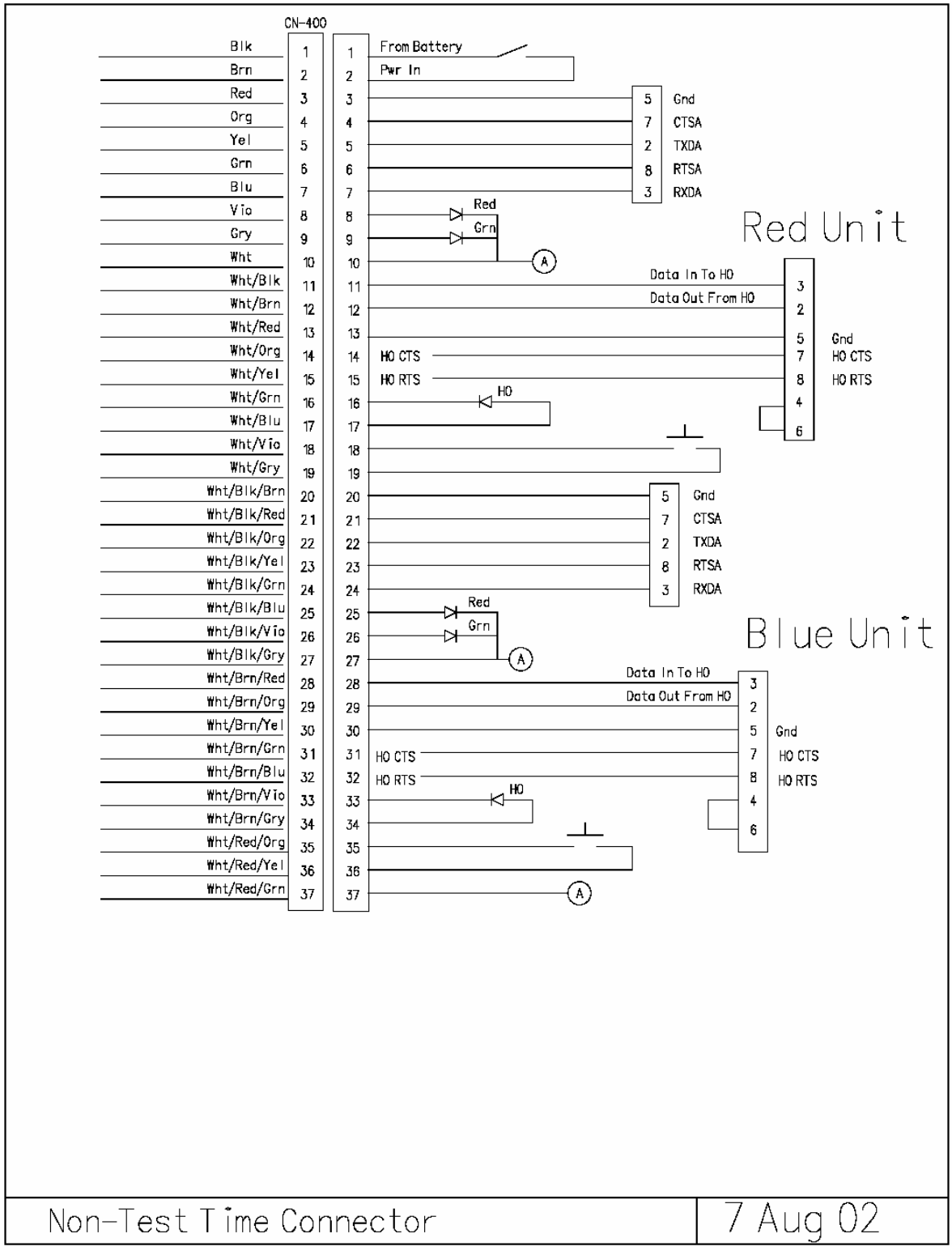

Figure 51. Dual GPS Receiver Non-Test Time Connector

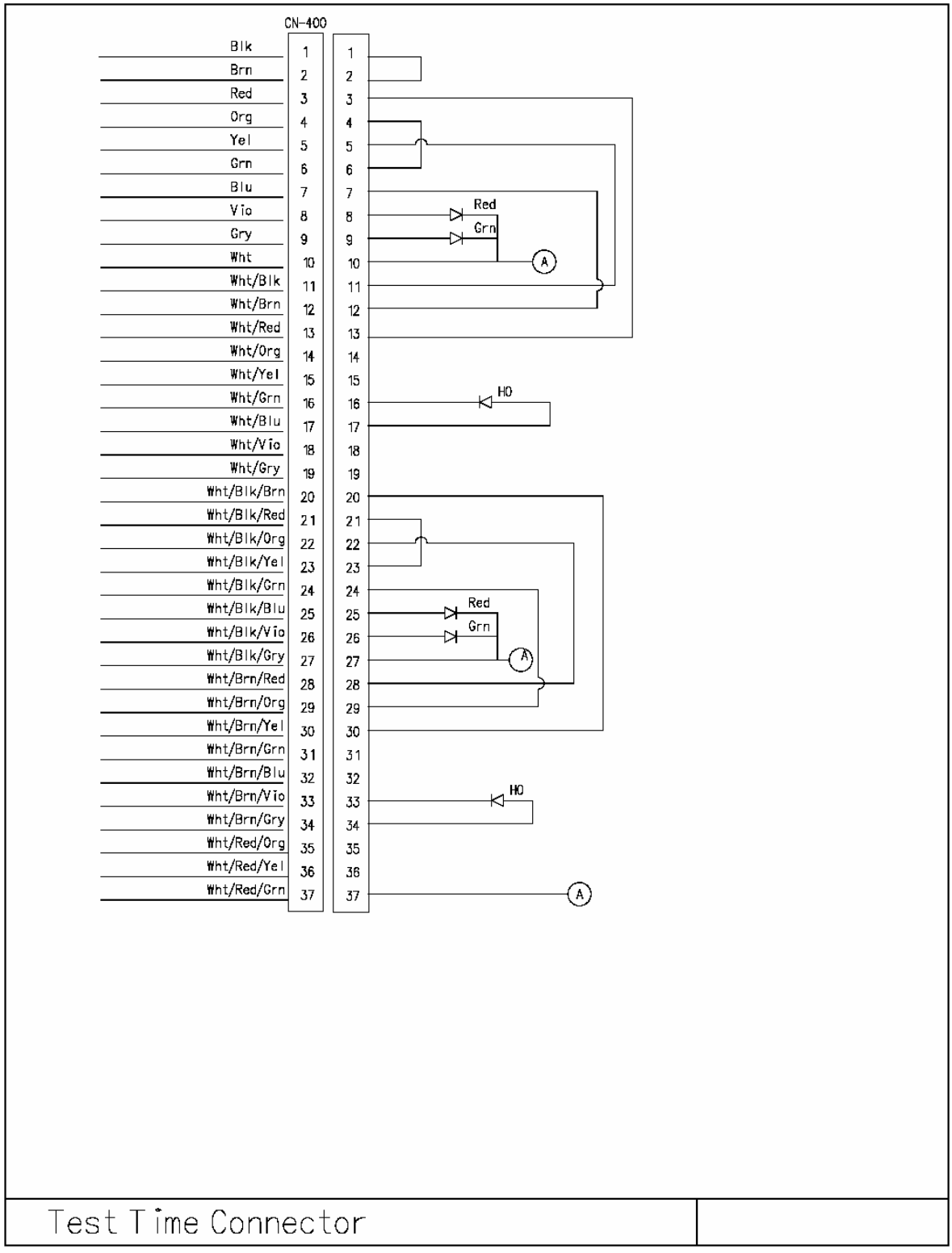

Figure 52. Dual GPS Receiver Test Time Connector

Appendix C. Compact Dual DIVEPACS Configuration

Appendix C is the schematic for the dual DIVEPACS configuration for future testing.

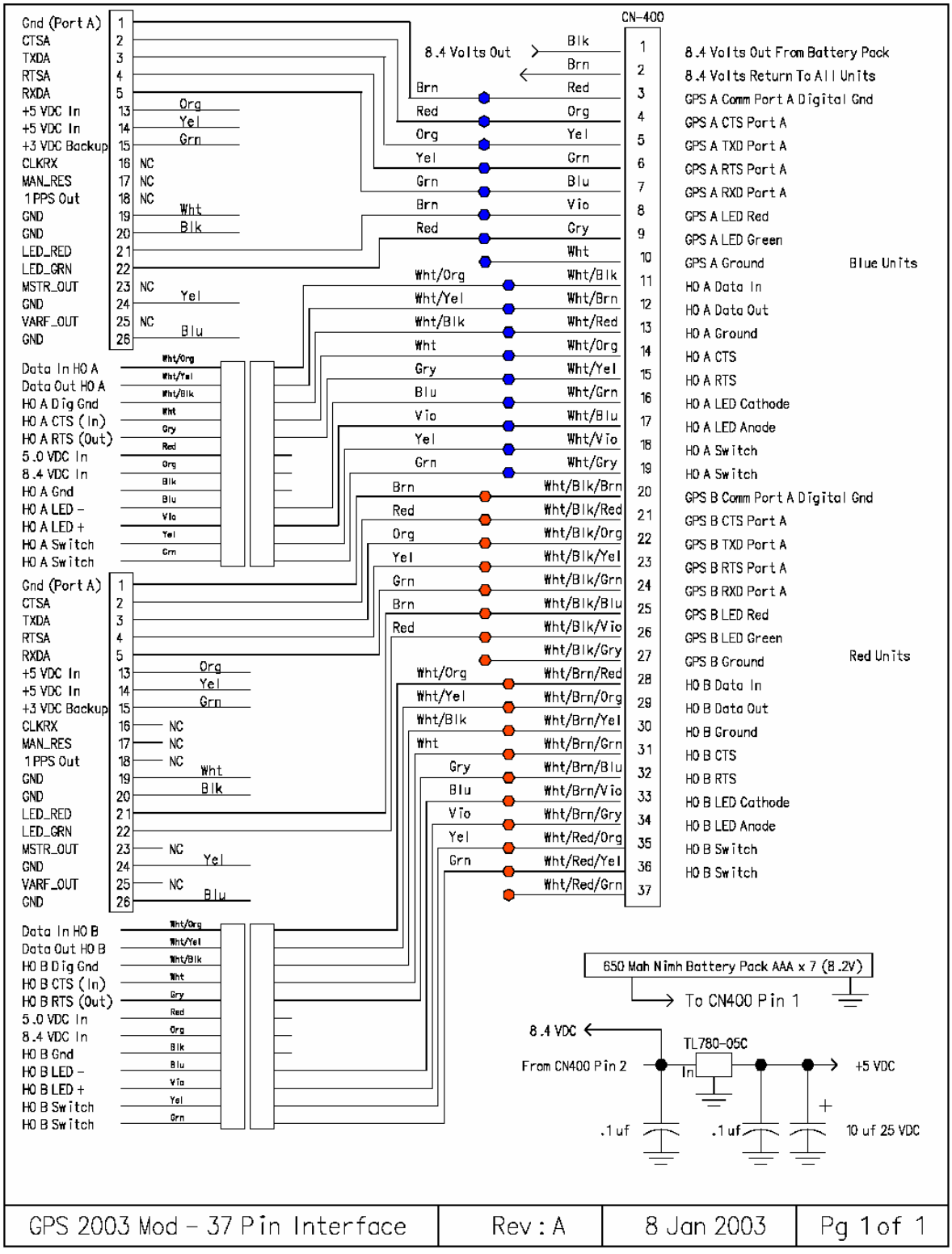

Figure 53. Compact Dual DIVEPACS Internal

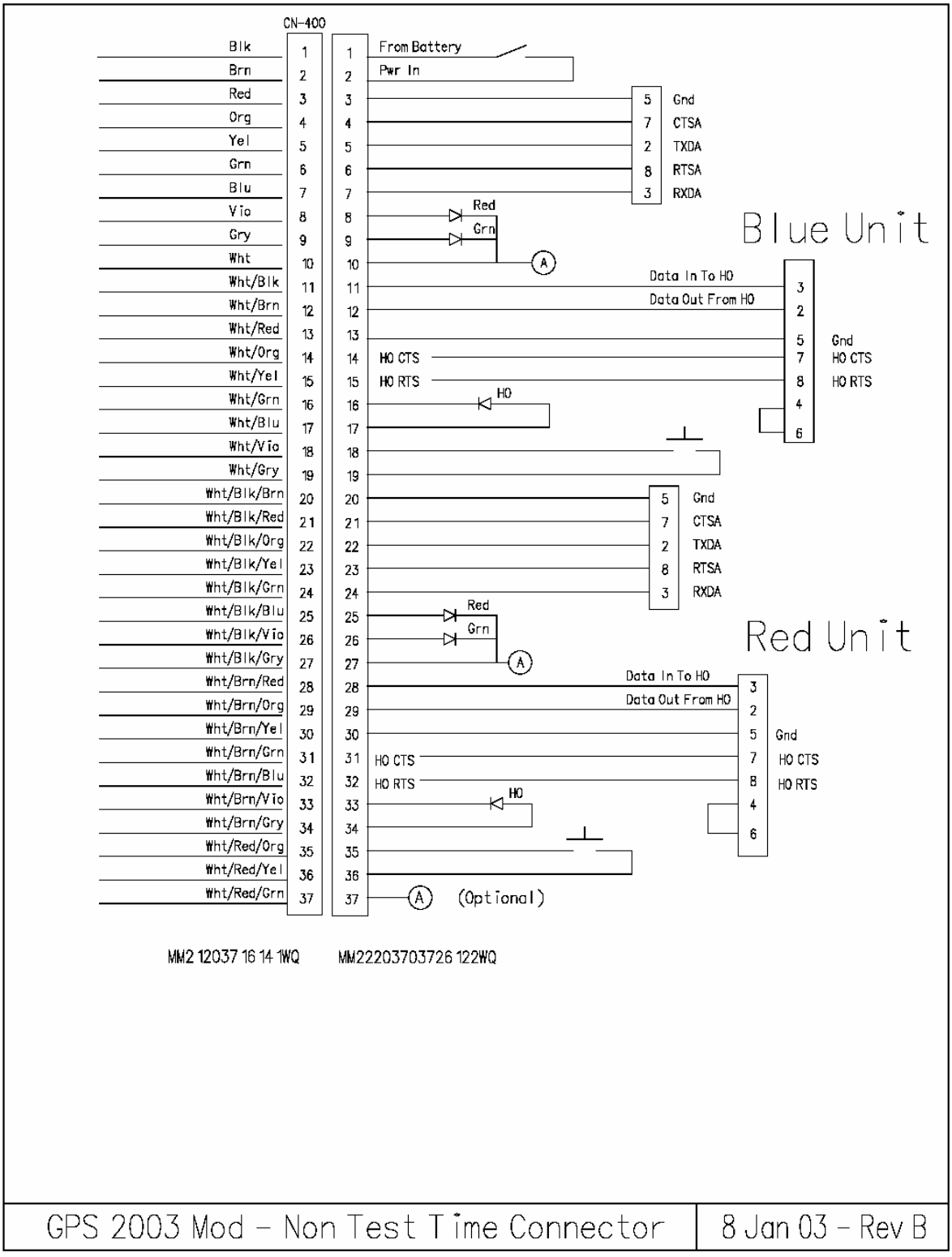

Figure 54. Compact Dual DIVEPACS Non Test Time Connector

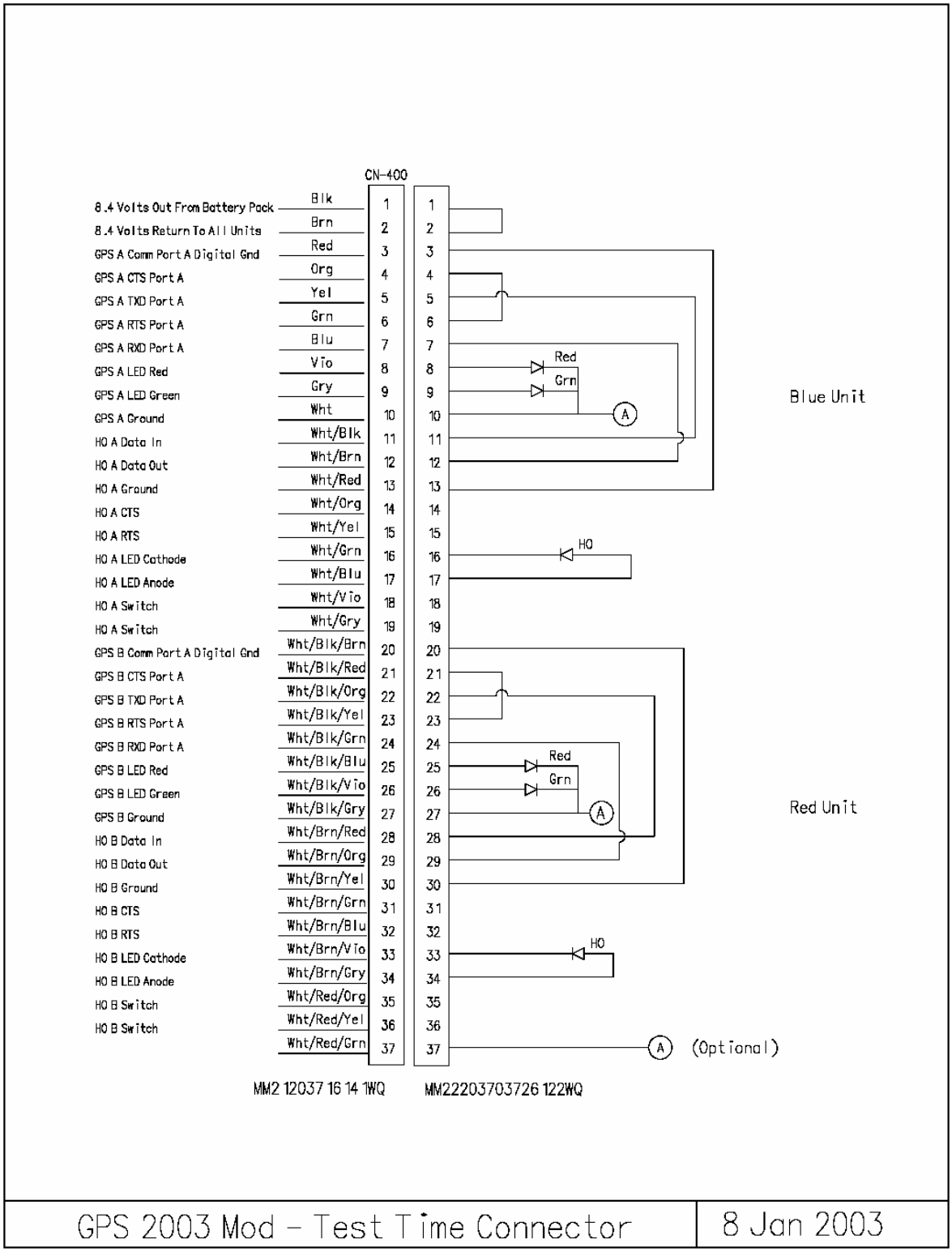

Figure 55. Compact Dual DIVEPACS Test Time Connector

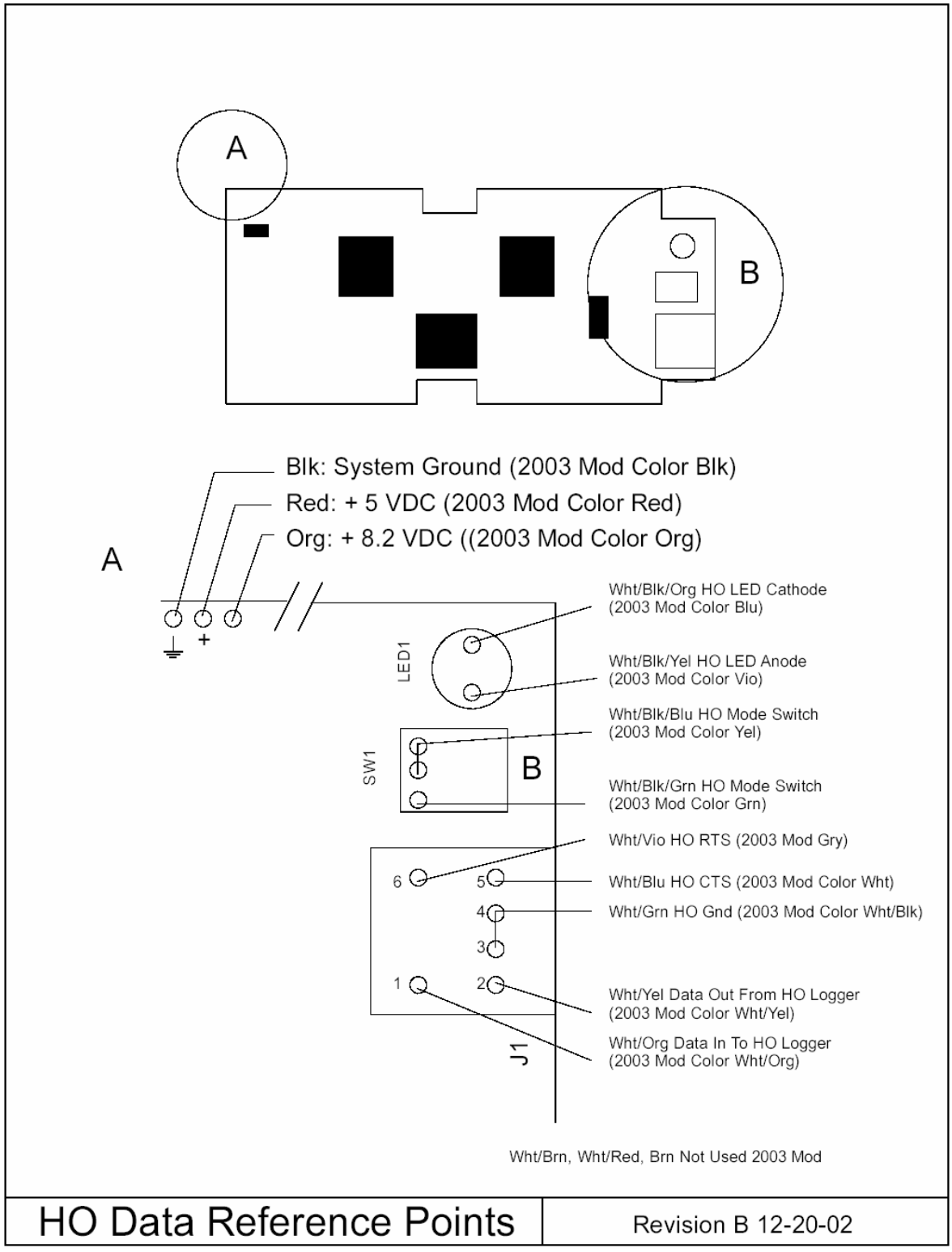

Figure 56. Compact Dual DIVEPACS H.O. Data Reference Points

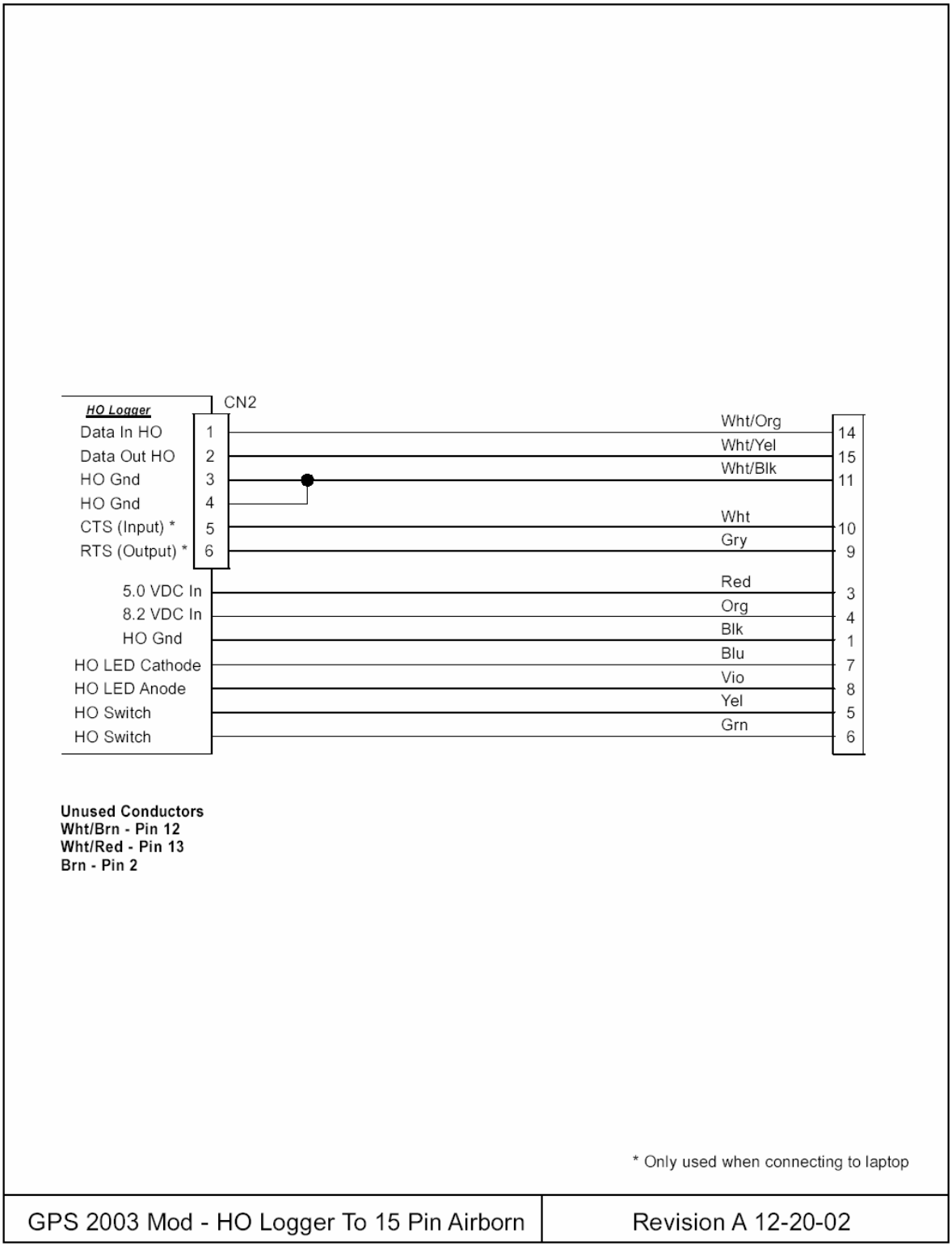

Figure 57. Compact Dual DIVEPACS H.O. Logger 15-Pin Airborn

Appendix D. Hurricane Mesa Test Track Flash Report

Appendix D is the flash report from the Hurricane Mesa Test Track and contains all the meteorological information for the test day [12].

HURRICANE MESA TEST TRACK

FLASH REPORT

CUSTOMER: Veridian/USAF

PROJECT TITLE: BRIM

TEST No: BRIM – 8 **HMTT RUN No:** 759

TEST DATE: 21 Nov 2002 **TEST TIME:** 11:04:30 PM

METEROLOGICAL CONDITIONS: Clear and sunny

TEMPERATURE: 59 °F **BAROMETRIC PRESSURE:** 64.2 CMHg

HUMIDITY: 17 %

WIND VELOCITY: 3 KNOTS **WIND DIRECTION:** From 90 (East)

TARGET SLED VELOCITY: 600 **KEAS TRAP TIME** .176 +. 005 sec =. 181

ACTUAL SLED VELOCITY: 602 **KEAS, CORRECTED FOR WIND**

SLED START STATION: 4510

SLED STOP STATION: Measured at left front slipper: F-15 11,604, Box Boy 7756, and 4668 Flat Boy

TEST SUMMARY AND OBSERVATIONS:
Run 759 was launched at 11:04:30 AM. This run was a test of the small female with the BRIM using the F-15 test sled. Target velocity was 600 KEAS. The run was programmed for 605 KEAS and actual velocity was 602 KEAS corrected for wind or 0.3% above nominal, which was well within the target velocity of 600 Keas +/- 10%. Posttest examination confirmed the BRIM and other equipment on the mannequin to be intact. All propulsion fired and there were no observed track operational anomalies.

PREPARED BY: Richard R. Higgins, Manager HMTT **DATE:** 21 Nov 2002

Appendix E. Antenna Data Sheets

Appendix E provides the data sheet and specifications for the Sarantel GeoHelix-H [30], the SM-66 [4], and the Mighty Mouse II [36] antennas used for this research. The data sheets presented in this appendix were taken directly from the web sites referenced in the bibliography.


SARANTEL
INSTALLATION GUIDE
UP CLOSE PERFECTION

Using GeoHelix™ antennas in GPS receivers

The GeoHelix™ antennas have been designed for use in L1 Band GPS (Global Positioning System) receivers. There are three different versions of the antenna, all of which have been designed to simplify the integration process.

GeoHelix-P is a passive antenna

GeoHelix-M

An active antenna with built in low noise amplifier (LNA) with a typical gain of 10dB.

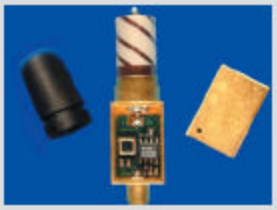

GeoHelix-H

An active antenna with built in low noise amplifier (LNA) with a typical gain of 20dB.

Electrical Characteristics

Parameter	GeoHelix-P	GeoHelix-M[1]	GeoHelix-H[2]	Units
Frequency Band	1575.42 ±2	1575.42 ±2	1575.42 ±2	MHz
Typical Gain	> -4	10	20	dBi
Maximum Noise Figure	N/A	1.50	1.50	dB
Output Impedance	50	50	50	Ohms
Maximum VSWR	2.0:1	2.0:1	2.0:1	
Supply Voltage	N/A	2.75 - 5.5	3.0 - 5.0	V
Typical Current Consumption	N/A	7	20	mA
Input Third-Order Intercept Point	N/A	+2.8	-14	dBm
Temperature Range	-40 to +85	-40 to +85	-40 to +85	°C

(1) All specifications at Vcc = 3.30V and frequency = 1575.42 ±2MHz at +23°C ±5°C unless otherwise specified

(2) All specifications at Vcc = 5.0 V and frequency = 1575.42 ±2MHz at +23°C ±5°C unless otherwise specified

The GeoHelix design offers many benefits over conventional antennas including;

- The antenna is a small ceramic cylinder (10mm diameter by 18mm length), which has a cardioid type Right Hand Circular Pattern (RHCP).
- The omni directional nature of the pattern, along with a 3 dBi beamwidth (greater than 120 degrees), gives the host GPS receiver a greater field of vision above the horizon and accessibility to more satellites.
- Ability to receive right-hand circularly polarised signals above the antenna's horizon and left-hand circularly polarised signals below the horizon, thus assisting GPS reception in built-up areas and other multi path environments. However, this is dependent on the architecture of the receiver.
- A very low Near-Field means that receiver performance is not affected when in close proximity to objects including human tissue. This ensures that the GPS receiver's sensitivity is not impaired when used in hand-held applications
- The balanced configuration of the design removes the need for a ground plane, making the antenna independent of the receiver design.
- An integral Balun ensures complete isolation of the antenna from its mounting, and allows adjacent use of multiple antennas, for example GPS and 3G mobile.

Pattern Performance

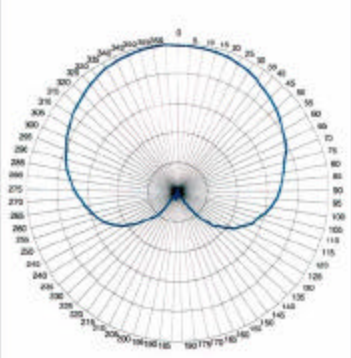

Application Guidelines

• Ensure that the antenna is mounted in such a way as to gain the maximum possible view of the sky during normal use.

• The correct antenna gain is dependent upon both the GPS receiver and the application. To select the correct antenna for your needs please consult Sarantel.

• Some GPS units have been designed to work with an active antenna only. Connecting a passive antenna to a receiver configured for an active antenna will cause a DC short and will risk damaging the receiver's power supply.

• For all active antennas, please ensure that the correct voltages are supplied to the LNA via the RF connectors. See the electrical characteristics table opposite for the correct operating voltages.

• The standard connector at the base of the antenna is a female MCX type connector. To test it please use a male MCX connector. If the antenna is to be installed on a PCB, the required connector is an SMT type right angle MCX plug (Supplier details available from Sarantel).

• Please avoid positioning the antenna near to large metal objects such as metal hydride batteries as this will degrade the signal efficiency.

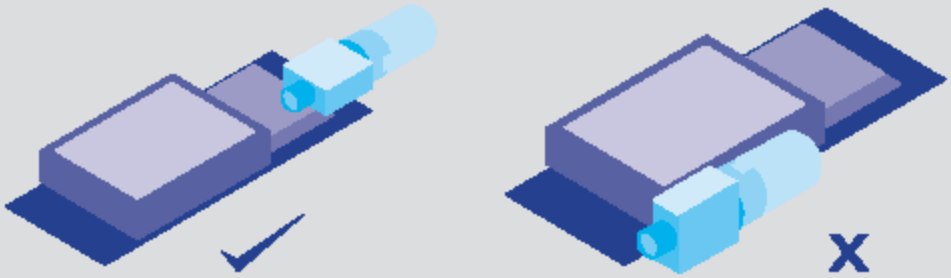

• The ring around the radome cap is designed to provide a weather seal and should not be used as the only mechanical fixing point.

• The antenna mounting box is designed to provide a Faraday Cage which offers protection against electrical interference. This is fitted during the manufacturing process and the protection will be damaged if the lid of the box is removed. Unauthorised removal will void any product warranty.

• The antenna has been extensively tested for temperature and humidity. However, additional protection is recommended below the radome to protect from wet or damp conditions that would damage the contents of the LNA box.

• The standard products are supplied with a rubberised plastic cap which has a known detuning effect. If an alternative material is to be used, please consult the factory about the material selection and the detuning effect thereof.

• If the antenna needs to be mechanically attached to a circuit board, a different box lid is available which has fixing lugs. Each lug has a 1.8mm diameter hole. The following screw types are recommended (Metric screw size M1.2 or American Standard 0-80UNF)

• The LNA box can be soldered directly on to a printed circuit board. To do this ensure that a low temperature solder paste is used with a melting temperature of less than 200°C. A hot air reflow method should be used.

SARANTEL

GEOHELIX-P: PASSIVE GPS ANTENNA ASSY

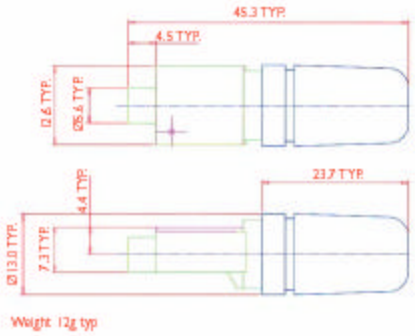

Weight 12g typ

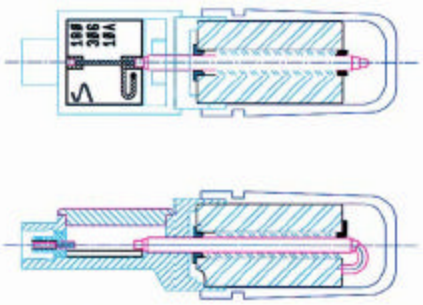

GEOHELIX-M: ACTIVE GPS ANTENNA ASSY

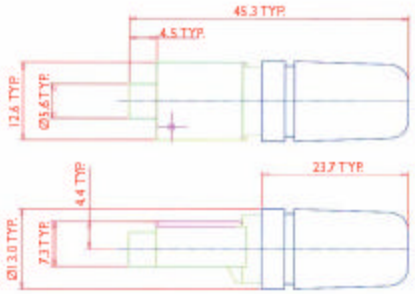

Weight 12g typ

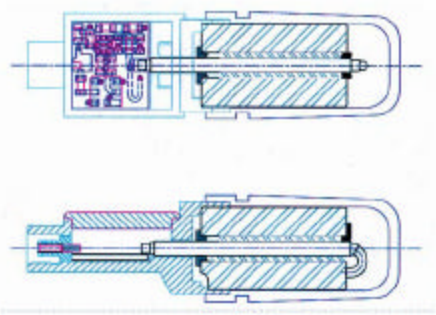

GEOHELIX-H: ACTIVE GPS ANTENNA ASSY

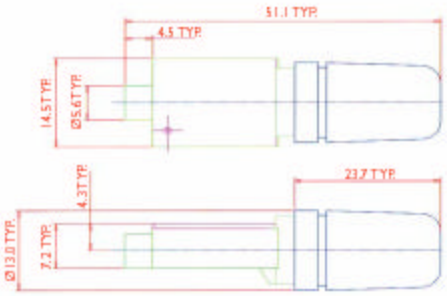

Weight 12g typ

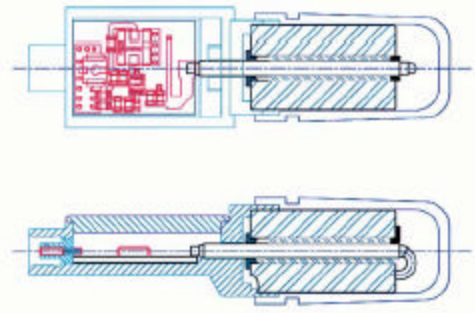

Distributor

SARANTEL

Sarantel Ltd, Unit 2, Wendel Point, Ryle Drive,
Park Farm South, Wellingborough NN8 6AQ

Tel: +44 (0) 1933 670560
Fax: +44 (0) 1933 401155
info@sarantel.com

Model SM-66

High Gain GPS Antenna with Low Noise Amplifier

The SM-66 is the integration of a high performance GPS patch antenna with a low noise amplifier into a state-of-the-art very low profile, extremely compact, fully waterproof antenna enclosure. The unit provides excellent amplification to any GPS Receiver with a +5vDC antenna power at the center pin.

The small size and ruggedness of this antenna is a pre-requisite for any antenna in the high demand of vehicle locating and car navigation GPS antenna that will sustain harsh outdoor environment while maintaining GPS signal stability.

Low noise figure / Fully weather proof
Ultra-high Sensitivity / Compact construction
Excellent temperature stability / Magnet or screw mount base
***Screw Mounting Base Optional**

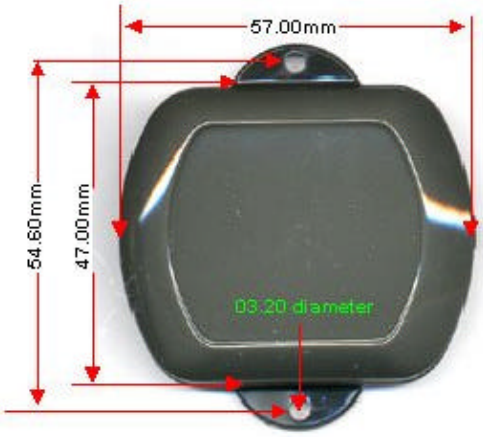

Specifications:

Physical Constructions:

Constructions: Polycarbonate radome enclosure, die-cast-shell at the bottom, water proof rubber gasket seals.
Dimensions:48mm(W)x 15mm(H). 58mm(L)x
Weight: 65grams.
Standard Magnetic Mounting: (With 2 M3 tapped holes on die-cast base, for use with "Optional" Mounting Plate)
Optional mounting plate: Metal flanges with holes for permanent mount.

Cable & Connector:

RF: 5 meter RG174/U cable
Pulling strength: 6 Kg @ 5sec.
Connector available:BNC, or MCX right angle.

Antenna Element:

Center Frequency: 1575.42 MHz +/-1.023 MHz
Polarization: R.H.C.P. (Right Handed Circular Polarization).
Absolute Gain @ Zenith: +5 dBi typical.
Gain @ 10° Elevation: -1 dBi typical.
Axial Ratio: 3 dB max.
Output VSWR: 1.5:1 max.
Output Impedance: 50 Ω

Low Noise Amplifier:

Center Frequency: 1575.42 MHz +/- 1.023 MHz.
Power Gain: 27 dB typical.
Bandwidth: 2 MHz min.
Noise Figure: 1.5 min.
Outer Band Attenuation: 20 dB min. @ Fo +/-50 MHz.
Supply Voltages: +4.5~5.5V DC.
Current Consumption: 28mA +- 3mA.
Output Impedance: 50 Ω

Overall Performance: (antenna element, LNA & coax cable)

Center Frequency: 1575.42 MHz.
Gain: 30 dB min.
Noise Figure: 2.0 max.
Axial Ratio: 3 dB max.
Bandwidth: 2MHz min.
VSWR: 2.0 max.
Output Impedance: 50 Ω

Environmental:

Operating Temperature: -40° C~ +85° C.
Storage Temperature: -50° C~ +90° C.
Relative Humidity: 95% non-condensing.
Water Resistance: 100% waterproof.

Mighty Mouse II

Active GPS Antennas

Features

- Universal connector, FME, which connects to SMB, SMA, BNC, TNC, MCX and NTYPE
- 5 meter cable
- -40°C to 85°C operating range
- Hermetically sealed, 100% waterproof
- Die-cast metal base plating ground plain
- Polycarbonate radome enclosure
- Magnetic and permanent mounting system

Mighty Mouse II (Extreme Low Power)

- 28dB gain low noise amplifier
- Maximum of 5mA current consumption (all voltages)
- 2.5V to 5.5V DC
- 3 stage amplifier and band pass filtering

Common Receivers and their Connectors

Receiver	Connector
Garmin 117	MCX
Garmin 12XL	MCX
Garmin 40	MCX
Garmin 45, 45XL, 48	BNC
Garmin 175	MCX
Garmin Chartplotters	BNC
Garmin II, II+	BNC
Garmin III, III+	BNC
Magellan ColorTRAK	SMB
Magellan Tracker	SMB
Motorola	SMA
Trimble CM3	SMB
Trimble SK-8 (Lassen)	SMB
Trimble SK II	SMB
Trimble ACE	SMB
Trimble SVee Six (+)	SMB

Ordering Information

Part Number	Description
MM2 GPS	Mighty Mouse II, 28 dB gain GPS Antenna with 5 meter cable (2.5V to 5.5V DC)
Options	
XXX	Straight connector; replace XXX with SMB, SMA, BNC, TNC, MCX or NTYPE
XXX-RA	Right angle connector; replace XXX with SMB, SMA, BNC, TNC, MCX or NTYPE

TRI-M SYSTEMS - ENGINEERING

Tri-M Systems and Engineering

1497 Kebet Way, Unit 109 • Port Coquitlam, BC V3C 6L3 • Canada

Tel: 604.945.9565 Fax: 604.945.9566 www.Tri-M.com

Appendix F. SAFE Association Paper

The following paper was presented to the SAFE Association Symposium on 2 October 2002. The results presented in the paper were the preliminary results from the Phase I and II testing conducted for this research.

Monitoring Air Force Aircraft Escape System Tests Using GPS-Based Position and Velocity

by
Capt Christina Schutte
Masters Student
Air Force Institute of Technology
2950 P Street Bldg. 640
Wright-Patterson AFB, OH 45433

Lt Col Mikel Miller
Deputy Department Head, Electrical Engineering and Computer Science Division
Air Force Institute of Technology
2950 P Street Bldg. 640
Wright-Patterson AFB, OH 45433

Capt Reece Tredway
Engineer, Navigation and Control Branch
Air Force Research Laboratory Munitions Directorate
101 West Eglin Blvd, Suite 152
Eglin AFB, FL 32542

ABSTRACT

Test and evaluation of the United States Air Force's latest aircraft escape system technology requires accurate position and velocity profiles during each test to determine the relative positions between the aircraft, ejection seat, manikin and the ground. Current rocket sled testing relies on expensive ground based multiple camera systems to determine the position and velocity profiles. While these systems are satisfactory at determining seat and manikin trajectories for sled testing, their accuracy decreases when they are used for in-flight testing, especially at high altitudes.

This paper presents the design and test results from a new GPS-based system capable of monitoring all major ejection test components (including multiple ejection seat systems) during an entire escape system test run. This portable system can easily be integrated into the test manikin, within the flight equipment, or in the ejection seat. Small, low-power, lightweight Global Positioning System (GPS) GPS receivers, capable of handling high-accelerations, are mounted on the desired escape system component to maintain track during the escape system test sequence from initiation until the final landing. The GPS-based system will be used to augment the telemetry and photography systems currently being used at the Air Force (AF) and other Department of Defense's (DoD) sled track test facilities to improve tracking accuracy and reduce testing costs.

In the preliminary stages of testing, a second generation GPS-based system has been modified to validate an ejection system's canopy deployment, and determine yawing motions of a Championship Auto Racing Team (CART) car using differential GPS. The preliminary results of both the first generation and second generation tests are provided in this paper.

INTRODUCTION

Shortly after man began to fly in the early 20th century, he realized the need to escape from a crippled aircraft, and that need spawned the growth of the ejection seat proving grounds. The AF and other DoD agencies maintain several test track facilities throughout the United States. The facilities missions may differ, but the equipment found at each one is primarily the same. Typically, each facility consists of a long sled track with the required telemetry and high-speed photography equipment to monitor, track and validate an aircraft escape system.

This paper provides a brief overview of and its capabilities and then describes the initial design of a GPS-based system used to augment the current monitoring systems to measure position, velocity and attitude for all the major ejection test components, and presents the results from its development.

Also, the paper outlines design changes and testing methodology for the second generation system, and presents some preliminary results from its initial testing phase.

GPS OVERVIEW

The GPS is a satellite-based radio navigation system developed and operated by the U.S. Department of Defense. The first GPS satellite was launched in the late 1970's. Although used for many years earlier, the system was not declared fully operational until 1995.[2]. The GPS is designed to give precise position, velocity, and time information to anyone with a GPS receiver. Figure 1 is an artist rendering of a GPS satellite in orbit around the earth.

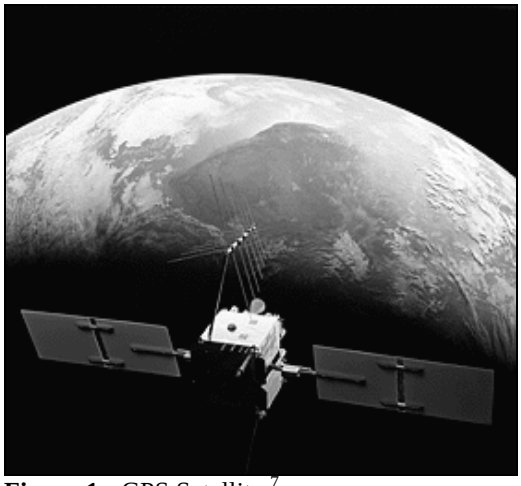

Figure 1: GPS Satellite.[7].

System Architecture. The three main parts of the Global Positioning System are the space, control, and the user segment as shown in Figure 2.

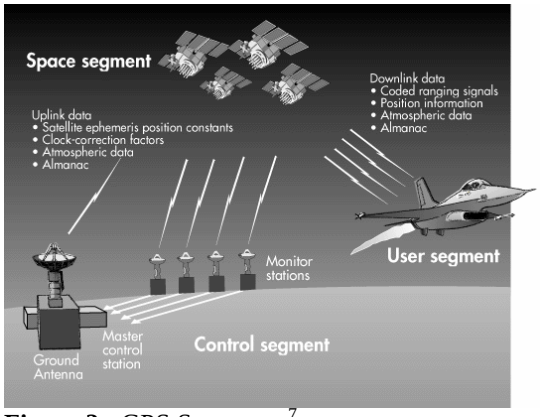

Figure 2: GPS Segments.[7].

Space Segment. The space segment is made up of the GPS satellites. The GPS constellation currently consists of 29 operational satellites. The satellites are located in one of six orbital planes set at 55 degrees inclination. The satellites are in a medium earth orbit (MEO) at an altitude of 22,200 km. Each GPS satellite has an orbital period of 11 hours and 56 minutes and remains in view above the horizon for approximately 5 hours on average.[2]. With the current 29-satellite constellation, a typical user can expect to have 6-8 satellites in view.

Control Segment. The Control Segment consists of a master control station (MCS) and five tracking stations located around the world. The MCS, located at Schriever AFB in Colorado Springs, is responsible for the command and control of the system, and continually monitors the satellite orbits and health. In addition to the MCS, the five remote tracking stations are located on the islands of Hawaii, Kwajalein, Ascension, Diego Garcia, and at Cape Canaveral. These unmanned stations are controlled by the MCS. The remote monitoring stations communicate with the satellites through dedicated ground antennas and with the MCS via ground and satellite links.

User Segment. The user segment is comprised of all the GPS receivers. Anyone with a GPS receiver can convert the satellite signals to precise position, velocity and time estimates. Today there are hundreds of models available on the market, ranging in price from less than one hundred dollars to tens of thousands of dollars. Normally with increased cost comes increased accuracy and capability. A typical GPS receiver's accuracy is approximately 16 meters spherical error probability (SEP).

Differential GPS (DGPS). To achieve the greatest possible accuracy from the GPS sensors, differential techniques must be used to remove the dominant error sources. A common real-time DGPS system is shown in Figure 3.

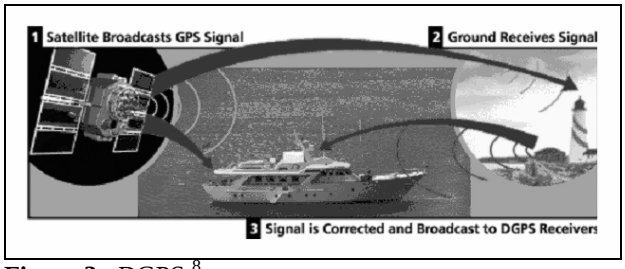

Figure 3. DGPS.[8].

The difference between DGPS and a GPS receiver operating as a stand-alone unit is the addition of a second independent GPS receiver operating as a reference station. The differences between the measured distances and the calculated distances to the satellites are continuously determined, and these differences are then transmitted as corrections to the mobile GPS receiver, or stored for post

processing. Post processing is often easier to implement because it doesn't require the additional hardware such as hard-wire data links or transmitters. Post processing also eliminates data latency because the corrections can be applied to the same time epoch for each measurement. The advantage of real-time corrections depends on the application. The increased accuracy of DGPS is based on the fact that errors such as satellite ephemeris and ionospheric delay are similar for receivers separated by distances as large as hundreds of kilometers. These errors in addition to being spatially correlated tend to vary slowly over time. The reference station estimates the errors for each satellite and provides them to the mobile receiver with some delay called latency. The further the mobile user is from the reference station, or the longer the latency, the less benefit derived from the differential correction. Depending on the DGPS technique, position accuracy can be improved to the sub meter level.

RESEARCH GOALS

The goal of this research is to improve the design and performance of Differential GPS (DGPS), Independent Velocity, Position and Attitude Collection System (DIVEPACS), and augment the current video monitoring and tracking systems used at the AF and other DoD sled track testing facilities. The design improvements will combine two DIVEPACS into a single package to meet the same size and weight constraints of a single DIVEPACS. The multiple receiver configuration will improve the DGPS capabilities to provide sub-meter accuracy for position, velocity, and attitude determination of the major ejection system components during the sled track ejections and actual in-air ejection test.

SYSTEM CONFIGURATION

First Generation System Configuration

The DIVEPACS is designed to fit into the pockets of a standard aircrew survival vest. Figure 4 shows the DIVEPACS as it is configured for Phase II freefall testing as described in the next section.

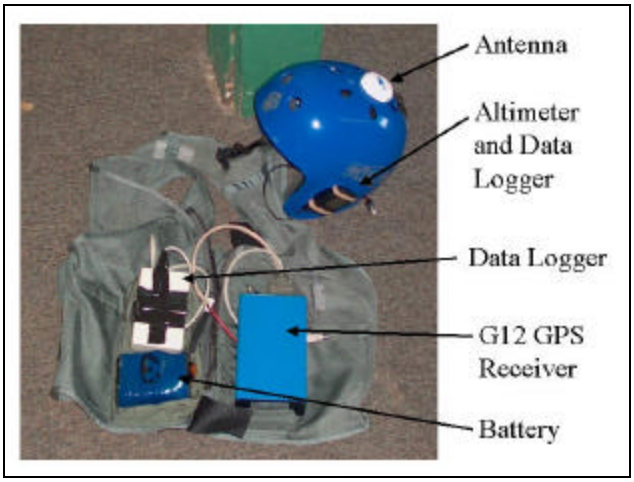

Figure 4: DIVEPACS configured for freefall testing

The components are shown on the aircrew survival vest that is worn by the manikin. This configuration keeps the components located close to the center of mass of the manikin. It is important that any bulky items placed on the manikin are positioned symmetrically around the manikin center so that the equipment doesn't cause the manikin to become unstable in flight and tumble when it enters the airstreams. The helmet shown in Figure 4 is not the type worn by the manikins during actual ejection trials, but is a standard skydiving helmet. The helmet and barometric altimeter were used for initial testing only during skydiving tests conducted at the Skydive Green County dropzone. The results are presented later in the paper.

GPS Receiver and Antenna

In a typical ejection sequence the ejection components experience accelerations as high as 20g's.[3]. In order to handle the high dynamics, the DIVPACS incorporated the Ashtech® G12 GPS Receiver. The G12 is an original equipment manufactured (OEM), 12-channel, single frequency (L1), coarse acquisition (C/A) code and carrier receiver. The receiver offers consistent and reliable tracking with peak acceleration rates greater than 23g's, over 450 g/s of jerk, and vibration levels of $01G^2/Hz$.[5]. The re-acquisition time is 2 seconds, and the hot start time to first fix is 11 seconds. The G12 can output National Marine Electronics Association (NEMA) messages, Ashtech proprietary messages, and raw measurements. The DIVEPACS G12 is limited to a 20Hz sampling rate, but based on the test data from previous ejections, a 20 Hz sample rate should be adequate to determine the manikin's position and velocity.[3]. In addition, when the G12 sample rate is set to either 10 or 20 Hz, only 8 satellites are used to calculate a position solution.

One of the design constraints on the system is that it is small enough to fit into the pockets of the survival vest shown in Figure 4. The size of the G12 is 108mm x 58.4mm. It weights 2.8 ounces and has a power consumption of 2.1 Watts including the power applied to the antenna. The antenna is external from the receiver and is located on top of the helmet shown in Figure 4. The manikin will wear a standard Air Force issue aircrew helmet with the antenna located inside the plastic shell toward the front of the helmet. A typical aircrew helmet and ejection harness is shown in Figure 5.

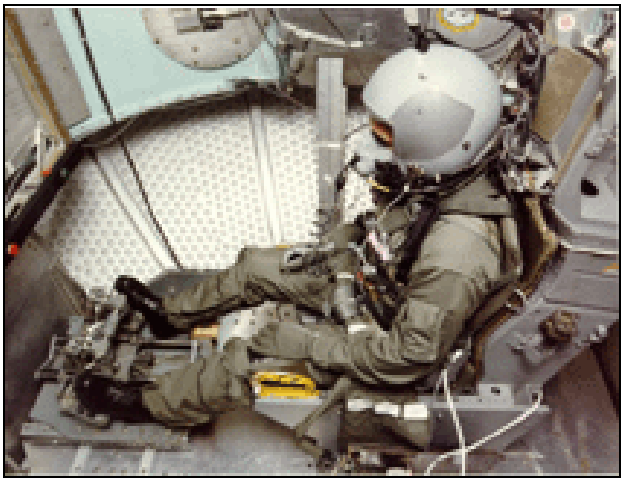

Figure 5: Aircrew member in ejection seat

Data Logger

All the data collected from the DIVEPACS GPS receiver is stored in an H.O. Data Compu-Log RS-12DD data logger for post processing. The data logger is designed to collect and store the output from any RS-232 source at a rate of up to 115,000 bps. A separate 9v battery powers the data logger. The data is placed into non-volatile memory so it is protected in the event of power loss. Due to the high dynamics, the original container and I/O connections will be replaced with a ruggedized container and connectors prior to the start of actual ejection tests.

Post Processing Software

After test completion, the data is downloaded from the data logger and reference receiver, and the files are processed using MATLAB® and Ashtech® software loaded on a desktop PC or laptop. At this point, the files can be processed separately to provide a stand-alone GPS position, velocity, and attitude solution from the data logger, or the files can be synchronized and processed together for a more accurate differential position, velocity, and attitude solution. The method of differential correction dictates the accuracy level of the solution. The three types of differential correction methods are code corrected, carrier smoothed code, and carrier phase differential. Carrier phase differential is the most accurate.

Second Generation System Configuration

The second generation of DIVEPACS will incorporate two Ashtech® G12 GPS Receivers and two H. O. Data Compu-Log RS12-DD data loggers into one package. The single package must still meet the size constraints listed above. Since two antennas must be mounted on the manikin, the Sarantel GeoHelix-H antenna replaced the Antenna Technologies Inc antenna for a better form fit. Although the Sarantel GeoHelix-H has a lower overall gain specification, the difference in mounting placement should compensate for it. The original antenna had to be mounted inside the helmet during an ejection, and the new antenna will be mounted on each shoulder without any obstructions. Figure 6 depicts the size difference between the two antennas.

In addition to the hardware changes, modifications to the differential functions in MATLAB® are needed to improve the carrier phase integer ambiguity resolution. Through the use of several algorithms, the functions will be more robust, and will be able to handle cycle slips in the data easier.

Figure 6: Antenna Technology Inc (Left) and Sarantel GeoHelix-H (Right)

TESTING METHODOLOGY

First Generation Systems

After selecting the hardware, the first generation systems underwent three phases of testing. Each phase had passing criteria established, and provided logical build up to the

next phase of testing. The phased approach ensured that the DIVEPACS could operate reliably during an ejection seat test.

Phase I Testing

Phase I testing integrated the receiver and data logger into a single package and bench tested them using different satellite configurations. One of the most challenging aspects of this phase was developing a hardened case able to withstand 15g's and ensure the data logger was able to retain the data even if the I/O cables were damaged and the battery disconnected. Phase II results are provided below.

Phase II Testing

Phase II testing was the first step in validating the DIVEPACS ability to track enough satellites to calculate a three-dimensional position and velocity solution in a medium dynamic environment. The DIVEPACS was configured for freefall flight. Figure 7 shows the DIVEPACS freefall configuration.

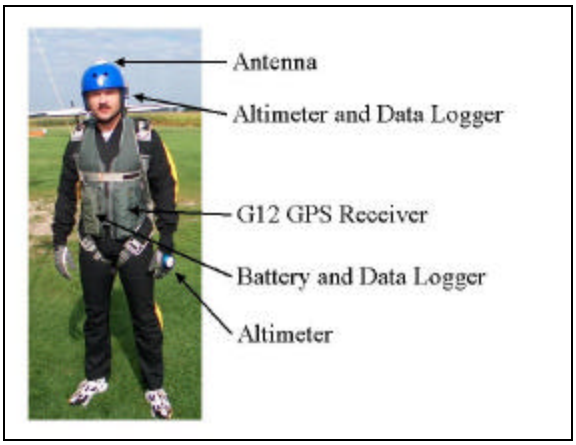

Figure 7: DIVEPACS Freefall Configuration

Freefall flight simulates a portion of the manikin's natural flight profile during an ejection sequence. Although the maximum velocity and acceleration experienced during a freefall don't match those of an actual ejection seat test prior to the parachute opening, they are very similar after the parachute has been deployed. The freefall tests provided a low cost test alternative to evaluate the DIVEPACS performance in a medium dynamic environment.

Phase III Testing

The last phase of testing consisted of configuring the DIVEPACS to be placed onto a manikin for an actual ejection seat test. The manikin's survival vest radio pocket held the DIVEPACS, and the antenna was mounted inside the manikin's aircrew helmet. To provide a differential GPS solution, a reference station was established within 5 km of the sled track.

Second Generation Systems

The second generation systems also have a phased approach for testing that is similar to the first generations' testing. For each test one aspect of the DIVEPACS is altered isolate one performance area of the system, and validate its impact on the DIVEPACS ability to provide an accurate position, velocity and or attitude solution. For all phases of testing a reference receiver will be used for differential GPS post processing.

Phase IA Testing

This phase consists of repackaging the two DIVEPACS into a single unit. By mounting the two antennas within the same plane on the manikin, a two dimensional attitude determination can be made provided the resolution for differential GPS solution is high enough. After the differential MATLAB® has been modified, a baseline will be established for the minimum separation of the antennas. The single DIVEPACS was then mounted into a Barber Dodge Championship Auto Racing Team (CART) car, and data was collected as the car qualified for an upcoming race. Figures 8 and 9 show the placement of the DIVEPACS and antennas on the CART car.

Figure 8: Dual DIVEPACS Configuration

Figure 9: Antenna Locations

Phase IIA Testing

Phase IIA testing is a follow-on to the freefall testing, and has two parts. The first part expands on the initial freefall tests. In the previous tests a human subject completed the freefall, and he was able to keep the GPS antenna oriented toward the sky minimizing the loss of lock. In this part of phase IIA, one DIVEPACS is mounted internally to a manikin, and the manikin is pushed from an aircraft on a static line. The natural tumbling and rotations of the manikin before its parachute deployment will help characterize the rotating motion of the manikin in a freefall state, and the system's ability to maintain lock through the rotations. Figure 10 shows the deployment configuration for the manikin.


Figure 10: Manikin Deployment Configuration

The second part of this phase uses the DIVEPACS dual configuration for attitude determination. Once the minimum separation of the antennas can be validated, the dual DIVEPACS will be mounted into a survival vest similar to the previous freefall testing with the use of two antennas. One antenna will be mounted on each shoulder of the parachutist.

Phase IIIA Testing

Phase IIIA testing consists of placing the dual DIVEPACS on a manikin for an actual ejection seat test. Due to the cost and limited availability of these tests, the data collected from phases IA and IIA will be used as the primary data source for analysis.

RESULTS

First Generation System Results

The first generation tests from the phase II testing appeared promising. The freefall test shown in Figure 11 shows that the DIVEPACS was able to maintain lock and provide a good position solution for the entire flight profile once the jumper exited the aircraft. Even through multiple spiral turns at the end of the freefall the DIVEPACS maintained lock, and proved the DIVEPACS could be used in this type of flight environment.

The first generation phase III testing did not fare as well. For the first test, the DIVEPACS was able to provide a position and velocity solution through the first four rocket motor firings. It was initially tracking six satellites, and at each subsequent motor firing, the system dropped a satellite. Figure 12 shows the correlation between the rocket motor firing sequence and the DIVEPACS ability to track satellites. The loss of lock at the motor firings may be due to inertia of the manikin's head motion. In the second ejection seat test the DIVEPACS lost lock almost immediately after the first rocket motor fired.

Second Generation System Results

Recommendations from the first generation tests were incorporated into the second generation systems tests when possible. The second generation tests are preliminary and do not necessarily reflect the overall performance of the DIVEPACS.

The preliminary results from the CART test look promising. Both receivers in the dual DIVEPACS configuration tracked the car's position and velocity through the entire qualifying period. The track had three bridges that obstructed the antennas sky view, and these outages are clearly visible in both the data files.

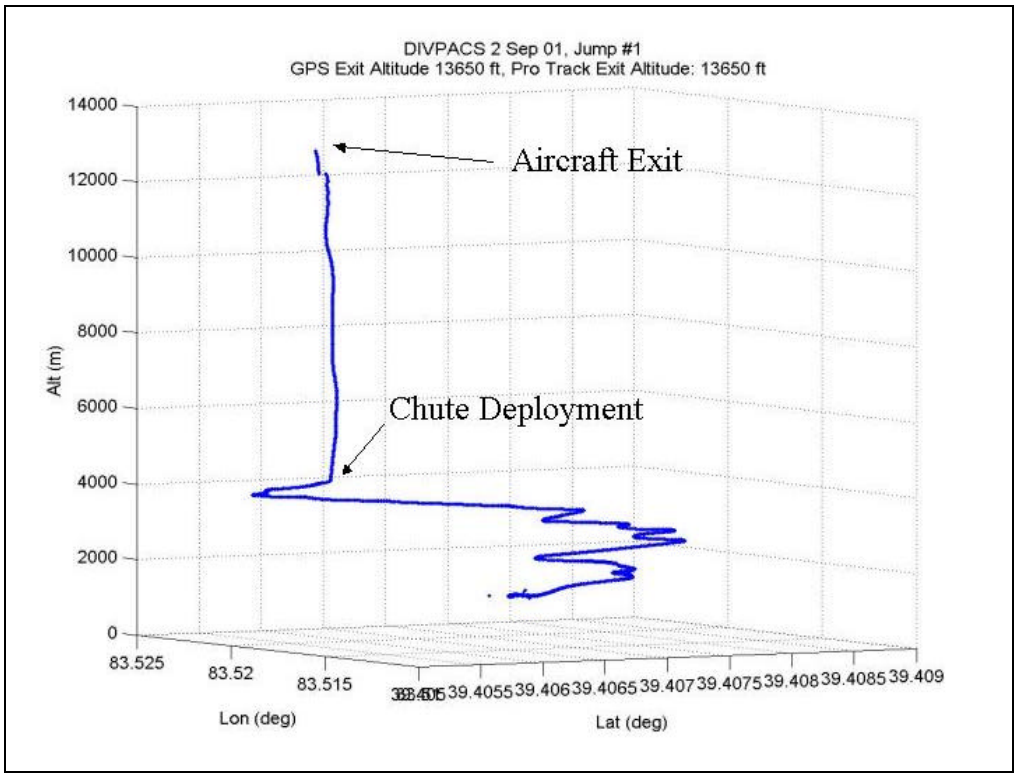

Figure 11: Phase II results in freefall configuration

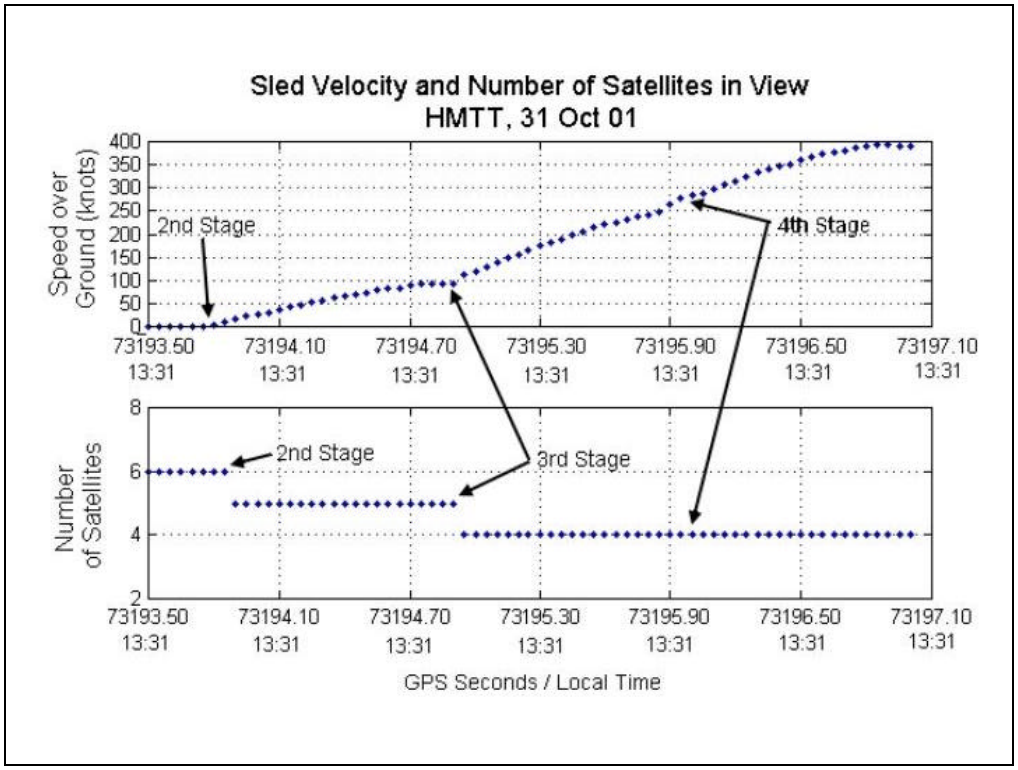

Figure 12: Sled Velocity and Number of Satellites in view, HMTT, 31 Oct 01

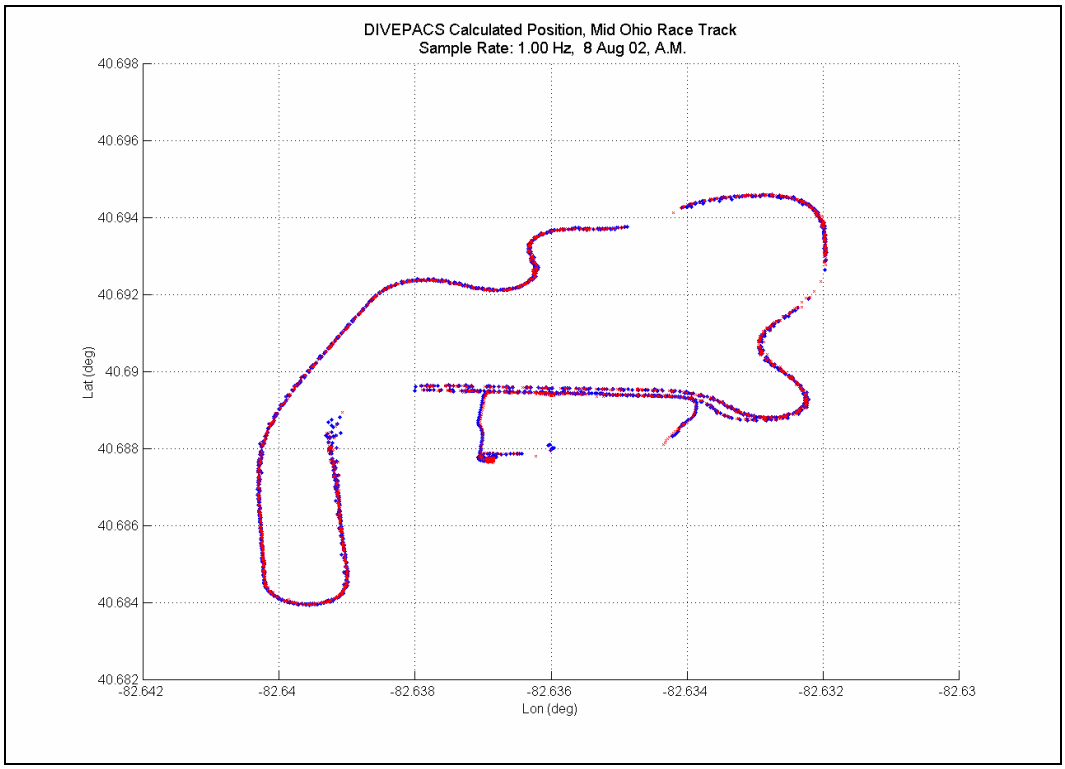

Figure 13: Mid Ohio Dual DIVEPACS Stand Alone GPS Position Solution

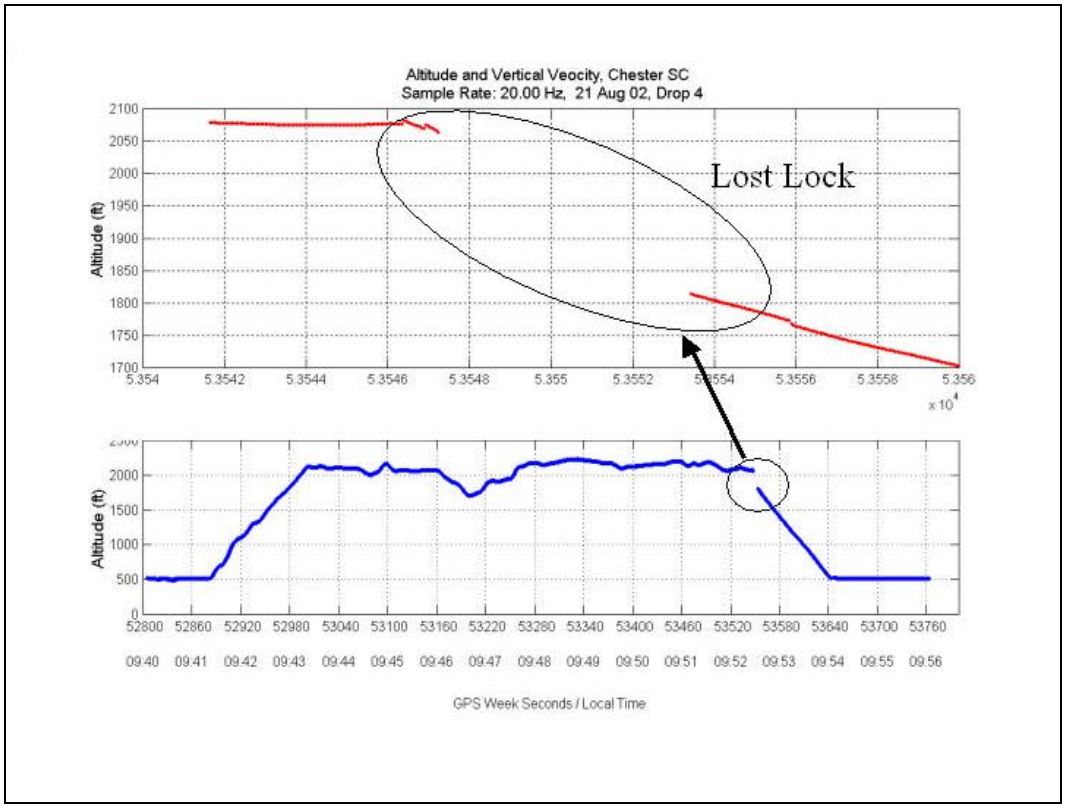

Figure 14: Loss of Lock

Figure 13 overlays the stand alone receivers position solutions. With the outages from the bridges, calculating a carrier phase differential GPS solution will be challenging.

The preliminary results from the first part of the phase IIA tests show that the manikin experiences more tumbling and rotations than the initial freefall tests using a human subject. The additional tumbling caused the DIVEPACS to lose lock and re-acquisition took up to six seconds. The discontinuity in Figure 14 illustrates the loss of lock. Prior to the loss of lock, the DIVEPACS was tracking seven satellites. The additional time to reacquire the satellites was due to the fact that the manikin was not in a position such that the GPS antenna could receive the GPS signals.

CONCLUSIONS

In this paper the initial design, preliminary test results, and problems associated with the new GPS-based system used to augment the current tracking and monitoring systems for position, velocity, and attitude solutions at the AF and other DoD sled track facilities. The DIVEPACS can provide an accurate position, and velocity solution in the low to medium dynamic environments, but some modifications still need to be made to produce good position and velocity solutions in a high dynamic environment. One strong possibility is the integration of a micro-electro-mechanical system (MEMS) based inertial measurement unit (IMU).

ACKNOWLEDGEMENT

The authors would like to thank the Air Force Research Laboratory, Human Effectiveness division, especially Mr. John Plaga and Mr. Doug Coppess for their contributions during the hardware acquisition and configuration. In addition the authors would like to thank the Air Force Research Laboratory, Munitions Directorate for their financial support and providing additional testing opportunities.

DISCLAIMER

The views expressed in this article are those of the authors and do not reflect the official policy or position of the United States Air For, The Department of Defense, or the U. S. Government.

BIOGRAPHY

Capt Christina Schutte is a Masters student at the Air Force Institute of Technology (AFIT). She received her BS in Electrical Engineering from Colorado Technical College in 1993. Her interests include GPS and GPS/INS integration.

Lt Col Mikel Miller is an Assistant Professor of Electrical Engineering at the Air Force Institute of Technology where he is responsible for teaching and research related to integrated GPS and inertial navigation systems. He has been involved with GPS testing and development since 1989.

Capt Brian Reece Tredway is currently assigned to the Air Force Research Laboratory Munitions Directorate at Eglin AFB, Florida. He received his BS in Electrical Engineering form Arizona State University in 1997, and his MS in Electrical Engineering from AFIT in 2002. He is actively involved with the integration of the GPS with Air Force munitions.

REFERENCES

[1] Tredway, Brian R. *Using GPS to Collect Trajectory Data for Ejection Seat Design, Validation, and Testing*. MS thesis, AFIT/GE/ENG/02M-27. Air Force Institute of Technology School of Engineering (AU), Wright-Patterson AFB OH, March 2002 (ADA401521).

[2] Misra, Pratap and Per Enge. *Global Positioning System; Signals, Measurements, and Performance.* Lincoln, Massachusetts: Ganga-Jamuna Press, 2001.

[3] Air Force Research Lab, Crew Escape Technologies. *"Design, Validation and Testing of the Russian K-36 Derivative Ejection Seat,"* Report K-36F – 3.5A.

[4] Titterton, D. H. and J. L. Weston. *Strapdown Inertial Navigation Technology*. Peter Peregrinus Ltd, on Behalf of the Institution of Electrical Engineers, London, United Kingdom, 1997.

[5] Haax, Lin, Abousalem Mohamed, and James Murphy. "The Ashtech G12-HDMA: A Low Cost, High performance GPS Space Receiver," *Procdeedings of ION National Technical Meeting 2000*, Salt Lake City, UT, 19-22 September 2000.

[6] *G12™ GPS OEM Board and Sensor Reference Manual*. Part Number 630068, Revision C. Santa Clara: Magellan Corporation Ashtech Precision Products, September 2000.

[7] Spilker, J.J. (1994). *"GPS Navigation Data," in Global Positioning System: Theory and Applications I.* Ed B. Parkinson, J. Spilker, P. Axelrad and P. Enge. Washington DC: AIAA, 1996.

[8] Dana, Peter H. *"The Geographer's Craft Project."* Department of Geography, The University of Colorado at Boulder. 1 May 2000.

[9] Bracy, Brian L. *Evaluation of a Method for Kinematic GPS Carrier-Phase Ambiguity Resolution Using a Network of Reference Receivers.* MS thesis, AFIT/GE/ENG/00M-05. Air Force Institute of Technology School of Engineering (AU), Wright-Patterson AFB OH, March 00 (ADA380761).

[10] Raquet, John R. Class Handout, EENG 533, Navigation Using GPS, Air Force Institute of Technology School of Engineering (AU), Wright-Patterson AFB OH, Spring 2002.

[11] Raquet, John R. Class Handout, EENG 633, Advanced GPS Theory and Applications, Air Force Institute of Technology School of Engineering (AU), Wright-Patterson AFB OH, Summer 2002.

[12] Miller, Mikel M. Class Handout, EENG 635, Inertial Navigation Subsystems, Air Force Institute of Technology School of Engineering (AU), Wright-Patterson AFB OH, Spring 2002.

[13] Pachter, Meir. Class Handout, EENG 534, Fundamentals of Aerospace Instruments and Navigation, Air Force Institute of Technology School of Engineering (AU), Wright-Patterson AFB OH, Winter 2002.

Bibliography

[1] Air Force Research Lab, Crew Escape Technologies. *"Design, Validation and Testing of the Russian K-36 Derivative Ejection Seat,"* Report K-36F – 3.5A.

[2] Bouska, Terry J. *Design and Simulation of a Pseudolite-Based Flight Reference System.* MS thesis, AFIT/GE/ENG/03M-03. Graduate School of Engineering and Management Air Force Institute of Technology (AU), Wright-Patterson AFB OH, March 03.

[3] Bracy, Brian L. *Evaluation of a Method for Kinematic GPS Carrier-Phase Ambiguity Resolution Using a Network of Reference Receivers.* MS thesis, AFIT/GE/ENG/00M-05. Graduate School of Engineering and Management Air Force Institute of Technology (AU), Wright-Patterson AFB OH, March 00 (ADA380761).

[4] Cables.com by Datacomm Cables. *Model SM-66 High Gain GPS Antenna with Low Noise Amplifier*, http://www.gpscables/sm66.htm. 29 October 2002.

[5] Cunningham, Joseph R. *Performance of GPS-Aided INS During High-Dynamic Maneuvers*. MS thesis, AFIT/GE/ENG/87D-12. Graduate School of Engineering and Management Air Force Institute of Technology (AU), Wright-Patterson AFB OH, December 1987 (ADA194624).

[6] CSM GmbH, *CSM Produkte*, http://www.csm.de/html/d/produkte_komponenten/frm/xmain.htm. 4 November 2002.

[7] Dana, Peter H. *"The Geographer's Craft Project."* Department of Geography, The University of Colorado at Boulder. 1 May 2000.

[8] Garmin, *About GPS*, http://www.garmin.com/aboutGPS. 15 December 2002.

[9] *G12™ GPS OEM Board and Sensor Reference Manual.* Part Number 630068, Revision C. Santa Clara: Magellan Corporation Ashtech Precision Products, September 2000.

[10] Haax, Lin, Abousalem Mohamed, and James Murphy. "The Ashtech G12-HDMA: A Low Cost, High performance GPS Space Receiver," *Procdeedings of ION National Technical Meeting 2000*, Salt Lake City, UT, 19-22 September 2000.

[11] Henderson, Paul E. *Development and Testing of a Multiple Filter Approach for Precise DGPS Positioning and Carrier-Phase Ambiguity Resolution*. MS thesis, AFIT/GE/ENG/ 01M-15. Graduate School of Engineering and Management Air Force Institute of Technology (AU), Wright-Patterson AFB OH, March 2001 (ADA392028).

[12] Higgins, Richard. *"FWD: Run 759 Flash Report"* Electronic Message. 4 March 2003.

[13] H. O. Data Compu-Log Type RS-xxDD User's Guide. Part Number RS-12DD, Revision1.04. H. O. Data, 18 June 2001.

[14] JAVAD Navigation Systems, http://www.javadgps.com. 20 November 2002.

[15] Kaplan, E. *Understanding GP: Principles and Applications*. Boston: Artech House Inc., 1996

[16] Loughran, Eileen. *"9/11 Test Photos"* Electronic Message. 25 September 2002.

[17] Maybeck, Peter S. *Stochastic Models, Estimation, and Control, Volume I.* Arlington, Virginia: Navtech Book and Software Store, 1994.

[18] Maybeck, Peter S. *Stochastic Models, Estimation, and Control, Volume II.* Arlington, Virginia: Navtech Book and Software Store, 1994.

[19] Maybeck, Peter S. *Stochastic Models, Estimation, and Control, Volume III.* Arlington, Virginia: Navtech Book and Software Store, 2001.

[20] Mercator GPS Systems, *Quest Quality Engineering & Survey Technology* http://www.mercat.com/QUEST/gpstutor.htm. 15 December 2002

[21] Miller, Mikel M. Class Handout, EENG 635, Inertial Navigation Subsystems, School of Engineering Air Force Institute of Technology, Wright-Patterson AFB OH, Spring 2002.

[22] Misra, Pratap and Per Enge. *Global Positioning System; Signals, Measurements, and Performance.* Lincoln, Massachusetts: Ganga-Jamuna Press, 2001.

[23] MSN TerraServer, http://www.terraserver.homeadvisor.msn.com. 23 February 2003

[24] National Air and Space Museum, *GPS: A New Constellation* http://www.nasm.edu/galleries/gps. 15 December 2002

[25] Pachter, Meir. Class Handout, EENG 534, Fundamentals of Aerospace Instruments and Navigation, School of Engineering Air Force Institute of Technology, Wright-Patterson AFB OH, Winter 2002.

[26] Plaga, John. *"RE: ENU Files from HMTT"* Electronic Message. 12 December 2002.

[27] Raquet, John R. *Development of a Method for Kinematic GPS Carrier-Phase Ambiguity Resolution Using Multiple Reference Receivers*, PhD Dissertation, Department of Geomatics Engineering, University of Calgary, Alberta, May 1998 (ADA359919).

[28] Raquet, John R. Class Handout, EENG 533, Navigation Using GPS, School of Engineering Air Force Institute of Technology, Wright-Patterson AFB OH, Spring 2002.

[29] Raquet, John R. Class Handout, EENG 633, Advanced GPS Theory and Applications, School of Engineering Air Force Institute of Technology, Wright-Patterson AFB OH, Summer 2002.

[30] Sarantel, http://www.sarantel.com/geohelix-h.html. 29 June 2002.

[31] The Aerospace Corporation, *"GPS Segments."* http://www.aero.org/publications/GPSPRIMER/GPSElements.html. 12 March 2003.

[32] The MathWorks Inc., 21 Elliot Street, Natick MA 01760. *MATLAB®*. Version 6.0.0.42a Release 12, November 2002

[33] Titterton, D. H. and J. L. Weston. *Strapdown Inertial Navigation Technology*. Peter Peregrinus Ltd, on Behalf of the Institution of Electrical Engineers, London, United Kingdom, 1997.

[34] Tredway, Brian R. *Using GPS to Collect Trajectory Data for Ejection Seat Design, Validation, and Testing*. MS thesis, AFIT/GE/ENG/02M-27. Graduate School of Engineering and Management Air Force Institute of Technology (AU), Wright-Patterson AFB OH, March 2002 (ADA401521).

[35] Triangle Digital Services LtD, *TDS2020F Technical Data*, http://www.TriangleDigital.com. 16 December 2002

[36] Tri_M Systems Engineering, *GPS Antennas*, http://www.tri-m.com/products/systems/mm2.html. 29 October 2002.

[37] U. S. Coast Guard Navigation Center, *The Navigation Center of Excellence*, http://www.navcen.uscg.gov. 15 December 2002

[38] U. S Geological Survey, *USGS National Mapping Information*, http://mapping.usgs.gov. 23 February 2003.

[39] Z-Family Technical Reference Manual. Part Number 630203-01, Revision A. Magellan Corporation, May 1998.

REPORT DOCUMENTATION PAGE

Form Approved
OMB No. 074-0188

1. REPORT DATE *(DD-MM-YYYY)*	2. REPORT TYPE	3. DATES COVERED *(From – To)*
25-03-2003	**Master's Thesis**	May 2002 – Mar 2003

4. TITLE AND SUBTITLE

USING THE GPS TO IMPROVE TRAJECTORY POSITION AND VELOCITY DETERMINATION DURING REAL-TIME EJECTION SEAT DESIGN, TEST AND EVALUATION

5a. CONTRACT NUMBER

5b. GRANT NUMBER

5c. PROGRAM ELEMENT NUMBER

6. AUTHOR(S)

Schutte, Christina G. Captain, USAF

5d. PROJECT NUMBER

5e. TASK NUMBER

5f. WORK UNIT NUMBER

7. PERFORMING ORGANIZATION NAMES(S) AND ADDRESS(S)

Air Force Institute of Technology
Graduate School of Engineering and Management (AFIT/EN)
2950 Hobson Way, Building 640
WPAFB OH 45433-7765

8. PERFORMING ORGANIZATION REPORT NUMBER

AFIT/GE/ENG/03-16

9. SPONSORING/MONITORING AGENCY NAME(S) AND ADDRESS(ES)

AFRL/HEPA
Attn: Mr. John Plaga
Q Street, Building 824 DSN: 785-1166
WPAFB OH 45433-7765 e-mail: John.Plaga@wpafb.af.mil

10. SPONSOR/MONITOR'S ACRONYM(S)

11. SPONSOR/MONITOR'S REPORT NUMBER(S)

12. DISTRIBUTION/AVAILABILITY STATEMENT

APPROVED FOR PUBLIC RELEASE; DISTRIBUTION UNLIMITED.

13. SUPPLEMENTARY NOTES

14. ABSTRACT

Test and evaluation of the United States Air Force's latest aircraft escape system technology requires accurate position and velocity profiles during each test to determine the relative positions between the aircraft, ejection seat, manikin and the ground. Current rocket sled testing relies on expensive ground based multiple camera systems to determine the position and velocity profiles. While these systems are satisfactory at determining seat and manikin trajectories for sled testing, their accuracy decreases when they are used for in-flight testing, especially at high altitudes.

This research presents the design and test results from a new GPS-based system capable of monitoring all major ejection test components (including multiple ejection seat systems) during an entire escape system test run. This portable system can easily be integrated into the test manikin, within the flight equipment, or in the ejection seat. Small, low-power, lightweight Global Positioning System (GPS) GPS receivers, capable of handling high-accelerations, are mounted on the desired escape system component to maintain track during the escape system test sequence from initiation until the final landing. The GPS-based system will be used to augment the telemetry and photography systems currently being used at the Air Force (AF) and other Department of Defense's (DoD) sled track test facilities to improve tracking accuracy and reduce testing costs.

15. SUBJECT TERMS

Global Positioning System, GPS, Differential GPS, DGPS, Ejection Seats, Navigation, Theodolite

16. SECURITY CLASSIFICATION OF:			17. LIMITATION OF ABSTRACT	18. NUMBER OF PAGES	19a. NAME OF RESPONSIBLE PERSON
a. REPORT	b. ABSTRACT	c. THIS PAGE			Mikel M. Miller, Lt Col, USAF (ENG)
U	U	U	UU	127	19b. TELEPHONE NUMBER *(Include area code)* (937) 255-7777, ext 3295; e-mail: Mikel.Miller@afit.edu

Standard Form 298 (Rev. 8-98)
Prescribed by ANSI Std. Z39-18